STUDIES ON HYDROGEN SULFIDE
DISPOSAL SYSTEMS

STUDIES ON HYDROGEN SULFIDE DISPOSAL SYSTEMS

SECTION ONE:

A PRELIMINARY STUDY OF THE ELECTROCHEMICAL DECOMPOSITION OF HYDROGEN SULFIDE: THE DETERMINATION OF THE CONDUCTIVITY DISPLAYED BY H_2S - SOLUTE MIXTURES

AND

SECTION TWO:

THE EVALUATION AND CHARACTERIZATION OF THE VANADIUM(IV) SPECIES PRESENT IN AQUEOUS SOLUTION CONTAINING CITRATE LIGAND

BY

THOMAS A. WALKER, B.Sc.

A Thesis
Submitted to the Faculty of Graduate Studies
in Partial Fulfillment of the Requirements
for the Degree Master of Science

McMaster University
Hamilton, Ontario

September 1985

To

my Parents,

who gave me the opportunity

to learn.

Master of Science (1985) McMaster University
Hamilton, Ontario

Title: Studies on Hydrogen Sulfide Disposal Systems

Section One: A Preliminary Study of the Electrochemical Decomposition of Hydrogen Sulfide: The Determination of the Conductivity Displayed by H_2S - Solute Mixtures

Section Two: The Evaluation and Characterization of the Vanadium(IV) Species Present in Aqueous Solution Containing Citrate Ligand

Author: Thomas A. Walker, BSc. (McMaster University)

Supervisor: Dr. O.E. Hileman Jr.

Number of Pages: xvi, 195

NOTE TO THE READER:

The following Thesis is comprised of two separate and individual parts, both of which relate to the disposal of hydrogen sulfide. Section One is an investigation into the possibility of developing a hydrogen sulfide decomposition process which would produce both hydrogen and elemental sulfur. Section Two deals with the speciation study of a catalyst used in a traditional process which converts hydrogen sulfide gas into elemental sulfur.

Abstract:

Section One: A Preliminary Study of the Electrochemical Decomposition of Hydrogen Sulfide: The Determination of the Conductivity Displayed by H_2S - Solute Mixtures

The disposal of hydrogen sulfide by electrolysis to produce both hydrogen and sulfur appears to an interesting alternative to the conventional Claus process which wastes the hydrogen content of hydrogen sulfide. The electrolysis at room temperature has been reported in the literature, however, the investigation was somewhat limited by the low conductivity displayed by the electrolysis solution (pyridine/hydrogen sulfide mixture).

The primary goal of this research was to construct a suitable apparatus and carry out a series of conductivity measurements of liquid hydrogen sulfide at room temperature with and without the addition of possible electrolytes. The objective was to determine if an electrolyte could be found that would increase the conductivity to a suitably high level to warrant the further investigation of the electrolysis process.

Of the six possible electrolytes, only tetrapropyl ammonium iodide increased the conductivity to a desirable level. A 0.4034 M solution of this alkyl ammonium iodide in liquid hydrogen sulfide increased the conductivity (at 23 C) from 7.00 X 10^{-8} $ohm^{-1}cm^{-1}$ for the pure solvent to 1.13 X 10^{-2} $ohm^{-1}cm^{-1}$. This increase was attributed to the formation of the corresponding hydrogen sulfide adduct and its subsequent dissociation in liquid hydrogen sulfide.

Now that it has clearly been established that appropriately high conducting solutions of hydrogen sulfide can be prepared, the further investigation of the electrolysis of hydrogen sulfide as a viable industrial process is warranted.

Section Two: The Evaluation and Characterization of the Vanadium(IV) Species Present in Aqueous Solution Containing Citrate Ligand.

This section deals with the investigation of species present in vanadium(IV): citrate solutions over a wide range of pH values. Various spectroscopic methods (UV/VIS, ESR, vanadium-51 FT-NMR) were used to probe this specific system. The accumulated spectroscopic data were rationalized on the basis of thirteen vanadium(IV) containing species, four of which were proposed to be vanadium(IV): citrate species. Based on the observed spectroscopic data an equilibrium diagram was prepared which illustrates the vanadium(IV) species present as a function of pH.

Acknowledgements:

I deeply appreciate the co-operation and friendly advise that I have received from the research group during my graduate years at McMaster. In addition, I would like to thank Mr. I. Thompson and Mr. B. Sayer for their technical assistance.

Table of Contents

Section One: Determination of the Conductivity Displayed by H_2 - Solute Mixtures

Chapter One - Introduction

Chapter Two - Properties of Hydrogen Sulfide

Table of Contents: Cont'd | Page

Chapter Two - Properties of Hydrogen Sulfide Cont'd

Chapter Three - Research Goals

Chapter Four - Experimental Details

Chapter Five - Results and Discussion

Table of Contents: Cont'd Page

Chapter Five - Results and Discussion Cont'd

Chapter Six - Summary and Conclusions

Appendices

Appendix C: Selected Physical Properties of the Electrolytes

Table of Contents: Cont'd Page

Appendix D: Detailed Operation Procedures

Section Two: Speciation Study of Vanadium(IV): Citrate Solution

Chapter One - Introduction

Table of Contents: Cont'd Page

Chapter Two - Experimental Details

2.2 Sample Analysis

Chapter Three - Resuls and Discussion

Table of Contents: Page

Appendices

Appendix E: Determination of the Percent Composition of Vanadium in Vanadyl Sulfate

Appendix F: Preparation and Handling of Samples

Appendix G: Tabulated ESR and NMR Results

List of Tables

Table No. Page

Section One:

Section Two:

List of Tables: Cont'd

List of Figures

List of Figures: Cont'd

List of Figures: Cont'd

SECTION ONE:

A Preliminary Study of the Electrochemical Decomposition of Hydrogen Sulfide: The Determination of the Conductivity Displayed by H_2S - Solute Mixtures

CHAPTER ONE:

INTRODUCTION

Chapter One - Introduction

1.1 Background:

Our society is faced with many very serious and complex problems attributable to our technological and industrial development and the associated energy requirements. At the present time, most of these energy requirements are meet by the consumption of non-renewable natural resources. Such a heavy reliance on these resources has, and will continue to have, very serious repercussions throughout our society, as was illustrated during the mid-1970's when the the supply of oil was depressed due to the oil embargo imposed by the OPEC nations.

These are only one set of the more obvious problems that arise from the reliance of our society on petroleum. Perhaps one of the most significant disadvantages is the effect of combustion of these fuel sources on our environment. As prime quality fossil fuels resources have been depleted, we have been forced to use less desirable resources. These lower grade fossil fuels contain higher levels of sulfur and other contaminates. Upon combustion these yield significant quantities of sulfur dioxide which is often, subsequently, vented into the atmosphere. In 1982, the United States National Emission Data System (NEDS) estimated that in the United States alone, approximately 29.1 million tons of sulfur dioxide and related species (ie. SO_X) were released into the atmosphere[1]. Table 1.1.1 contains a break down

Table 1.1.1: Estimated SO_X Emission for the United States in 1982(1)

Major Source Category	Estimated SO_X Emissions (million tons)		Percentage of Total for USA	
Stationary fuel Combustion	22.8		78.5%	
Coal		18.2		62.5%
Oil		4.3		14.8%
Gas		0.2		0.7%
Industrial	5.3		18.2%	
Primary metal		2.5		8.8%
Chemical production		0.97		3.3%
Petroleum		0.88		3.0%
Mineral production		0.52		1.8%
Transportation	0.91		3.1%	
Gasoline		0.23		0.8%
Diseal fuel		0.43		1.5%
Total Emissions:	29.1 million tons			

of this 29.1 million tons as a function of originating source, and clearly shows that the combustion of coal is by far the greatest single source of sulfur dioxide emissions.

Once in the environment, the conversion of sulfur dioxide to sulfuric acid may result from one of the two following pathways[1]. In polluted regions, the sulfur dioxide may collide in the gas phase with strong oxidizing radicals such as $HO^{\bullet}$, $HO_2^{\bullet}$ and $CH_3^{\bullet}$ and undergo homogeneous oxidation. These oxidizing radicals are produced as intermediate products in the daytime photo-oxidation of hydrocarbon-nitrous oxide emissions. The second possible reaction route involves both gaseous and liquid or solid phases and may proceed by one of the following heterogeneous mechanisms:

(1) Catalytic oxidation in water droplets by transition metals;
(2) oxidation in the liquid phase by ozone or hydrogen peroxide; or,
(3) surface catalyzed oxidation of sulfur dioxide on collision with solid particles such as elemental carbon (soot).

Regardless of the exact reaction pathway, the overall result is the same: the production of acidified precipitation. Upon deposition, this "acid rain" subsequently has the effect of decreasing the pH of our lakes and streams and increasing the corrosion rate to our man-made structures. This pH drop has a significant effect on aquatic life and the "death" of hundred of lakes in North America, as well as in Europe[1] is credited to this effect.

So it would appear that our society not only has to deal with the problems associated with the depletion of our energy resources, but also the related pollution problems caused by using these resources. It is obvious, on the long-term scale, that the only real solution is the development of new "clean" energy sources. Currently there is substantial research in the fields of solar, geothermal and nuclear energy. It, however, is uncertain when, or even if, these alternatives will be able to economically meet our energy demands.

On the short-term scale, it is apparent that conservation of existing fossil fuels resources combined with methods to decrease sulfur dioxide emissions is the only answer. Emissions levels of sulfur dioxide can be reduced in one of two ways:

(1) low grade fuel source, especially coal, could be upgraded prior to combustion thus eliminating the production of sulfur dioxide; or,

(2) the flue gas resulting from the combustion of low grade fuel could be treated, thus removing sulfur dioxide and other pollutants before entering the environment.

Of the two methods, the treatment of flue gas has the disadvantage of being more expensive and suffers from the problems associated with the disposal of the resulting waste sludge or by-product acid.

1.2 Fuel Desulfurization

Currently, within the industry, there is increasing activity to upgrade fuels such as lignites, coals, cokes, pitches, residues, heavy oils and bitumen and thereby reducing the sulfur content. In gaseous fuel, the majority of the sulfur exists as hydrogen sulfide and is easily extracted by solvent scrubbing systems. In liquid and solid fuels the sulfur is present in many chemical forms, but exists primarily as various sulfur containing organic molecules such as sulfides, disulfides and mercaptans. The sulfur content of these fuels can be decreased to an acceptable level by treatment of the fuel with hydrogen at elevated temperatures. This reaction can be represented as follows:

$$\underset{\text{(containing sulfur)}}{\text{Fuel}} + H_2 \text{ ---> } \underset{\text{(with less sulfur)}}{\text{Fuel}} + H_2S$$

The overall result is that large portions of the sulfur are removed, yielding a higher grade fuel source and hydrogen sulfide. Since hydrogen sulfide is toxic and corrosive in nature it must be appropriately handled and disposed of. At the present time, most of the hydrogen sulfide produced in this way is disposed of by means of the Claus Kiln process.

The Claus process is a well established industrial process which involves the partial oxidation of hydrogen sulfide to sulfur and water with the net release of heat.[2] The reaction actually proceeds via a two step process initially involving a highly exothermic oxidation step in which a portion of the hydrogen sulfide is oxidized to sulfur dioxide (equation 1).

$$H_2S + 3/2\ O_2 \dashrightarrow SO_2 + H_2O \qquad (1)$$

This step is followed by a less exothermic redox reaction whereby the sulfur dioxide reacts with the remainder of the hydrogen sulfide to produce elemental sulfur and water (equation 2).

$$2H_2S + SO_2 \dashrightarrow 3S + 2H_2O + \text{heat} \qquad (2)$$

The overall reaction is self-sustaining and produces elemental sulfur as well as approximately 218 KJ of heat per mole of hydrogen sulfide (equation 3).

$$3H_2S + 3/2\ O_2 \dashrightarrow 3S + 2H_2O \qquad (3)$$

The Claus process, as it is used by industry, has a number of significant disadvantages. Typically, the Claus process has an efficiency rating of about 94% to 98%. This may appear to be efficient, however, when considering the large quantity of hydrogen sulfide being disposed of in this way, it is apparent that substantial amounts of hydrogen sulfide and/or sulfur dioxide are being released into the atmosphere.

Perhaps the most significant disadvantage of this process is that there are only two recoverable products: elemental sulfur and low grade heat. In 1979, 6.1 million tons of sulfur were recovered in

Canada, while 4.07 million tons were recovered in the United States.[3] This amount of sulfur represents the loss of approximately 7.5 X 10^9 m^3 (approx. 250 X 10^9 SCF) of hydrogen. It has been estimated that if the majority of this hydrogen could be recovered, it would be enough to hydrogenate one million tons of coal to produce 59 X 10^6 bbl of high-grade liquid hydrocarbon fuel.[3] This lost hydrogen represents a substantial cost, and if even a small amount of the hydrogen could be effectively recovered, the cost of the upgrading process could be significantly reduced.

Not only is the Claus process wasteful of hydrogen but at the present time much of the hydrogen which is being used for fuel up-grading is derived from natural gas or naphtha. If a process to recover both the hydrogen and the sulfur was developed this would not only decrease the cost of fuel up-grading but would also reduce the consumption of prime non-renewable resources.

1.3 Hydrogen Sulfide Decomposition

The decomposition of hydrogen sulfide into hydrogen and sulfur is an endothermic process which requires the net input of approximately 80 KJ of energy per mole of hydrogen sulfide for the reaction to proceed. The advantage of such a process is the production of two recoverable products: hydrogen and sulfur (equation 4).

$$2H_2S + \text{energy} <\!\!==\!\!> 2H_2 + 2/X\ S_X \qquad (4)^*$$

The first reported studies on the direct thermal decomposition were by Taylor and Pickett.[4] The decomposition reaction was carried out on a platinum wire which was electrically heated to about 1000C. They concluded that the reaction which proceeded could be broken into three distinctive steps:

(1) absorption of the hydrogen sulfide onto the surface of the wire;
(2) decomposition with the immediate loss of hydrogen; followed by,
(3) the evaporation of the sulfur from the surface of the wire.

Under these conditions, they found that the decomposition of hydrogen sulfide only went to about 10% completion.

More recently Raymont[5] studied the thermal decomposition and reported that hydrogen sulfide is quite thermodynamically stable and does not undergo thermal decomposition to any significant amount at

---

* NOTE: <===> is used in this thesis to represent equilibrium, not resonance

temperatures below 1800K. Even at these high temperatures, the kinetic rate of the uncatalyzed reaction is still very low. For these reasons, the uncatalyzed direct thermal decomposition of hydrogen sulfide is unfavorable from thermodynamic and kinetic considerations.

Raymont[6] pointed out that it maybe possible that the decomposition reaction could be carried out under more moderate reaction conditions by "side stepping" the thermodynamic limitations while the kinetic limitation could be eliminated by the use of appropriate catalysts. Presently, there are five main approaches which are being investigated in an effort to develop a viable industrial process for the decomposition of hydrogen sulfide:

(1) upset equilibrium;

(2) closed loops;

(3) open loops;

(4) hybrid electro-thermochemical closed loops; and,

(5) electrolysis.

1.3.1 Upset Equilibrium

Upset equilibrium techniques make use of the LeChatelier principle whereby a reaction can be forced to proceed by the continuous removal of one or all of the products.

In the decomposition of hydrogen sulfide (equation 4) the reaction could be forced to proceed by selectively removing the produced hydrogen through a diffusion membrane. Molecular sieves would appear ideal for this type of process except that they degrade at even moderate temperatures. Palladium and platinum metal alloy membranes have received some investigation and actually appear to catalyze the reaction. Such membranes, however, are very expensive and may be adversely affected by sulfur deposition.

Even with the use of a diffusion membrane, the reaction rate of the system would need to be increased to make it a viable industrial process. There is evidence from Hyne[7] and Kotera[8] that some transition metal sulfides such as, cobalt or molybdenum sulfides, maybe able to catalyze the decomposition reaction. In general, it was found that the activity of the catalysis was dependent on the stoichiometry of the metal sulfides and was greatest when the metal to sulfide ratio was near unity or greater.

A major disadvantage to diffusion separation approach is that the technique is ultimately limited by the Grahams Diffusion Law Limit which would make it necessary to pass the hydrogen/ hydrogen sulfide gas stream over the membrane a number of times to obtain significant yields of hydrogen. This approach has the further disadvantage that if the sulfur is not removed also, the vapour pressure would be great enough to depress the forward rate of the reaction.

An alternative approach was investigated by Kotera, et al.,[9] in which the sulfur was removed from the product stream. The necessary change in reaction conditions, however, were found to be very extreme. This, coupled with the fact that the yield per pass was extremely low, excluded this approach from being considered a viable one.

Overall, the upset equilibrium approach appears to be somewhat limited due to the expense of the membranes which would be required, as well as kinetic and mass action limitations effects.

1.3.2 Closed Loops

Often, a single unfavourable reaction can be broken into several reactions which proceed under more favourable conditions. In its simplest form this maybe represented by equations (5) and (6).

$$H_2S + X \longrightarrow XS + H_2(g) \qquad (5)$$

$$XS \longrightarrow X + S \qquad (6)$$

The system is referred to as a closed loop because the "X" species is not consumed by the process and is recycled to react with more hydrogen sulfide.

Most research in this area has been conducted by two independent groups in Japan.[10,11] Their work has dealt with the use of transition metal sulfides, such as the sulfides of iron, cobalt and molybdenum. The following is one of the typical reaction sequences which was studied:

$$Co_3S_4 + 2H_2S \longrightarrow 3CoS_2 + 2H_2 \qquad (7)$$

$$3CoS_2 + \text{heat} \longrightarrow Co_3S_4 + 2S \qquad (8)$$

The first reaction (equation 7) was found to be kinetically slow but did occur at a temperature of 550-800K, while the second (equation 8) appears to proceed fairly quickly at temperatures of 950-1200K.

This type of approach seems attractive except that if a batch process is used, the quantity of material required to convert even small quantities of hydrogen sulfide would be enormous. For example, in the case of the cobalt sulfide cycle (reaction 7 and 8) the efficiency was determined to be only 60% to 70%, making it necessary to have approximately 7.3 tons of cobalt sulfide for every ton of sulfur produced by the process. This drawback could possibly be overcome by the use of fluidized beds, if the existing kinetic limitations and byproduct formation could be resolved.

1.3.3 Open Loops

Open loops result from the combination of an unfavourable reaction with a series of favourable reactions, in order to increase the yield of the desired products. These loops differ significantly from closed loops in that auxiliary reagents are consumed and waste products are subsequently formed.

The following is only one of many possible open loops suggested by Raymont[6] for the conversion of hydrogen sulfide to hydrogen and sulfur.

$$2H_2S + 2CO \longrightarrow 2H_2 + 2COS \qquad (9)$$

$$2COS + SO_2 \longrightarrow 2CO_2 + 3/2\ S_2 \qquad (10)$$

$$1/2\ S_2 + O_2 \longrightarrow SO_2 \qquad (11)$$

Overall Reaction:

$$2H_2S + 2CO + O_2 \longrightarrow 2H_2 + S_2 + 2CO_2 \qquad (12)$$

These types of multi-step processes are often expensive because separate processing units are required for each segment of the reaction sequence (equations 9 through 11). A further disadvantage to this approach is that often side reactions occur. This coupled with the fact that separation of the products is often difficult results in contamination of the product stream. Since most often these coproducts are toxic and pollutants, the subsequent disposal problem is often complex and expensive.

1.3.4 Hybrid Electro-thermochemical Closed Loop

Recently, Kalina and Maas Jr.[12,13] reported a process whereby hydrogen sulfide was chemical oxidized to sulfur (see equations 13 through 20). This was followed by an electrochemical step in which the reduced iodine oxidant was regenerated, accompanied by the production of hydrogen equal to the quantity that was present in the hydrogen sulfide. They found that the chemical oxidation of hydrogen sulfide by iodine occurred in acidic solutions (pH= 0-1) and in basic solutions (pH= 13-14).

Regardless of the pH of the solution, the process can be divided into two distinctive steps: (1) the oxidation of the hydrogen sulfide to sulfur in a chemical reactor; followed by, (2) the electrochemical regeneration of the oxidizing iodine species in an electrochemical cell equipped with a membrane to separate cathodic and anodic reactions.

In acidic solutions[12], the iodine exists primarily as I_3^- and oxidizes the hydrogen sulfide to sulfur (equation 13).

$$I_2 \text{ (as } I_3^-) + H_2S \longrightarrow 2H^+ + 2I^- + S \qquad (13)$$

This reduced solution is then circulated to the electrochemical cell where the oxidizing species is regenerated with the production of hydrogen (equation 14 and 15).

Anode Reaction	$3I^- \longrightarrow I_3^- + 2e^-$	(14)
Cathode Reaction	$2H^+ + 2e^- \longrightarrow H_2$	(15)

Combination of these two half reaction results in the following overall reaction (equation 16):

$$3I^- + 2H^+ \longrightarrow I_3^- + H_2 \qquad (16)$$

The overall result of the process is the oxidation of hydrogen sulfide to sulfur followed by the electrolysis of the acid solution to yield hydrogen and the regenerated iodine species.

Kalina and Maas reported excellent sulfur and hydrogen recovery for the above process, as well as high current efficiency. The major disadvantage which they pointed out were problems associated with scrubbing hydrogen sulfide gas streams with an acidic solution. They found that the absorption of hydrogen sulfide into the acidic iodine solution proceeded fairly well, but was less effective than traditional caustic scrubbers. This would result in the need for larger scrubbing systems if the process was expanded to the industrial scale and would represent a significant increase in cost.

This process was also evaluated in basic solutions[13], which solved the problem of hydrogen sulfide absorption into the solution. In basic solution iodine disproportionates quickly to form IO_3^- which oxidizes hydrogen sulfide to sulfur with the production of water and I^- ions (equation 17).

$$3H_2S + IO_3^- \longrightarrow 3S + 3H_2O + I^- \qquad (17)$$

The resulting reduced solution is circulated to an electrochemical cell where the I^- is oxidized back to iodine which quickly disproportionates again. This results in the following overall reaction occurring in the anode compartment of the electrochemical cell (equation 18):

$$I^- + 6OH^- \longrightarrow IO_3^- + 3H_2O + 6e^- \qquad (18)$$

At the cathode, water is reduced to hydrogen with the production of hydroxide ions (equation 19).

$$2H_2O + 2e^- \longrightarrow H_2 + 2OH^- \qquad (19)$$

The overall reaction in the electrochemical cell is the production of hydrogen and IO_3^- ions (equation 20).

$$I^- + 3H_2O \longrightarrow IO_3^- + 3H_2 \qquad (20)$$

As was previously mentioned, this approach has the advantage of quick and efficient hydrogen sulfide absorption. It was found, however that the sulfur recovery was only about 66%. This low yield was caused by the reaction of the sulfur in basic solution to form soluble sulfates.

The two process, as presented, appear promising if a few basic limitations can be resolved. In the case of the acidic process, the hydrogen sulfide absorption problem still represents a major limitation, as does sulfur recovery in the basic process.

A similar approach was investigated in our lab by Prosser,[14] in which spent Stretford liquors were successfully regenerated with no observed deterioration in the performance of the process.

1.3.5 Electrolysis

The electrochemical decomposition of hydrogen sulfide is assumed to proceed in an analogous manner to the electrolysis of water. At the cathode, hydrogen sulfide is reduced, producing hydrogen and sulfide ions (S^{2-}) (equation 21).

$$\text{Cathode Reaction: } H_2S + 2e^- \text{--->} H_2(g) + S^{2-} \qquad (21)$$

Once produced, the sulfide ions migrate to the anode where they are oxidized to elemental sulfur (equation 22).

$$\text{Anode Reaction: } S^{2-} \text{--->} 1/2\ S_2 + 2e^- \qquad (22)$$

Combination of these two half reactions results in the overall reaction in which hydrogen and elemental sulfur are produced by the application of an external electrical power source (equation 23).

$$H_2S + \text{electrical energy} \text{--->} H_2(g) + 1/8S_8 \qquad (23)$$

Recently, Landau[15] reported the first electrolysis of liquid hydrogen sulfide. The electrolysis was carried out in a pressurized manifold at room temperature using aluminum electrodes. Pyridine was added to the liquid hydrogen sulfide to act as a supporting electrolyte, thereby increasing the conductivity of the solution.

In electrolysis processes, electrode reactions often have to be carefully monitored and controlled to prevent further oxidation from taking place at the anode resulting in unwanted by-product formation and consumption of excess power. Landau found that the electrolysis produced only hydrogen and sulfur. The current efficiency for hydrogen production was determined to be 99.7 +/- 0.5%, while that for sulfur was only 84.2%.

Landau[15] considered that the low anodic current efficiency may have resulted from the formation of an insulating layer of sulfur on the anode, thereby reducing the formation of more sulfur. This possibility was rejected since the presence of an insulating layer of sulfur would also decrease the overall cell current efficiency, which was not the case. It was therefore suggested that the low current efficiency may have been due to limitation in the extraction of sulfur from the cell following electrolysis.

Using these experimentally obtained current efficiencies and electrode over potentials, Landau[16] carried out a preliminary optimization and economic analysis of the electrolysis process. He estimated that an electrolysis plant for handling the acid gas from a 250 X 10^6 SCFD coal gasification plant would yield hydrogen and sulfur worth approximately $7.4 million per year, while consuming electricity worth $15.6 million. He therefore concluded that if hydrogen sulfide electrolysis is to become a commercial process, then electrodes with lower over potentials must be developed and the conductivity of the electrolysis solution must be significantly increased by at least a factor of 500. This would reduce the electricity cost in the above example to $4.2 million, resulting in a net profit of $3.2 million.

The conductivity of pure liquid hydrogen sulfide is very low only of the order of 10^{-8} to 10^{-9} $ohm^{-1}cm^{-1}$. For an electrolysis process to be efficient the conductivity of the electrolyzed solution must be substantially higher. Landau's work indicates that the conductivity of the electrolysis solution must be increased to about 10^{-2} $ohm^{-1}cm^{-1}$ for the process to become economically viable. In the case of hydrogen sulfide this could be achieved in a number of ways. The conductivity can be increased by the addition of small amounts of supporting electrolytes, as Landau[15] has done, or conversely by dissolving the hydrogen sulfide in an appropriate solvent which has a high conductivity. Another interesting proposal, made by Raymont[6], was the possibility of high temperature electrolysis of sulfide salts.

This approach was investigated by Lim and Winnick[17], who considered the removal of hydrogen sulfide from the product stream of a modern air-blown coal gasifier. This approach has the advantage of operating at or near typical gasifier temperatures (700 to 1000C). The product gas stream from the coal gasifier, which contains hydrogen sulfide is fed to a porous carbon cathode in the electrolysis cell (see figure 1.3.1). Here, the hydrogen sulfide is reduced to produce hydrogen and sulfide ions (equation 21). These sulfide ions diffuse into the sodium-lithium semi-solid electrolyte (see figure 1.3.1) and migrate to the anode through a membrane where they are oxidized at a porous carbon anode, to produce elemental sulfur vapour (equation 22).

Presently, the major disadvantages stem from concern about the possibility of side reactions occurring thereby reducing the efficiency of the system. As it can be seen from Table 1.3.1, the product stream from a typical gasifier contains significant levels of carbon monoxide and carbon dioxide, which could react with hydrogen

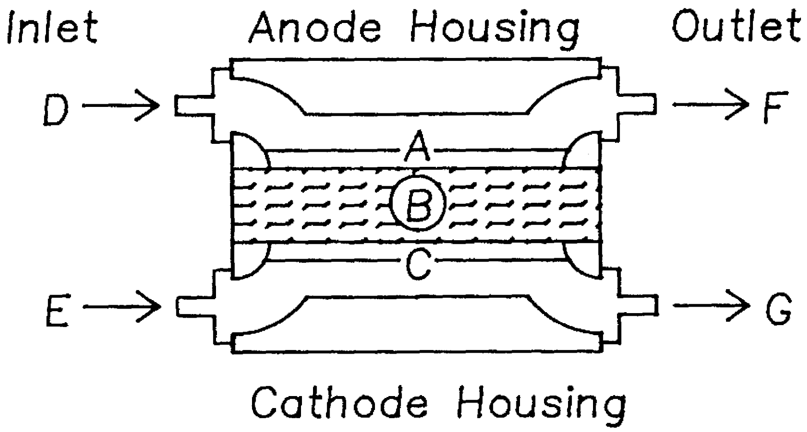

Figure 1.3.1: High Temperature Electrolysis Cell For Use In Conjuction With A Modern Coal Gasifier

The product stream from the gasifier enters the cell through inlet (E). The hydrogen sulfide in the gas stream is reduced at the cathode (C) producing hydrogen gas and sulfide ion. The hydrogen passes with the product stream through outlet (G). The sulfide ions migrate through the sodium/potassium sulfide salt electrolyte (B) to the anode (A) where they are oxidized to elemental sulfur vapour.
The sulfur vapour is carried away by the nitrogen gas stream which enters through inlet (D) and exits through outlet (F).

Table 1.3.1: Typical Gas Composition from an Advanced Air-blown Coal Gasifier[17]

Component	Mole Percent
H_2	14.0
N_2	48.0
CO	29.0
CO_2	3.0
CH_4	3.3
H_2S	0.7
COS	trace
H_2O	2.0

sulfide (equation 24 and 25).

$$CO_2 + H_2S <===> COS + H_2O \qquad (24)$$

$$CO + H_2S <===> COS + H_2 \qquad (25)$$

It is also possible that at these temperatures (700 to 1000C), the hydrogen sulfide could react with the carbon electrode to produce carbon disulfide (equation 26).

$$C + H_2S ---> CS_2 + H_2 \qquad (26)$$

The presence of water (see table 1.3.1) as well as carbon dioxide in the produce stream also may give rise to undesirable reactions with the sulfide salt electrolyte as shown in equations 27 through 30.

$$M_2S + H_2O <===> M_2O + H_2S \qquad (27)$$

$$M_2S + 2H_2O <===> MOH + H_2S \qquad (28)$$

$$M_2S + 4H_2O <===> M_2SO_4 + 4H_2 \qquad (29)$$

$$M_2S + H_2O + CO_2 <===> M_2CO_2 + H_2S \qquad (30)$$

From their preliminary work, Lim and Winnick[17] found that these possible side reactions (equations 24 to 30) did not occur to any significant degree. They observed hydrogen sulfide removal efficiencies in excess of 98.8%, which appeared to be independent of carbon dioxide levels. The porous carbon electrodes, as well as the electrolyte, were stable during the course of their experiments. This preliminary study indicates that the high temperature electrolysis of sulfide salts may be an economically feasible process for use in connection with advanced coal gasifier.

Advantages of electrochemical decomposition stem from the basic simplicity of the process coupled with the flexibility of unit size and inherent "cleanliness" of electrochemical processes. Electrical energy, however, is generally more expensive and the higher cost represents a major disadvantage to the electrolysis process. It has been suggested that a fraction of the hydrogen produced from the electrolysis process could be used to produce the necessary electrical energy. Calculations by Hileman and Hepler[18] indicate that if the electrical energy is produced by conventional combustion technology, then anywhere from one-third to one-half of the produced hydrogen would be consumed to keep the process going. Fletcher[3] has suggested that a high efficiency hydrogen-oxygen fuel cell could be connected in series with the electrolysis process to provide the required electrical power. He estimated that only a maximum of 20% of the hydrogen produced from the electrolysis would be consumed in order to supply the necessary electrical energy.

1.4 Summary

In this era of industrial and technological advances we are faced with the challenge of finding and developing new non-polluting energy resources. What has been overlooked for many years is that what appears to be a waste product can often turn out to be an energy source in itself, as in the case of hydrogen sulfide.

Hydrogen sulfide is obtained in large quantities as a naturally occurring contaminate in gaseous fuel as well as from the desulfurization processing of liquid and solid fossil fuel. At present, this hydrogen sulfide is disposed of utilizing the Claus process in which only the sulfur is recovered and the hydrogen content is effectively lost as water (see figure 1.4.1).

If industrial processes could be developed to recover both the sulfur and the hydrogen, the economic benefits would be substantial. The hydrogen recovered by such processes could either be used as a fuel itself or it could be recycled for further use in the desulfurization of fossil fuels, or both (see figure 1.4.2).

Presently, a number of approaches are being investigated to facilitate the decomposition of hydrogen sulfide into hydrogen and sulfur. Of these methods the electrolysis approach appears to be the most promising. It has the advantage of basic simplicity combined with flexibility of unit size and "cleanliness" of operation.

The electrolysis of liquid hydrogen sulfide has been reported by Landau[15]. From his data he concluded that the electrolysis is a

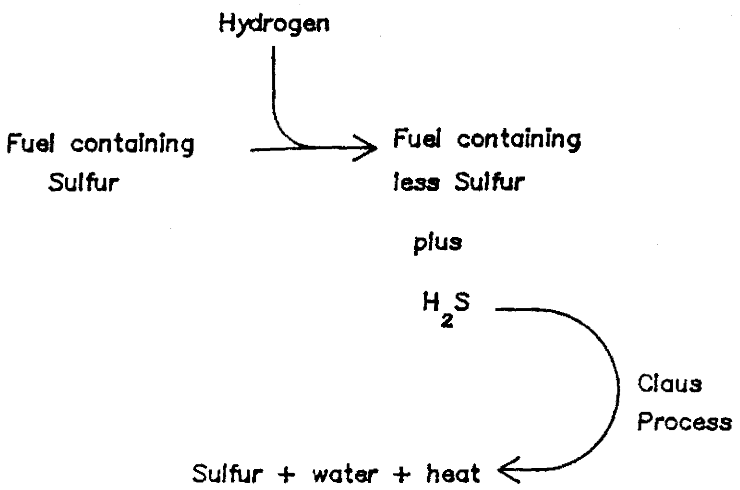

Figure 1.4.1:

At the present, most hydrogen sulfide obtained from fuel desulfurization is converted to elemental sulfur, water and low grade heat by the Claus Process. This process wastes the hydrogen content of the hydrogen sulfide.

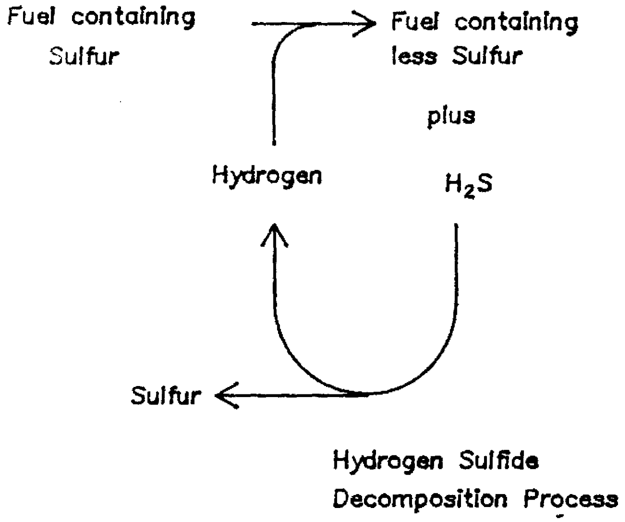

Figure 1.4.2:

Proposed hydrogen sulfide decomposition process would produce both hydrogen and sulfur.

very promising process if a few limitations could be resolved. Specifically, he pointed out the necessity for the development of electrodes with smaller over potentials and the need to increase the conductivity of the solution, if the electrochemical decomposition is to become a viable industrial process.

CHAPTER TWO

Properties of Hydrogen Sulfide

Chapter Two - Properties of H_2S

2.1 Molecular Structure

Structurally, hydrogen sulfide and water are similar in that they both exist as non-linear molecules with C_{2V} symmetry[19]. The bond angle in hydrogen sulfide varies to different degrees depending on physical state. In contrast to water, liquid hydrogen sulfide has a dihedral angle of almost 90 degrees, while water has a dihedral angle of just slightly less than 105 degrees. This would infer that the bonding of the hydrogen to the sulfur in hydrogen sulfide results from an almost pure p-p orbital interaction with very little orbital hybridization. In the water molecule, the bonding is a result of interactions of the hydrogen with a sp^3 hybridized orbital on the oxygen. This results in greater delocalization of the lone electrons on the oxygen atom and accounts for the high degree of hydrogen bonding which is present in water. In hydrogen sulfide such delocalization is not possible and is consistent with the observation that liquid hydrogen sulfide shows little tendency to hydrogen bond.

2.2 Physical Properties

This lack of hydrogen bonding primarily explains why hydrogen sulfide only exists as a liquid at atmospheric pressures over a narrow 25 degree temperature range, extending from -85.5C to -60.0C. This low boiling point is not a serious problem, since the liquid state can be extended up to the critical temperature of 100.4 C by the use of a pressure manifold. The vapour pressure between the boiling point and the critical temperature is estimated to fit equation (31)[19].

$$\log P = 8.370 - 1341.408\ T^{-1} - 0.012734\ T + 0.00001381\ T^{2} \qquad (31)$$

From this equation, it is estimated that the vapour pressure at 23C is approximately 19 atm (279 psi). This high vapour pressure coupled with its corrosive nature and extreme toxicity (see table 2.2.1) has severely limited the amount of research which has been carried out on liquid hydrogen sulfide. The majority of the work which has been done was carried out under atmospheric pressure at low temperatures (approx. -70C).

Table 2.2.1: Physiological Effects of Hydrogen Sulfide

Concentration of Hydrogen Sulfide in Air	Physiological Effect
0.05 ppm	-Detectable by odour, no health hazard
0.1 ppm	-Irritation to eyes and throat -Prolonged exposure causes sensory loss
50 ppm	-Complete sensory loss
>50 ppm	-Nausea, headaches, coughing, dizziness -Prolonged exposure may result in pulmonary edema.
500 ppm	-Immediate loss of consciousness -Depressed respiration -Death in 30-60 minutes

2.3 Solvent Properties

Liquid hydrogen sulfide is considered to be a protonated solvent in which the protons exist as H_3S^+ species (equation 32).

$$2H_2S \Longleftrightarrow H_3S^+ + HS^- \qquad (32)$$

$$K = [H_3S^+]\,[HS^-] / [H_2S]^2 = 25 \times 10^{-34} \qquad (33)$$

The equilibrium dissociation constant for this reaction is extremely low (equation 33) and has been estimated from conductivity data to be 25×10^{-34} at -78C[19].

Table 2.3.1 lists various solvent properties for liquid hydrogen sulfide, as well as the hydrides of neighbouring elements. In comparison to neighbouring hydrides, liquid hydrogen sulfide displays rather unique solvent properties. It possesses a small dielectric constant and dipole moment, while it displays a large molar volume and a high degree of polarizability. This low dipole moment coupled with the large molar volume would indicate that the tendency of polar compounds to dissolve in liquid hydrogen sulfide might be severely limited. However, due to the high degree of polarizability of the hydrogen sulfide molecule, polar materials such as acetone, ethyl ether, ethanol, carbon disulfide, and alkyl halides are all soluble to some degree. In general, many organic compounds are soluble in hydrogen sulfide while ionic compounds show very little tendency to dissolve, unless they contain large anions, such as ammonium alkylates.

Table 2.3.1: Solvent Properties of Various Hydrides[19]

Solvent	Dielectric Constant	Dipole Moment (esu)	Molar Volume (cm^3/mole)	Polarizability (cm^3)
HCl	8.85	1.03×10^{-18}	30.6	3.1×10^{-24}
H_2S	10.2	0.88×10^{-18}	35.9	3.82×10^{-24}
NH_3	22.0	1.50×10^{-18}	25.0	2.21×10^{-24}
H_2O	81.0	1.74×10^{-18}	18.8	1.475×10^{-24}
HF	83.6	2.00×10^{-18}	20.2	1.0×10^{-24}

The dielectric constant for hydrogen sulfide is substantially lower than that of water. This constant is a measure of the solvent's effect on coulombic interactions within the solution. The force of attraction or repulsion of two charged particles in a solvent can be expressed as a function of charge, separation and dielectric constant of the solvent, as illustrated by equation (34).

$$F = K\, Q_1 Q_2 / c\, R^2 \qquad (34)$$

Where F is the force between the charged particles

K is a constant

Q_i is charge on specific particle i

c is the dielectric constant

R is distance between the charged particles

As can be seen from the equation (34), the lower the dielectric constant, the greater the force of interaction between charged particles. This explains why ionic materials dissolve well in solvents of high dielectric constants, while they are insoluble in solvents of low dielectric constant.

2.4 Conductivity

There is some controversy in the literature as to the specific conductivity of liquid hydrogen sulfide. This discrepancy is due to the fact that at the time most of these experiments where conducted, it was not possible to obtain hydrogen sulfide commercially. Liquid hydrogen sulfide was produced on site by reacting dilute hydrochloric acid with ferrous sulfide. The produced gas then had to be purified and dried before subsequent use. The presence of even a small amount of water has been shown to result in a significant decrease in the conductivity.[20]

The best estimate of the conductivity of liquid hydrogen sulfide at -78C is in the range 10^{-9} to 10^{-11} ohm^{-1} cm^{-1}.[19,20,21,22,25] It has been assumed that this low conductivity value is the result of the small equilibrium constant for the dissociation reaction of hydrogen sulfide (equation 35 and 36).

$$2H_2S \Longleftrightarrow H_3S^+ + HS^- \qquad (35)$$

$$K = [H_3S^+]\ [HS^-]\ /\ [H_2S]^2 \qquad (36)$$

$$= 25 \times 10^{-34} \text{ at } -78C$$

The first reported conductivity measurements of liquid hydrogen sulfide near to room temperature were made by Landau[15]. He reported that the specific conductivity at 0C and 10C were 9.3×10^{-9} ohm^{-1} cm^{-1} and $1.8 \times 10^{-8} ohm^{-1}$ cm^{-1}, respectively. These values appear to be consistent with earlier values obtained at lower temperatures.[21]

One of the first studies of the conductivity of organic reagents dissolved in liquid hydrogen sulfide was carried out by Walker, McIntosh and Archibald in 1904[22]. They qualitatively examined the conductivity of some 80 organic materials in hydrogen sulfide, at -70C, and found that the conductivity increased significantly only in the case of pyridine, piperidine, nicotine and quinoline. This increase in conductivity was attributed to their basic nature. The conductivity was also observed to increase, but only slightly when acetonitrile was dissolved in the liquid hydrogen sulfide.

The first systematic investigation into the conductivity of liquid hydrogen sulfide was carried out by Quam and Wilkinson[23] in 1925. They found that the conductivity of hydrogen sulfide at -80C could be increased significantly by the addition of iodine. Iodine was observed to dissolve quickly, and to increase the specific conductivity of the solution from 10^{-11} to 1.36×10^{-5}. Quam and Wilkinson[23] agreed with the conclusion of Walden[24] that the liquid hydrogen sulfide acted as a inert solvent and this increase in conductivity was due to the subsequently dissociation of I_2 (equation 37).

$$I_2 \Longleftrightarrow I^+ + I^- \qquad (37)$$

Later studies by Lineken[25], however indicated that the hydrogen sulfide may not act as an inert solvent in this system, but may actually react with the iodine. He found that even though the iodine dissolved rapidly, the conductivity increased slowly with time indicating some slow chemical reaction maybe taking place. This was further supported by the presence of volatile iodine compounds in the hydrogen sulfide which was allowed to boil out of the conductivity cell. This evidence in itself is not conclusive, but later independent studies[26] have confirmed the existence of anions of the form HI_2^-. This adds additional support for the proposal that the hydrogen sulfide may actually interact with the iodine to form conductive species.

Quam and Wilkinson[23] also tried ammonium chloride and found it was insoluble in liquid hydrogen sulfide and had no effect on the conductivity. Substitution of methyl groups onto the ammonia, however, was found to increase the solubility and resulted in increased conductivity of the hydrogen sulfide solution. This increase in conductivity with increasing substitution is attributed to the effect of the bulky alkyl groups, which reduces the equilibrium constant of reaction (38).

$$NHX_3^+ + Cl^- \Longleftrightarrow NX_3 + HCl \qquad (38)$$

The forward reaction reduces the conductivity of the solution since HCl is a weak acid in a solvent of low dielectric solvent and therefore does not dissociate. This results in a subsequent loss of charge carriers thereby reducing the conductivity.

The investigation of various substituted ammonium chloride effects on conductivity of hydrogen sulfide was further extended by Lineken and Wilkinson[27] in 1940. They investigated the conductance effects of mono-, di-, tri-, and tetra-substituted methyl, ethyl and n-propylammonium chlorides. They found that conductance increased with the number and size of the substituted groups, and that the number of groups appeared to have a greater effect than size of the groups.

It was also observed that the molar conductivity as a function of concentration of these substituted alkyl ammonium chlorides initially decreased with increasing concentration until a minimum was reached. As the concentration was further increased the molar conductivity also increased. This behaviour was shown by Fuoss and Kraus to be typical of electrolytes in solvents of low dielectric constants,[28,29] where the possibility of triple ions formation exists (equation 39 through 41).

$$NX_4^+Cl^- \Longleftrightarrow NX_4^+ + Cl^- \qquad (39)$$

$$NX_4^+ + NX_4^+Cl^- \Longleftrightarrow NX_4^+Cl^-NX_4^+ \qquad (40)$$

$$Cl^- + NX_4^+Cl^- \Longleftrightarrow Cl^-NX_4^+Cl^- \qquad (41)$$

where X= $-H$, $-CH_3$, $-C_2H_5$, $-C_3H_7$

It is the formation of these triple ions (and ions complexes of higher number) which explains the observed change in conductivity with concentration.

In 1966, Cotton and Waddington[30] investigated the effect on the conductivity of various amines and phosphines (at -78C), as well as various substituted ammonium chloride compounds including their corresponding hydrogen sulfide adducts. These values are presented in table 2.4.1 along with corresponding values taken from earlier work carried out by Lineken[27]. From these results, they concluded that amines and phosphines are readily protonated in liquid hydrogen sulfide resulting in an observed increase in conductivity. They also

Table 2.4.1: Conductivity Data for Various Electrolytes in Liquid Hydrogen Sulfide at -78 C[25]

Compound	Concentration (moles/litre)	Specific Conductance ($10^{-6}ohm^{-1}cm^{-1}$)	Molar Conductance ($cm^2ohm^{-1}mole^{-1}$)
Me_3N	0.011	0.3	0.025
	0.104	10.4	0.100
	0.611	179.0	0.294
Et_3N	0.111	51.4	0.463
C_5H_5N	0.018	1.15	0.066
PH_3	0.101	0.068	0.001
Me_2PH	0.076	0.582	0.008
NH_3	saturated	0.020	-----
HCl	0.092	0.025	2.72×10^{-4}
HBr	0.169	0.138	8.17×10^{-4}
HI	0.31	0.53	17.1×10^{-4}
Me_4NSH	0.0150	33.0	2.2
	0.0782	68.3	8.7

Table 2.4.1: Cont'd

Compound	Concentration (moles/litre)	Specific Conductance ($10^{-6}ohm^{-1}cm^{-1}$)	Molar Conductance ($cm^2ohm^{-1}mole^{-1}$)
Et_4NSH	0.0128	79.0	6.2
	0.0245	173.0	7.1
	0.0521	740.0	14.2
	0.0620	999.0	16.1
Pr_4NSH	0.0184	171.0	9.3
	0.0265	301.0	11.4
	0.0851	1750.0	20.6
Me_4NCl	0.0577	129.0	2.23
	0.0578	149.0	2.58*
Et_4NCl	0.0317	194.0	6.1
	0.0670	697.0	10.4
	0.0268	63.2	2.66*
Pr_4NCl	0.0746	645.0	8.64*
	0.0685	728.0	10.62
Bu_4NCl	0.0380	194.0	5.1
Bu_4NI	0.0667	814.0	12.2

Note: * indicates values taken from reference 20 to compare with other values from reference 25 observed that the conductivity could be increased significantly more by the addition of hydrogen sulfide adducts of tetra-alkylammonium chloride than by the addition of the respective tetra-alkylammonium chloride.

They postulated that the increase in conductivity by the adducts was due to dissociation of these adducts in liquid hydrogen sulfide to yield hydrogen sulfide ions. This would suggest that the hydrogen sulfide ions must interact with solvent and perhaps some type of Grotthus mechanism maybe operative in the conduction process[30].

The first conductivity measurements at room temperature and elevated pressure where reported by Landau[15]. Their investigation focused on the possible electrolysis of liquid hydrogen sulfide at room temperature. Initially, pyridine was used as a supporting electrolyte and the electrolysis was observed to proceed with good current efficiency. However, they found that if the process was to be considered a industrially viable one, the conductivity of the solution must be significantly increased. Efforts were made to find a better electrolyte and several were tried. The values obtained for conductivity of the solution with the addition of pyridine and these other possible electrolytes is presented in table 2.4.2 . As can be seen from their results, their efforts to find a better electrolyte were unsuccessful.

Table 2.4.2: Conductivity Data Reported by Landau[15] for Liquid Hydrogen Sulfide

Solute	Temperature (degrees C)	Concentration (mole fraction)	Conductivity ($ohm^{-1}cm^{-1}$)
None	0		9.3×10^{-9}
None	10		1.8×10^{-8}
Pyridine	25	0.300	1.8×10^{-4}
Na_2S	0	0.057	4.5×10^{-8}
Mixture of			
Na_2S	0	0.001	1.4×10^{-9}
S		0.004	
CO_2		1.227	

2.5 Summary

The conductivity of liquid hydrogen sulfide has been shown to increase significantly with the addition of various amines, phosphines and alkyl substituted ammonium chlorides (see table 2.4.1). Even though the majority of the measurements were made at low temperatures it is reasonable to expect that the conductivity of liquid hydrogen sulfide at room temperatures would also increase with the presence of these compounds.

CHAPTER THREE

Research Goals

Chapter Three: Research Goals

3.1 Objectives

The electrochemical decomposition of hydrogen sulfide has had limited investigation, but appears to a promising process with a number of significant advantages. It is apparent, however, from Landau's[15,16] work that before any development of an industrially viable electrolysis process can proceed, it is necessary to carry out a fundamental study of the electrical conductivity of liquid hydrogen sulfide with the addition of electrolytes. Specifically, the following research goals were defined:

(1) Construction and testing of a pressure manifold and conductivity cell which will allow the safe handling and disposal of liquid hydrogen sulfide at room temperatures.

(2) Selection of a series of possible electrolytes based upon available information from the literature.

(3) Determination of the conductivity of liquid hydrogen sulfide with and without addition of the possible electrolytes. The primary goal is to find a electrolyte which will increase the conductivity of liquid hydrogen sulfide to the point where it becomes feasible to consider the electrolytic decomposition of H_2S as a possible industrial process.

CHAPTER FOUR

Experimental Details

Chapter Four - Experimental Details

4.1 Pressure Manifold:

A pressure manifold for the direct delivery of liquid hydrogen sulfide to the conductivity cell was constructed as shown in figure 4.1.1 . The material of construction of all connecting tubing and swagelok joints was nylon, which is pressure rated to 1000 psi. Stainless steel inserts were placed into the ends of the nylon tubing at the joints to allow safe operation at the required pressure. The valves were all of stainless steel construction and were lubricated with a mixture of graphite and silicone grease to prevent them from seizing.

The manifold was pressure tested up to at least 450 psi before each run. The pressure was then monitored as a function of time by a pressure gauge and a closed loop manometer. This step was necessary to evaluate the safety of the manifold and to reduce the possible risk of line ruptures.

At the conclusion of each run the pressure manifold was vented directly to a cold trap and subsequently to a flame, where the exhaust was thermally combusted (see figure 4.1.2). A vacuum pump was connected in parallel to permit evacuation of the manifold. An emergency pressure release loop was also built into the manifold. This closed loop consisted of 100 feet of the nylon tubing which could be used to relieve pressure in the manifold should the necessity arise.

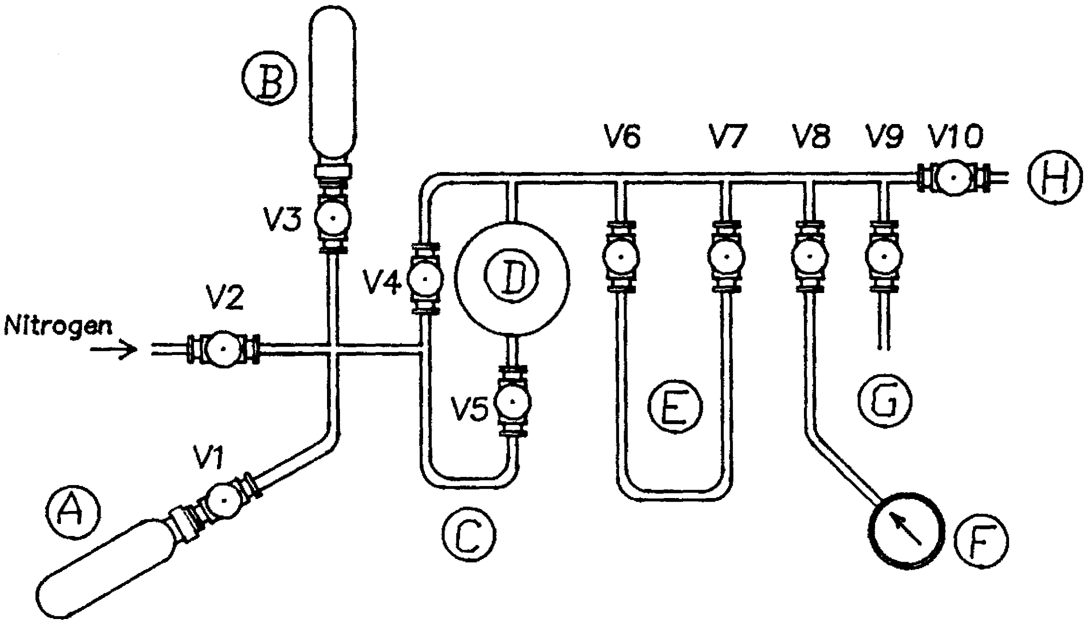

Figure 4.1.1: Pressure Manifold for Measuring the Conductivity of Liquid Hydrogen Sulfide at Room Temperature

Legend

V1–V10: Stainless Steel Valves
A: Tank A
B: Tank B
C: Sample Loop
D: Conductivity Cell
E: Closed Loop Manometer
F: Pressure Gauge
G: Emergency Pressure Release Loop
H: To Disposal Unit

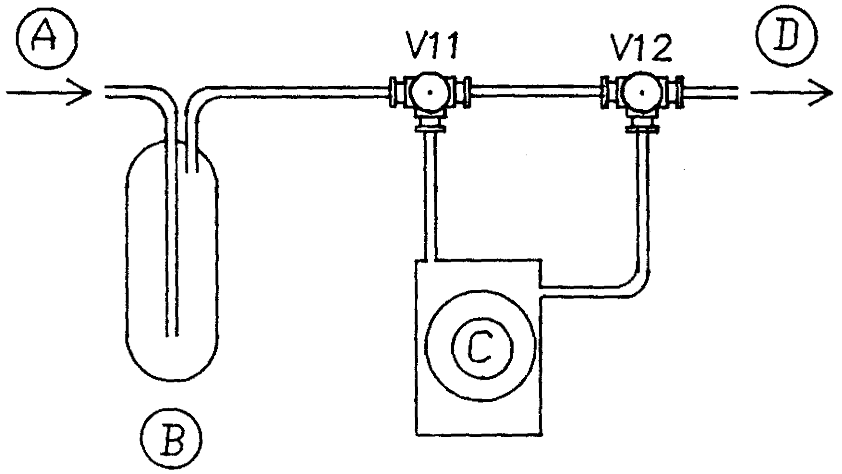

Figure 4.1.2: Thermal Disposal Unit For The Exhaust From The Pressure Manifold

Legend:

V11–V12: Three–way Valves
A: From Pressure Manifold
B: Cold Trap
C: Vacuum Pump
D: To The Flame

4.2 Isolation Chamber:

Due to the toxic nature of hydrogen sulfide and the relatively large quantity used in this experiment, it was deemed necessary to isolate the pressure manifold from the laboratory. To this end, it was mounted in a fume hood fitted with sliding plexiglas windows. Manipulation of the manifold was gained through the use of dry box gloves which were mounted on plexiglas rings, which were fitted into circular openings in the sliding windows. The manifold was connected to a thermal disposal unit located in an adjacent fume hood.

4.3 Conductivity Cell:

The conductivity cell consisted of two 3.81 cm diameter platinum electrodes embedded in the ends of a teflon cavity with a separation of .5 cm (see figure 4.3.1). The teflon cavity was contained within a stainless steel jacket which allowed safe operation at the necessary pressures. O-rings were used throughout the stainless assembly to provide a seal between the pressure plates and the external body. Liquid hydrogen sulfide entered the cell from the bottom through a small orifice and the excess was allowed to flow out through a similar orifice in the top of the cell.

Electrical connection with the electrodes was achieved by silver soldering a platinum rod to the back of the platinum electrode. This platinum rod passed through the teflon cup, an O-ring, and the pressure plate. A stainless steel rod was soldered to the end of this rod and passed through the steel end cap of the cell, where electrical connection was made to conductivity bridge.

The cell constant was determined with a .001M solution of KCl as outlined in Appendix A.

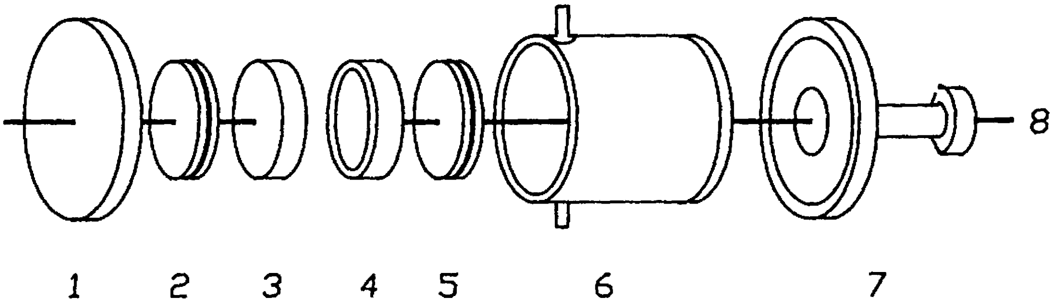

Figure 4.3.1: Expanded View of
the Conductivity Cell

Legend:

(1) End Cap
(2) Pressure Plate with O-rings
(3) & (4) Teflon Cup with Electrodes
(5) Pressure Plate with O-rings
(6) Stainless Steel Body
(7) End Cap with Pressure Spindle
(8) Contact Rod

4.4 Conductivity Measurements:

Conductivity measurements were made utilizing both DC and AC techniques (see appendix B for details) where possible. As outlined by Shedlovsky,[31] DC conductivity measurements are only possible with solutions which exhibit low conductivity. In solutions of higher conductivity polarization occurs instantaneously, resulting in lower than actual conductivity values.

AC measurements were obtained at a frequency of 3 KC using a "Industrial Instruments" conductivity bridge. This bridge allowed direct balancing up to a maximum of 99,999.9 ohms. Resistances of higher magnitude were obtained by using a shunt in parallel with the bridge. The total measured resistance can then be related to the resistance of the cell by equation (42).

$$R_T^{-1} = R_S^{-1} + R_C^{-1} \qquad (42)$$

where R_T is the total measured resistance

R_S is the known resistance of the shunt

R_C is the unknown resistance of the cell

DC measurements were made using a Model 4410 Beckman 4-1/2 digit multimeter. As can be seen from the simplified block diagram (see figure 4.4.1) the heart of the multimeter is an analog to digital converter. Multimeters measure resistance by a ratio technique, where an unknown resistance is compared to an internal standard resistance.

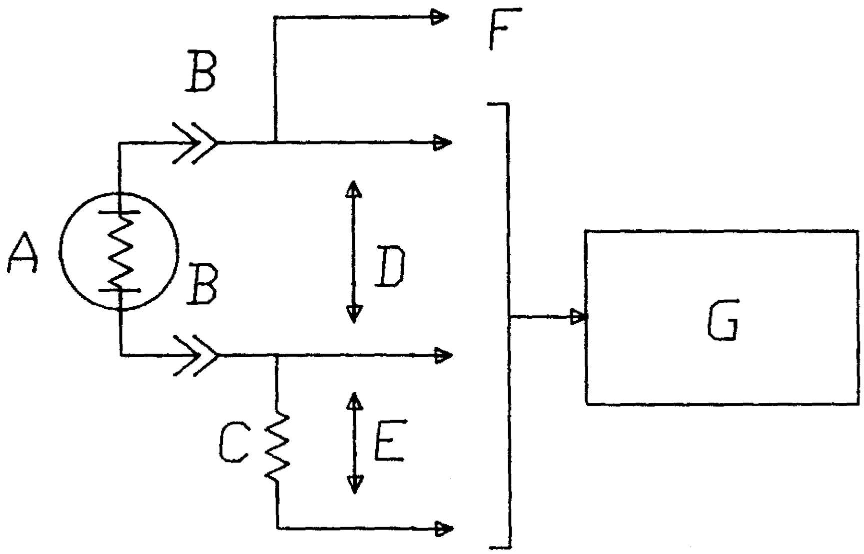

Figure 4.4.1: Simplified Block Diagram of Conductivity Cell and Multimeter

Legend:

A: Conductivity Cell
B: Multimeter Inputs
C: A Standard Reference Resistor
D: Voltage Drop Across the Cell
E: Voltage Drop Across Reference Resistor
F: Current Source (battery)
G: A/D Converter

As shown in the block diagram, the cell is connected in series with a selected standard resistance and a current source. Since there is negligible loading at the sensing terminals of the A/D converter, the ratio of the two resistors is equal to the ratio of their respective voltage drops. Because of this fact, the A/D converter then uses a ratiometric conversion technique which is based solely on the ratio of the unknown voltage to the reference voltage, thereby determining the unknown resistance of the cell. This particular multimeter has a accuracy rating of approximately 0.3% over the measured resistance range.

4.5 Reagents:

Certified pure (99.5% pure) hydrogen sulfide was obtained from Matheson Gas Products Canada and was used without further treatment. The following six possible electrolytes were obtained from Aldrich and were also used without further purification:*

(1) acetonitrile

(2) N-methyl pyridone

(3) pyridine

(4) N-methyl piperdine

(5) 1-methyldiethanol amine

(6) tetrapropylammonium iodide

* For physical properties of these reagents consult appendix C.

4.6 Experimental Procedure:

An overview of the experimental procedure is presented in the following section, for the detailed procedure consult Appendix D.

The desired amount of electrolyte was placed in the bottom of the sample loop (see figure 4.1.1). The manifold was subsequently flushed with ultra-pure nitrogen and evacuated. The gaseous hydrogen sulfide was allowed to enter the manifold from tank A. When the pressure in the manifold was equal to that in tank A, the valve was closed. Liquid hydrogen sulfide was then introduced into the manifold from tank B. At this point the valve below the cell was still closed. The liquid hydrogen sulfide was allowed to come into contact with the electrolyte and the resulting solution was observed for any physical change (eg. change in colour). After sufficient time was allowed for mixing and reacting, the valve below the cell was opened and the solution was forced into the conductivity cell. The valve was then closed and the appropriate AC or DC conductivity measurements were made, as outlined in Appendix D.

After the measurements were complete, the exit valve was opened and the hydrogen sulfide was vented through the cold trap and subsequently to a flame where it was thermally decomposed (see figure 4.1.2). The manifold was subsequently evacuated and flushed with nitrogen several times to remove any remaining hydrogen sulfide. The cell and manifold were then disassembled and cleaned for the next run.

CHAPTER FIVE

Results and Discussion

Chapter Five - Results and Discussion:

5.1 Pressure Manifold

Due to the physical properties of liquid hydrogen sulfide a pressure manifold had to be constructed to allow the measurement of the conductivity of liquid hydrogen sulfide solution at room temperatures. The manifold which was developed had the following features:

(1) All parts, with the exception of the stainless steel valves, were constructed of nylon which had a bursting pressure of 1000 psi. These materials were necessary due to the corrosive nature and high vapour pressure of liquid hydrogen sulfide at room temperature. The manifold could withstand internal pressures in excess of 450 psi. This was achieved by the use of stainless steel inserts in the nylon tubing at the connection joints.

(2) Waste liquid hydrogen sulfide was disposed of by venting to a cold trap and then to a flame. In the flame, the hydrogen sulfide was converted to sulfur dioxide and vented to the atmosphere.

(3) Liquid hydrogen sulfide was introduced into the cell at room temperature. This is contrast to all previously reported conductivity studies in which the hydrogen sulfide was condensed into the cell at low temperatures (-70C) using a dry ice/ether mixture.

(4) A sample loop was present which allow direct observation of the

interaction between the electrolyte and the solvent.

(5) Pressure in the manifold was monitored by an pressure gauge and a closed loop manometer.

(6) An emergency pressure release loop was present to allow the release of pressure from the manifold should the need arise.

5.2 Conductivity of Liquid Hydrogen Sulfide

The conductivity of pure liquid hydrogen sulfide was determined periodically throughout the course of the experiments. This was done to ensure that no contamination of the tubing occurred from the successive runs. Though the conductivity did fluctuate, as shown in table 5.2.1, the results were all of the same magnitude and did not drift in a systematic manner.

The conductivity of liquid hydrogen sulfide at 23C was determined to be approximately $7.00 \times 10^{-8} \text{ohm}^{-1}\text{cm}^{-1}$, which compares favourably with values reported by Landau[15]; $9.3 \times 10^{-9} \text{ohm}^{-1}\text{cm}^{-1}$ at 0C and $1.8 \times 10^{-8} \text{ohm}^{-1}\text{cm}^{-1}$ at 10C. This low conductivity is attributed to the low equilibrium constant for the dissociation of hydrogen sulfide.

From conductivity studies conducted at low temperatures it is apparent that most organic reagents that dissolve in liquid hydrogen sulfide do not increase the conductivity of the resulting solution. It has been shown, however, that amines, nitriles, aldehydes and ketones do react with liquid hydrogen sulfide and produce solutions that exhibit increased conductivity. Most ionic materials are insoluble in liquid hydrogen sulfide due to the low dielectric constant, but ionic compounds with low lattice energy, such as alkylammonium halides, have been found to be soluble and result in strongly conducting solutions.

With these facts in mind, the following reagents were chosen to be tested as possible electrolytes to increase the conductivity of liquid hydrogen sulfide:

Table 5.2.1: Conductivity Data for Liquid Hydrogen Sulfide at 23C

Electrolyte	Concentration moles/litre (mole fraction)	Specific Conductivity $ohm^{-1}cm^{-1}$	Molar Conductance $cm^2ohm^{-1}mole^{-1}$
None		7.26 X 10^{-8}	
		6.52 X 10^{-8}	
		6.94 X 10^{-8}	
Acetonitrile	0.636	1.84 X 10^{-7}(DC)	2.89 X 10^{-4}
	(.027)		
1-methyl-2-pyridone	0.1678	7.82 X 10^{-7}(DC)	4.66 X 10^{-3}
	(.00715)	7.56 X 10^{-7}(AC)	4.51 X 10^{-3}
Pyridine	0.2207	7.83 X 10^{-7}(DC)	3.55 X 10^{-3}
	(.0094)	7.61 X 10^{-7}(AC)	3.45 X 10^{-3}
1-methyl piperdine	0.2746	3.15 X 10^{-5}(DC)	1.15 X 10^{-1}
	(.01253)	2.91 X 10^{-5}(AC)	1.06 X 10^{-1}
1-methyldiethanol amine	0.1564	1.98 X 10^{-7}(DC)	1.27 X 10^{-3}
	(.0067)		
tetrapropyl-ammonium iodide	0.3826	9.84 X 10^{-3}(AC)	2.57 X 10^{1}
	(.0175)		
	0.4034	1.13 X 10^{-2}(AC)	2.80 X 10^{1}
	(.0184)		

(1) acetonitrile

(2) N-methyl pyridone

(3) pyridine

(4) N-methyl piperdine

(5) 1-methyldiethanol amine

(6) tetrapropylammonium iodide

* For physical properties of these reagent consult appendix C.

Using these reagents, the conductivity measurements were made and the results are reported in table 5.2.1 .

5.2.1 Acetonitrile:

Acetonitrile, dissolved in liquid hydrogen sulfide, was found to increase the conductivity only slightly to about 1.84 X 10^{-7} ohm^{-1} cm^{-1}, even through the acetonitrile did react with the solvent.

Upon exposure to hydrogen sulfide the acetonitrile was observed to expand in volume. This is consistent with the known reaction of between nitriles and hydrogen sulfide.[19] Initially, hydrogen sulfide adds across the triple bond in the nitrile yielding the corresponding addition product (equation 43).

$$CH_3CN + H_2S \text{ ---> } CH_3\text{-}CS\text{-}NH_2 \qquad (43)$$

Proton loss does not occur since the amino nitrogen is less positive in liquid hydrogen sulfide than in the corresponding aqueous system. At room temperature, under the slightly acidic condition present in liquid hydrogen sulfide, this addition product undergoes thiohydrolysis quickly (equation 44).

$$CH_3\text{-}CS\text{-}NH_2 + H_2S \text{ <===> } CH_3\text{-}CS\text{-}NH_3^+ + HS^- \qquad (44)$$

It is this thiohydrolysis product which results in the formation of current carrying species. Apparently, from the low conductivity valves obtained, the reaction either has a low equilibrium constant or the produced ions must have limited mobility in the resulting solution.

5.2.2 Amines:

It has been suggested by Cotton and Waddington[30] that amines increase the conductivity of liquid hydrogen sulfide by undergoing an acid-base reaction with the solvent, whereby the amine abstracts a proton from the hydrogen sulfide (equation 45). The ions produced by this reaction have the effect of increasing the conductivity of the solution.

$$R_3N + H_2S \Longleftrightarrow R_3NH^+ + HS^- \qquad (45)$$

In our investigation, the conductivity of hydrogen sulfide was measured with the addition of pyridine, as well as a derivative of pyridine: N-methyl pyridone. These two possible electrolytes were chosen for a number of reasons:

(1) Pyridine was chosen because the conductivity of hydrogen sulfide/pyridine solutions have been measured at room temperature and are reported in the literature by Landau[15].

(2) N-methyl pyridone was chosen because of its similarity to pyridine and less less toxic nature. Comparison between this derivative and pyridine might also provide information concerning the effect of the presence of functional groups on the conductive process.

The conductivity observed for pyridine and N-methyl pyridone dissolved in hydrogen sulfide was determined to be virtually the same: approximately $7.75 \times 10^{-7} ohm^{-1} cm^{-1}$. Landau[15] reported that the conductivity of hydrogen sulfide containing pyridine increased to a maximum with increasing concentration. He found that the conductivity reached a maximum of $1.81 \times 10^{-4} ohm^{-1} cm^{-1}$ at a .3 mole fraction of pyridine.

Landau's solutions were approximately 300 times more concentrated than the one used in this experiment. His reported conductivity value is also approximately 300 times greater than was observed for our solution. If we assume that the increase in conductivity is a result of a quick acid-base reaction which virtually goes to completion and that the ions so produced do not interact, then we can conclude that our conductivity data is consistent with that of Landau.

This statement can be made since conductivity is actually a measurement of the number of charge carriers in the system. If the number of charge carriers is double, then the conductivity also doubles. This is assuming there is no interaction between the ions at higher concentration and that the mobility of these ions is not significantly changed due to concentration changes.

One advantage of our experimental design was the possibility to observe the interact between the test electrolytes and the liquid hydrogen sulfide outside of the conductivity cell. In the case of pyridine, as well as N-methyl pyridone, the amine was observed to expand in volume slightly upon the exposure to gaseous hydrogen sulfide. However, upon the introduction of liquid hydrogen sulfide, it was found that the solute in the sample loop was immiscible with the solvent stream. Subsequently, when the solution was forced into the conductivity cell, a large plug of solute was observed to settle out, due to its higher density. Regardless of the absence of pyridine in the cell, the conductivity was significantly increased. It maybe possible that as the hydrogen sulfide stream passed over and through the amine plug the acid-base reaction occurred with the sulfide ions travelling along with the solvent stream while the pyridium ions remained behind. This may infer that the sulfide ions play a much more important role in the conductive process than the pyridium ion.

The observation that pyridine and N-methyl pyridone gave rise to similar conductivity measurements at similar concentration would infer that the presence of additional functional groups (at least ketones) have very little effect on the conductivity.

Another amine which was chosen as a possible electrolyte due to the significant promise it has shown in hydrogen sulfide scrubbing systems[32] was 1-methyldiethanolamine. Upon exposure to gaseous hydrogen sulfide, the reddish-brown colour of the amine faded quickly and the volume was observed to increase slightly. These observations are consistent with the fact that this specific amine is known to react quickly with hydrogen sulfide. However, upon introduction of the liquid hydrogen sulfide, it was found that the amine was immiscible with the solvent stream. When the solution in the sample loop was forced into the conductivity cell the amine settled back into the sample loop. The resulting conductivity of the solution was observed to be $1.98 \times 10^{-7} ohm^{-1} cm^{-1}$, only slightly higher than that observed for pure liquid hydrogen sulfide. This low conductivity value may reflect that even though the hydrogen sulfide reacted with the amine, the products formed may not have diffused significantly into the solvent stream. This could be due to possibility of hydrogen bonding between the alcohol groups on the amine and the sulfide ions produced in the acid-base reaction.

Of the four amines which were tested, N-methyl piperdine was observed to give rise to the highest conductivity value: 3.00×10^{-5} $ohm^{-1}cm^{-1}$. Physically, this amine reacted with the gaseous hydrogen sulfide in the same manner as pyridine. However, upon introduction of the liquid hydrogen sulfide, the amine was observed to diffuse quickly into the solvent stream and did not settle back into the sample loop after the conductivity cell was loaded. This increased conductivity is attributed to ions which are formed in the acid-base reaction with the solvent (equation 45). The conductivity was much higher than that observed for pyridine. This is probably due to the fact that this amine did diffuse easily into the solvent, showing a high degree of mobility.

5.3 Alkylammonium Halide:

Previous conductivity data from the literature indicated that the conductivity of hydrogen sulfide could be significantly increased by the presence of alkylammonium halides. The conductivity and solubility was determined to increase with increasing substitution on the ammonium center. Cotton and Waddington[30] found that the hydrogen sulfide adducts of these corresponding alkylammonium halides displayed even higher conductivity in liquid hydrogen sulfide.

With these facts in mind, it was proposed to test tetrapropylammonium iodide as a possible electrolyte, due to its high degree of substitution. Upon exposing the solid to gaseous hydrogen sulfide, it was observed to absorb hydrogen sulfide rapidly forming a clear liquid layer over what appeared to be crystalline ionic material. Contact with liquid hydrogen sulfide immediately caused further dissolution of the ionic material even though the two solution were immiscible. A further half hour was required before all of the ionic material in the loop dissolved. The sample was then forced into the conductivity cell, with no indication of any material settling back into the sample loop. Apparently, this was due to the similar densities of the solute and solvent.

The conductivity of the resulting solution were extremely high, $1.1 \times 10^{-2} ohm^{-1} cm^{-1}$ (see table 5.2.1), but were consistent with values obtained by Cotton and Waddington[29] for tetrapropylammonium hydrogen sulfide at -78C. This would infer that the reaction between the gaseous hydrogen sulfide and tetrapropyl-ammonium iodide probably produced the corresponding hydrogen sulfide adduct. It has been proposed by Cotton and Waddington that this increase in conductivity maybe the result of the hydrogen sulfide adduct acting as a sulfide donour. In our case, it is also possible that the I^- counter ion may also have played a role in the conductive process.

CHAPTER SIX

Summary and Conclusions

Chapter Six - Summary and Conclusions:

6.1 Summary

The conductivity of liquid hydrogen sulfide at 23 C was determined to be 7.00 X 10^{-8}ohm^{-1}cm^{-1}, which is consistent with values determined by Landau[15]. An increase in conductivity was observed in every case upon addition of test electrolytes (see table 5.2.1). This conductivity increase was a result of a variety of reactions between the different solutes and the solvent.

Acetonitrile reacted with the solvent to form an addition product which quickly underwent thiohydrolysis to produce the corresponding thioacid. The resulting conductivity was only slightly higher than the neat solvent reflecting the fact that either the reaction has a low equilibrium constant or the ions produced have a limited mobility in the solvent.

The amines which were tested as possible electrolytes were also observed to undergo reaction with the solvent. It has been suggested by Cotton and Waddington[30], that amines react via an acid-base reaction (equation 45) to produce sulfide ions and the corresponding protonated amine. The observed conductivity was the greatest when n-methyl piperdine was added to the hydrogen sulfide solvent stream. The major difference between this amine and the others tested was that it diffused into the solvent stream quickly. It is possible that the other amines may prove to be effective in increasing the conductivity, if they were used as solvents into which hydrogen sulfide could be dissolved.

The best conductivity values were obtained when tetrapropyl ammonium iodide was added to the hydrogen sulfide. The low lattice energy of this electrolyte resulted in an extensive reaction between the solute and gaseous hydrogen sulfide to produce the corresponding hydrogen sulfide adduct. As Cotton and Waddington found[30], the adducts of these alkyl ammonium halides increased the conductivity significantly. They concluded that the increase in conductivity was a result of the adduct acting as a sulfide ion donour in the resulting solution. The ease of diffusion of the adduct into the solvent stream also reinforces the notion that the ions produced by the reaction of the solvent with the solute are highly mobile in the resulting solution.

6.2 Conclusions:

It has been suggested by Landau[16], that electro-decomposition of hydrogen sulfide could be considered a viable alternative to the Claus process, if the solution conductivity could be increased to approximately $10^{-2}\text{ohm}^{-1}\text{cm}^{-1}$. His attempts to find a suitable electrolyte were unsuccessful and it was the primary goal of this study to evaluate possible electrolytes so as to determine if the further investigation of the electrolysis of hydrogen sulfide as a industrial process is warranted.

The data obtained in this study indicates that of all the electrolytes tested, tetrapropylammonium iodide was the only one to increase the conductivity of the solution to desired level as prescribed by Landau[16]. The conductivity increase due to the presence of alkyl ammonium halides is attributed to the formation of the hydrogen sulfide adduct which subsequently acts as a sulfide ion donours in the solvent, thereby increasing the observed conductivity.

Now that a suitable electrolyte has been found, further investigation of the electrolysis process is warranted to determine if the electrolytic decomposition of hydrogen sulfide is a possible route to a viable industrial process which would produce both hydrogen and sulfur.

References:

(1) Bubenick, D.V.; "Acid Rain Information Book", Second Edition, Noyes Publication, USA., 1984.

(2) Hahm, A.V.; "The Petrochemical Industry", McGraw-Hill Publications, New York, 1970.

(3) Fletcher, E.A., Energy, 8(11), 835(1983).

(4) Pickett, C.F., J. Phys. Chem., 31, 1212(1927).

(5) Raymont, M.E.D.; "Hydrogen Production and Marketing",ACS Symposium, 116, 335(1980).

(6) Raymont, M.E.D., Hydrocarbon Processing, 54(7), pp 139-142(1975).

(7) Chivers, T., Hyne, J.B., and Lau, C., Int. J. Hydrogen Energy, 5, 499(1980).

(8) Kotera, Y., Int. J. Hydrogen Energy, 1, 219(1976).

(9) Kameyama, T., Dodiya, M., Fukuda, K., and Kotera, Y., Separation Sci and Tech., 14, 953(1979).

(10) Kiuchi, H., Iwasaki, T., Nakamura, I., and Tanaka, T.,"Hydrogen Production and Marketing", ACS Symposium Series, 116, 349(1980).

(11) Dokiya, M., Fukuda, K., Yokokawa, H., and, Kammayamma, K., Bull. Chem. Soc. Japan, 51, 150(1978).

(12) Kalina, D.W., and Maas Jr., E.T., Int. J. Hydrogen Energy, Vol. 3(3), 157(1985).

(13) Kalina, D.W., and Maas Jr., E.T., Int. J. Hydrogen Energy, Vol. 3(3), 163(1985).

(14) Prosser, D., M.Sc. Thesis, McMaster University, Hamilton, Canada (In Preparation).

(15) Landau, U., J. Applied Electrochem., 10, 405(1980).

(16) Landau, U., NTIS Report, Aug.(1979).

(17) Lim, H.S., and Winnick, J., J. Electrochem. Soc., 131(3), 562(1984).

(18) Hepler and Hileman Jr., O.E., Research Proposal to AOSTRA, Edmonton, Alberta, Canada(1984).

(19) Feher, F., "The Chemistry of Non-Aqueous Solvents", Vol. 3, Chapter 4 (1976).

(20) Wilkinson, J.A., Chem. Rev. 8, 237(1931).

(21) Satwalekar, S.D., Butler, L.W., and Wilkinson, J.A., J. Am. Chem. Soc. 52, 3045(1930).

(22) Walker, J.W., McIntosh, D., and Archibald, E., J. Chem Soc., 85, 1098(1904).

(23) Quam, G.N., and Wilkinson, J.A., J. Am. Chem. Soc. 47, 989(1925).

(24) Walden, Z., Physik. Chem. 43, 385(1903).

(25) Lineken, E.E., J. Am. Chem. Soc. 68, 1966(1946).

(26) Harmon, K.M., and Gebauer, P.A., Inorg. Chem., 2, 1319(1963).

(27) Lineken, E.E., and Wilkinson, J.A., J. Am. Chem. Soc. 62, 251(1940).

(28) Kraus, C.A., and Fuoss, R.M., J. Amer. Chem. Soc. 55, 21(1933).

(29) Kraus, C.A., and Fuoss, R.M., J. Amer. Chem. Soc. 55, 2387(1933).

(30) Cotton, J.D., and Waddington, T.C., J. Chem. Soc.(A), 785(1966).

(31) Weissberger and Rossiter, "Physical Methods of Chemistry; Part IIA: Electrochemical Method", Vol. 1, chapter III (1971).

(32) Jou, F., and Otto, F.D., Ind. Eng. Chem Process Des. Dev.,21, 539-544(1982).

APPENDICES

Appendix A: Determination of Cell Constant

A cell constant had to be determined to allow the calculation of specific conductivity from resistance measurements. This was achieved by calibrating the cell using a solution of known specific conductivity. A .001M KCl solution was prepared and the resistance of this solution in the conductivity cell was measured using the AC conductivity bridge. The specific conductivity of this KCl solution is known to 0.0014836 $ohm^{-1}cm^{-1}$ at 25C. The cell constant can be determined by substitution into the following expression given the measured resistance of the .001 M KCl solution in the cell.

$k = C / R$ where k = the specific conductance
C = the cell constant
R = the measured resistance in ohms

Using this expression and the measured resistance values it was calculated that the cell constant for this cell was 0.0415408 cm^{-1}. This value was taken to be the cell constant throughout the course of the experiments.

The cell constant can also be obtained by direct measurement of the electrodes and the separation between them. This method is not very exact due to limitations in measuring the various components of the cell. However, it is useful to verify the magnitude of the cell constant. The cell constant, effective area of the electrodes and there separation are related by the following equation:

$C = L / A$ where C is the cell constant

L is the separation of the electrodes

A is the area of the electrode

For the cell used in this experiments, it was determined that the electrode have a area of 11.4 cm^2 and a separation of .5 cm. Substitution of these values into the above equation gives a cell constant of 0.0438596 cm^{-1}. This value is in good agreement with the value obtained from measuring the conductivity of the .001M KCl solution.

Appendix B: Conductivity Measurements

Conductivity of the hydrogen sulfide solutions were determined by measuring the resistance of the solutions by DC and AC techniques. The DC technique had the advantage of being much quicker than the AC technique. To relate these resistance measurements to specific conductivity it was necessary to determine a cell constant for the conductivity cell as outlined in appendix A.

The use of the DC method was restricted to measuring the resistance of the solutions which displayed high resistance. In solutions of low resistance, polarization with the DC method occurs instantaneously resulting in higher than actual resistance measurements. For this reason, all resistance measurements were initially made utilizing the DC method and were then confirmed using AC conductivity bridge.

This AC conductivity bridge allowed the direct balancing of resistance up to 50 kilo-ohms. Resistance values higher than this were determined by using a resistor of known value in parallel with the conductivity cell. The resistance of the cell could then related to the total observed resistance and the resistance of the shunt.

B1.1 Procedure for DC Measurements:

Once the cell was filled with the hydrogen sulfide solution, the multimeter was connected to the terminals of the conductivity cell. In between the multimeter and the cell was a contact switch which allowed the momentary contact between the cell and meter. This switch also allowed the polarity of the electrodes to be changed between successive measurements.

The actual measurements were determined by momentarily providing contact between the cell and meter. The first reading from the meter was taken, as the reading were observed to increase with time due to polarization. The contact was then immediately broken and the polarity of the electrode was reversed before taking another reading. This procedure was repeated several time to obtain a set of resistance measurements.

After the DC measurements were made, AC resistance measurements were determined as outlined in the next section.

B1.2 AC Measurements:

Once the DC measurements were complete, the AC conductivity bridge was connected to the terminals of the cell. A shunt of known resistance was placed in parallel with cell if the resistance measurements obtained from the DC method were high. The resistance of the cell was then determined at a frequency of 3 kilocycles.

Appendix C: Selected Physical Properties of the Test Electrolytes:

C1.1 Acetonitrile: CH_3CN

formula weight: 41.05
specific gravity: 0.783
melting point: -41 C
boiling point: 82 C
flash point: 42 F

Other properties: Soluble in water and alcohol,
Flammable liquid,high polarity,
high dielectric constant

C1.2 N-methyldiethanol amine: $CH_3N(C_2H_4OH)_2$

formula weight: 119.16
specific gravity: 1.0418 (20 C)
melting point: -21.0 C
boiling point: 247.2 C
flash point: 260 F

Other properties: irritant, low toxicity, combustible

C1.3 1-methyl-2-pyridone: $(C_5H_4ON)CH_3$

formula weight: 109.13
specific gravity: 1.027
melting point: -24 C
boiling point: 202 C
flash point: 204 F

Other properties: Soluble in water, various organic solvents,
and castor oil
Combustible

C1.4 1-methyl piperidine: $(C_4H_4N)CH_3$

formula weight: 99.18
specific gravity: 0.816
boiling point: 106-107 C
flash point: 38 F

Other Properties: irritant, flammable liquid

C1.5 Tetrapropylammonium Iodide: $(CH_3CH_2CH_2)_4NI$

formula weight: 313.27
melting point: 283 C

Other Properties: irritant, hygroscopic

Appendix D: Operation Procedures

Note: Refer to figure 4.1.1 and 4.1.2 for notation used in the following sections.

D1.1 Pressure Testing

(1) The desired amount of electrolyte was placed in the sample loop,

(2) initially V1,V2,V3,V9 and V10 are closed
and V4,V5,V6,V7 and V8 are open
and V11,V12 are switched to the flame position
and the two hydrogen sulfide cylinders are attached but still closed,

(3) V2 is opened and the manifold is pressurized with high purity nitrogen,

(4) V2,V6 are then closed (in that order),

(5) the pressure change is monitored by observing the closed loop manometer and the pressure gauge,

(6) if the rate of the pressure drop is acceptable, then V6 is opened,

(7) open V1,V3 and Close V6; this step is necessary to pressure test the cylinder connections,

(8) once again, the pressure change is monitored,

(9) if the pressure drop is acceptable, then V6 is opened,

(10) check emergency pressure release loop by opening V9,

(11) V2 is opened and the pressure increased to the desired level,

(12) close V2 and close V6,

(13) the pressure drop is monitored; if acceptable, then V6 is opened

(14) at this point the manifold has passed the pressure test.

D1.2 Loading the Manifold with Hydrogen Sulfide:

(1) open V10 and release the nitrogen into exhaust system,

(2) close V8 and V9

(3) switch V11 and V12 to the vacuum pump position and reduce pressure of manifold using vacuum pump,

(4) then close V10, V1 and V3,

(5) fill cold trap with a dry ice/ethanol mixture and have a supply of liquid nitrogen on hand in the fumehood with the manifold,

(6) switch V11 and V12 to flame position and ignite the flame,

(7) open tank A,

(8) open V1 and allow the manifold to come up to the vapour pressure of H_2S,

(9)open V8,

(10) observe electrolyte for any physical change,

(11) close V4 and V5, thereby isolating sample loop from the rest of the manifold,

(12) open tank B,

(13) open V3,

(14) at this point liquid hydrogen sulfide should flow into the manifold. If this does not occur then open V10 and V4 repeatedly to reduce the pressure in the manifold and cause the liquid hydrogen sulfide to flow from tank B.

(15) Fill the sample loop with liquid hydrogen sulfide and observe any reaction between the solvent and the solute.

(16) once sufficient time has passed, V5 is opened and the solution is forced into the conductivity cell. (It maybe necessary to open V10 to reduce pressure and force the solution into the cell).

(17) V5 is then closed, isolating the solution from the sample loop,

(18) AC and DC conductivity measurements were then taken as outlined

in Appendix B.

Note: If at any time during the experiment the odour of hydrogen sulfide is detected then the emergency procedure outlined in appendix D1.4 is followed.

D1.3 Exhaust Procedure

At the conclusion of conductivity measurements, the following exhaust procedure is followed.

(1) V11 and V12 on the disposal unit are set to the flame position,

(2) tank A and tank B are closed and V1,V3 and V5 are opened,

(3) V10 is then slowly opened and the hydrogen sulfide is exhausted to the disposal unit,

(4) the exhausted hydrogen sulfide condenses in the cold trap and is vented slowly to the flame,

(5) when all the liquid hydrogen sulfide in the manifold is evaporated, V11 and V12 are switched to the vacuum pump and the manifold is evacuated. The exhaust from the vacuum pump is passed into the flame,

(6) V10 is then closed,

(7) V11 and V12 are switched back to the flame position,

(8) V2 is opened and the manifold is pressurized with nitrogen,

(9) V10 is then opened,

(10) the nitrogen/hydrogen sulfide exhaust is vented to the flame,

(11) V11 and V12 are switched to the vacuum pump and the manifold evacuated,

(12) Steps 5 to 10 are then repeated until there is no further sign of hydrogen sulfide being combusted in the flame.

(13) At the conclusion of the exhaust procedure the manifold is left at atmospheric pressure.

D1.4 Emergency Procedure:

If any major leaks are detected the following procedure should be followed:

(1) open V9 to emergency pressure release loop,

(2) pour liquid nitrogen over Tank A,

(3) open V1 and allow H_2S to drain into Tank A,

(4) proceed with normal exhaust procedure.

Section Two:

The Evaluation and Characterization of the Vanadium(IV) Species Present in Aqueous Solution Containing Citrate Ligand

CHAPTER ONE:

INTRODUCTION

Chapter One - Introduction

1.1 Setting

The chemical industry as it exists today relies extensively on the refining of crude petroleum and natural gas as a source of feedstocks for numerous chemical processes. Upon initial extraction of petroleum or natural gas from sedimentary layers of rock, it is found to be contaminated with a number of components such as hydrogen sulfide, and water. Of these two common contaminates hydrogen sulfide constitutes the major problem due to its high toxicity and its behaviour as a catalyst poison in such processes as catalytic reforming of petroleum.

The hydrogen sulfide is extracted from the natural gas by passing the sour gas stream through a scrub bath which removes all the acidic components and a small quantity of hydrocarbons. Once the hydrogen sulfide is extracted it maybe disposed of by conversion to elemental sulfur. Usually this sulfur is subsequently used in the production of sulfuric acid, which is used as a feedstock in the production of fertilizers and various other chemicals. The elemental sulfur may also be used in the production of insulating foam and construction materials such as concrete and asphalt.

The method of choice for the conversion of hydrogen sulfide to elemental sulfur is often dependent on the estimated amount of sulfur to be produced on a daily basis. If the daily sulfur production is large, say greater than 100 tons per day, then the conversion is usually carried out in the gas phase using a process known as the Claus Kiln process. This specific process entails oxidizing the hydrogen sulfide gas in the presence of oxygen at controlled temperatures resulting in the production of elemental sulfur and low grade heat. If the amount of sulfur to be produced is rather small, say less than approximately five tons per hour, then the conversion may be handled more economically by washing the sour gas stream with an aqueous alkaline mildly oxidizing solution which results in the production of an effluent gas of diminished hydrogen sulfide content and elemental sulfur. The spent liquor is then reoxidized by aerial oxygen in the presence of a catalyst and recycled.

The Stretford process is one such industrial process. It utilizes vanadium (in oxidation states +4 and +5) along with 9,10-anthraquinone-2,7-disulfonate (ADA) dissolved in a carbonate/bicarbonate buffer (pH 8-10) containing citrate to desulfurize gaseous fuel and fuel by-products (see table 1.1 for typical composition of Stretford liquor). This dual catalyst process proceeds via a number of discrete steps:

(1) Initially the hydrogen sulfide is absorbed into a carbonate/bicarbonate buffer where the hydrogen sulfide dissociates into hydrosulfide ions with the release of protons (equation 1 and 2).

$$H_2S\ (g) <==> H_2S\ (solution) \qquad (1)$$

$$H_2S\ (solution) <==> H^+ + HS^- \qquad (2)$$

(in a carbonate/bicarbonate buffer, pH= 9 +/- 0.5)

Table 1.1: Typical Composition of Stretford Liquor

Reagent	Concentration (g/dm^3)
(1) sodium metavanadate $NaVO_3$	4.3
(2) sodium carbonate Na_2CO_3	25.0
(3) trisodium citrate - dihydrate $Na_3C_6H_5O_7 \cdot 2H_2O$	10.0
(4) 9,10-Anthraquinone-2,7-disulfonic Acid Disodium salt (ADA)	3.0

Since, the second ionization constant of hydrogen sulfide is very small at this pH only hydrosulfide ions are present in the liquor.

(2) The hydrosulfide ions produced are then oxidized to elemental sulfur by the reduction of vanadium(V) to vanadium(IV) (equation 3).

$$HS^- + 2\text{"}V^{5+}\text{"} \Longleftrightarrow 2\text{"}V^{4+}\text{"} + 1/8\ S_8 + H^+ \qquad (3)$$

(3) The vanadium(IV) is then reoxidized by aerial oxygen which is dissolved in solution (equation 4) to yield vanadium(V) (equation 5) which is recycled to produce more elemental sulfur.

$$1/2\ O_2(g) \Longleftrightarrow 1/2\ O_2\ (\text{soln.}) \qquad (4)$$

$$2\text{"}V^{4+}\text{"} + 2H^+ + 1/2\ O_2 \Longleftrightarrow 2\text{"}V^{5+}\text{"} + H_2O \qquad (5)$$

(4) To increase the rate of regeneration of the vanadium(V) species 9,10-anthraquinone-2,7-disulfonic disodium salt (ADA) is added to the system to catalytically produce activated oxygen in the form of hydrogen peroxide (equation 6). The hydrogen peroxide then reoxidizes the vanadium(IV) to vanadium(V) (equation 7).

$$O_2 \longrightarrow H_2O_2 \qquad (6)$$

(in the presence of H_2ADA/ ADA)

$$2\text{"}V^{4+}\text{"} + 2H^+ + H_2O_2 \Longleftrightarrow 2\text{"}V^{5+}\text{"} + 2H_2O \qquad (7)$$

Citrate is added to the system to act as a chelating agent to block the loss of vanadium from the process liquor through precipitation of sodium vanadyl vanadates. The redox reactions are separated in space and time to minimize the rate of built up of sulfur-oxy-acid anions and other polysulfide anions in the circulating liquor.

The overall result of the process is the conversion of hydrogen sulfide to elemental sulfur with the net comsumption of oxygen (equation 8).

$$H_2S(g) + 1/2\ O_2(g) \Longleftrightarrow H_2O(l) + 1/8\ S_8(s) \qquad (8)$$

Catalyst loss from this system represents a major operational problem due to high cost and low availability. Modifications to the existing process or development of a new, more economical catalyst system is hindered since the actual electron transfer mechanisms involved are not fully understood. To achieve any insight into these mechanisms, a rudimentary understanding of chemical properties of the individual catalytic species present in solution is necessary. The catalytic species for the vanadium(V) have been extensively studied[1], however, very little is known about the speciation of vanadium(IV).

1.2 Background

1.2.1 Chemistry of Oxovanadium (IV): Speciation in Aqueous Solutions

Vanadium is known to form complexes in oxidation states varying from -1 to +5. In the case of vanadium (IV), the majority of the aqueous chemistry is dominated by the presence of an oxygen multiple covalent bond. This covalently bonded oxygen in the VO^{2+} moiety remains intact during chemical reactions involving other ligands within the first coordination sphere of the vanadium [2]. In fact, Selbin[3] referred to oxovanadium(IV) as perhaps the most stable biatomic ion known. The resistance to protonation of the vanadyl oxygen can be understood in terms of molecular orbital bonding scheme whereby the oxygen 2p orbitals are used to pi bond to the vanadium leaving only the sp sigma hybrid orbital for proton attachment. Due to the high 2s character of this hybrid, it can be seen that this is energetically unfavourable[2].

Vanadium(IV) is a d^1 system with an electron configuration of $[Ar]3d^1$ and has four or five primary coordination sites available in addition to the one occupied by the multiple covalently bonded oxygen. This results in two possible structures - square pyramidal or octahedral - with the one being exhibited depending on the number of coordinated ligands.

In acidic aqueous solution it has been concluded from esr and oxygen-17 nmr[5,6,7] data that the vanadium nucleus is coordinated to six ligands of the form : $VO(H_2O)_5$ (see figure 1.1). On this structural assumption, Wuthrich and Connick[5] surmised that the line width of the oxygen-17 nmr resonance of this hydrated vanadyl ion could be influenced by the exchange rate of nuclei from four non-equivalent coordination sites, namely:

(1) the site of the multiple covalent bonded oxygen;

(2) the four equatorial positions;

(3) the axial position opposite the vanadyl oxygen; or,

(4) possibly additional coordination sites in a second coordination sphere.

Subsequent oxygen-17 nmr experiments led these investigators to report the following observations and conclusions. The exchange of the vanadyl oxygen was not observed since the rate was much too slow on the nmr time scale to be studied by the oxygen-17 nmr relaxation techniques. They further observed that the exchange rate of H_2O from the equatorial positions seemed to be the only reaction which greatly influenced the nuclear relaxation in the bulk of the solution. They found that this exchange rate was rather slow compared to that of other hydrated doubly charged 3d metal ions. The exchange rate was also found to be dependent on the presence of chelating ligands which were able to coordinate in adjoining equatorial positions. They attributed the slow exchange rate to a large electrostatic contribution of the VO^{2+} to the bonding of the water molecules. The increased rate of exchange caused by various chelating ligands might also then be attributed to a simple electrostatic interaction. The ligands which are able to occupy more than one position in the first

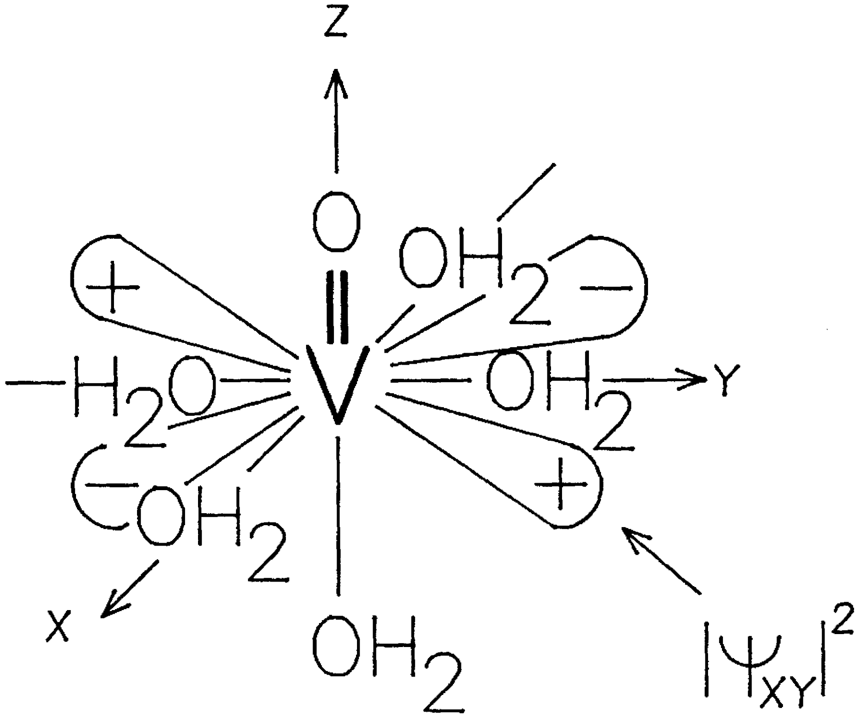

Figure 1.1

Structure of $VO(H_2O)_5^{2+}$. $|\Psi_{xy}|^2$ outlines the areas of high unpaired electron density for the ground state molecule.[19]

coordination sphere with negatively charged groups could neutralize part of the large positive charge on the VO^{2+}, which is effective in the bonding of water molecules. This would have the effect of decreasing the strength of the metal-water bond thereby increasing the exchange rate.

The rate of axial exchange was found to be much greater than that of the equatorial position by a factor of 10^6. This type of behaviour would be expected since group theoretical considerations indicate that different wave functions are involved in the bonding of the four equatorial and the axial ligands of the first coordination sphere.

From redox potential [8] and esr studies[9] on V(IV) and V(V) systems, it would appear that the VO^{2+} entity exists in acidic solutions and is stable against oxidation for a period of up to six months.[2] On the basis of pH titrations, Ducret[10] concluded that two hydrolyzed derivatives of the VO^{2+} entity were formed in solution as the pH increased; namely $VO(OH)^+$ and insoluble $VO(OH)_2$.

He estimated the pH required for the first hydrolysis reaction to occur was 4.8 (equation 9). The precipitation of the hydroxide was observed upon the addition of approximately 1:1 equivalents of base to VO^{2+}(equation 10), and the solubility product (S) was determined to be approximately 10^{-22} (equation 11).

$$VO(OH)^+ + H^+ \rightleftharpoons VO^{2+} + H_2O \qquad pK = 4.8 \quad (9)$$

$$VO^{2+} + 2OH^- \rightleftharpoons VO(OH)_2 \quad (10)$$

$$S = [VO^{2+}][OH^-]^2 = 10^{-22} \quad (11)$$

Later, Rossotti[11] suggested that when the pH of the solution was increased, a dimer formed in solution (equation 13) in addition to the formation of the $VO(OH)^+$ species (equation 12).

$$VO(OH)^+ + H^+ \Longleftrightarrow VO^{2+} + H_2O \quad pK = 6.0 \qquad (12)$$

$$(VOOH)_2^{2+} + 2H^+ \Longleftrightarrow 2VO^{2+} + 2H_2O \quad pK = 6.9 \qquad (13)$$

Dean and Herringshaw[12] investigated the air oxidation of vanadium (IV) in alkaline solution (0.006 - 3.8 N NaOH) and found that the reaction proceeds rapidly via the reduction of oxygen to peroxide (equation 14). The hydrogen peroxide produced, then oxidizes more vanadium(IV) to vanadium(V) with the production of hydroxide ion (equation 15).

$$O_2 + 2VO_3^{2-} + 2H_2O \longrightarrow 2VO_3^- + 2OH^- + H_2O_2 \qquad (14)$$

$$H_2O_2 + VO_3^{2-} \longrightarrow VO_3^- + 2OH^- \qquad (15)$$

The rate of the first step (equation 14) was found to be proportional to the concentration of the hydroxide and to be catalyzed by the presence of Fe(III).

Iannuzzi[13] reported that the addition of VO^{2+} to excess base gave a clear orange/brown solution which he ascribes to the presence of the mononuclear species: $VO(OH)_3^-$. At high pH levels (in excess of 12) these solutions exhibited an esr spectra with 8 lines with similar line splittings and intensities as that of an acidic solution containing VO^{2+} at the same analytical concentration. This would indicate that at pH levels in excess of 12, polynuclear vanadium(IV) species probably comprise only a small fraction of the total vanadium present in the solution.

The acid titration curve of $VO(OH)_3^-$ in excess base exhibits an endpoint one-half equivalent prior to the precipitation of $VO(OH)_2$. This has been attributed to the formation of $V_4O_9^{2-}$ and/or $V_2O_5^{2-}$ ions (equation 16 and 17)[13].

$$4\ VO(OH)_3^- + 2H^+ \rightleftharpoons V_4O_9^{2-} + 7H_2O \qquad (16)$$

$$4\ VO(OH)_2 + 2OH^- \rightleftharpoons V_4O_9^{2-} + 5H_2O \qquad (17)$$

Ostrowetsky[14] carried out a similar titration and observed the formation of a "light precipitate" at a point corresponding to $VO(OH)_2$ and then a clear solution one equivalent later, at a point corresponding to $VO(OH)^+$.

Polarographic evidence[15] suggests that two isopolyanions ($V_2O_5^{2-}$ and $V_4O_9^{2-}$) are of importance in the presence of such non-complexing ligands as SO_4^{2-}, Cl^- and F^-. The individual waves that Lingane associated with each of the species (in 0.03N KOH solutions) were observed to collapse into one in a carbonate buffer where the pH was less than 0.03N NaOH. This "new" wave was attributed to the $V_2O_5^{2-}$ ion. Ostrowetsky[14] observed a double wave at a pH of 11 in a similar solution containing ammoniacal buffer which collapsed into one wave when the pH was reduced to 9.7. He criticized Lingane's previous work because sulfite was used as an oxygen scavenger. This, he felt, was totally unacceptable. Lingane,[16] himself, pointed out that "the stabilizing effect of the sulfite [on vanadium solutions] is peculiar and warrants further investigation."

1.2.2 Complex Formation:

In later papers, Lingane[18] went on to demonstrate complex formation between vanadium (IV) and thiocynate, citrate, tartrate, borate and phosphate. He also found that no reaction occurred with sulfate, fluoride, chloride or pyrophosphate. Further, it was demonstrated by Pecsok and Juvet[19] that vanadium (IV) formed complexes with EDTA (ethylenediaminetetraacetate) up to a pH of 12. There are some x-ray studies[4] which indicate that under specific conditions VO^{2+} has a tendency to form pyramidal complexes in which the V^{4+} is not in the plane of the four equatorial ligands. Additional evidence for this pyramidal structure comes from oxygen-17 nmr experiments[5] which appear to indicate that the tetradentate ligands NTA (nitrilo- triacetate) and PIDA (2-picolyliminodiacetate) are coordinated to the four equatorial positions of VO^{2+}. From an examination of space filling models it seems rather unlikely that a planar structure would exist due to steric hinderance; thus, a square pyramidal structure should be favoured (see figure 1.2). In the pyramidal structure, the vanadium(IV) would then be five coordinated in complexes with tetradentate ligands, while for all other complexes there is probably at least a weak coordination of a sixth group in the axial position.

Based on data generated from conductance measurements, potentiometric titrations and UV/VIS spectroscopy of the vanadium(IV): citrate system, it was concluded that in neutral and basic solutions containing citrate a strong 1:1 (mononuclear) complex

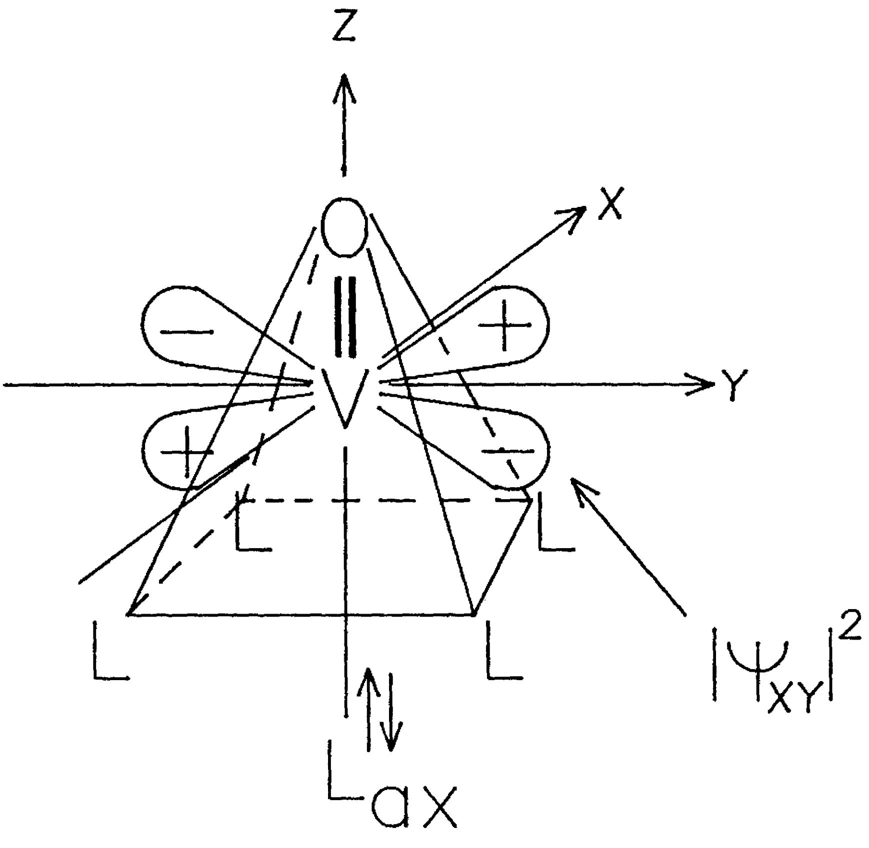

Figure 1.2

Pyramidal coordinaton of the hydrated vanadyl ion. $|\Psi_{xy}|^2$ outlines the areas of high unpaired electron density.[20]

with vanadium (IV) was formed[10]. In acidic solutions (pH < 6) with excess citrate present a 2:1 (binuclear) complex was also found. Nikolova[20], however, found that above pH of 4.5 only the 1:1 complex is stable.

Potentiometric evidence[21] suggests that citrate can act as a tetradentate ligand. This would infer that the hydroxyl group on the citrate participates in the coordination. Analytical results of Canneri[22] and the IR results of Nikolova[20], however, indicated that one hydrogen remains on the citrate ligand when it is complexed with vanadium. It has been found that the hydroxyl group on citric acid shows little tendency to ionize. This has caused Nikolova, et al.,[20] to conclude that the hydroxyl group of the citric acid may participate in coordination without deprotonation. This would suggest a tridentate structure which is consistent with the structure proposed by Selbin[2] and others[10,20,23](see figure 1.3).

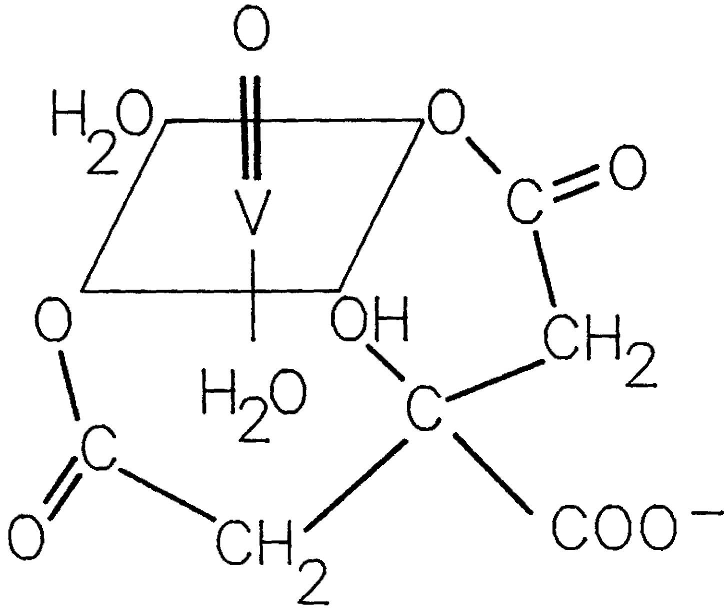

Figure 1.3

Proposed structure of vanadium(IV): citrate complex. (Ref. 2,10,20,23)

1.2.3 Summary of the Aqueous Chemistry of Oxovanadium(IV)

Vanadium (IV) tends to form six coordinate complexes with most ligands (such as EDTA, tartrate, citrate, oxalate and carbonate) and appears to have the capacity to form five coordinate complexes with tetradentate ligands. Aqueous solutions of vanadium(IV) are slow to attain equilibrium, and the equilibrium compositions appear to be highly pH dependent with a relatively large change in the relative ratios of the anions being possible over a very narrow pH range. Oxygen must be excluded from these solutions (especially basic solutions) to prevent the oxidation of vanadium(IV) to vanadium(V).

1.3 Spectroscopic Studies on Vanadium(IV)

1.3.1 UV/VIS

In aqueous solutions of VO^{2+} three low intensity absorption bands are generally observed[2]:

(1) 625-910 nm (16000-1000 cm^{-1});

(2) 526-689 nm (14500-19000 cm^{-1}); and,

(3) 333-476 nm (21000-30000 cm^{-1}).

The third band (333-476 nm) is often buried beneath a high intensity charge transfer band.

The wide energy ranges would tend to indicate a high degree of sensitivity of the electronic transitions to the environment of the first coordination sphere members. These transitions can be rationalized by the molecular orbital diagram (see figure 1.4) proposed by Ballhausen and Grey[23] in which the transitions are assigned in the following manner (equations 18-20):

Band I: $b_2 \text{--->} e_{pi}{}^*$ $({}^2B_2 \text{--->} {}^2E(I))$ (18)

Band II: $b_2 \text{--->} b_1{}^*$ $({}^2B_2 \text{--->} {}^2B_1)$ (19)

Band III: $b_2 \text{--->} Ia_1{}^*$ $({}^2B_2 \text{--->} {}^2A_1)$ (20)

There has been some argument over the exact ordering of two antibonding levels ($b_1{}^*$ and $e_{pi}{}^*$) but since these levels are so very close in energy it is not of major concern and the ordering could actually be a function of the complexing agent present in solution.[2]

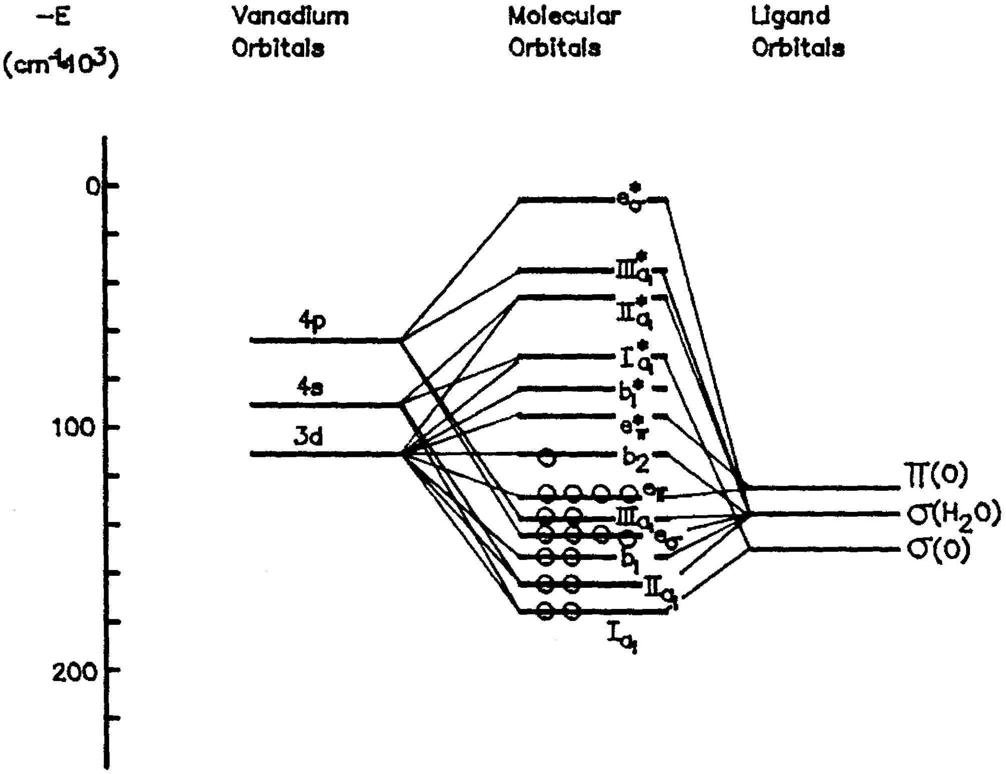

Figure 1.4

Energy diagram for $VO(H_2O)_5^{2+}$, according to Ballhausen and Gray.[14]

Iannuzzi[13] did considerable comparative work on UV/VIS spectra of acidic versus basic solutions of vanadium(IV). He observed a shift to higher energy of the second d-d band and shift to lower energy of the third d-d band (which is often buried under a charge transfer band in acidic solution) as the pH was increased (see table 1.2). On the basis of their data, he predicted the formation of a monomer in basic solution of the form $VO(OH)_3^-$ (equation 21)

$$VO(H_2O)_5^{2+} + 3OH^- \text{---->} VO(OH)_3(H_2O)_2^- + 3H_2O \qquad (21)$$

As was previously mentionged, data generated from conductance measurements, potentiometric titrations and UV/VIS spectroscopy suggests that in the presence of citrate, two citrato complexes are formed:

(1) A strong 1:1 complex (mononuclear with respect to vanadium) is present in the pH range 2 to 9; and,

(2) a 2:1 (binuclear with respect to vanadium) complex forms[10] in acidic solutions (pH < 6) even when excess citrate is present. Nikolova[20], however, found that above pH of 3.5 the predominant species was the 1:1 mononuclear complex between the vanadium(IV) and citrate.

This study was hampered, however, by the fact that in the pH region 4 to 9 the ratio of the vanadium to citrate was maintained at 1:5 to suppress the hydrolysis of the oxovanadium(IV). It was only when the pH was further decreased below 3.5 that the ratio of citrate ligand to vanadium could be reduced without hydrolysis occurring. Subsequent UV/VIS experiments by Nikolova[20] in this pH range revealed

Table 1.2: UV/VIS Data for Aqueous Solution of Vanadium(IV)[13]

pH	Band Maxima (in nm)		
	Band I	Band II	Band III
Acidic	763	625	223
Basic	780	520	410

the presence of a binuclear complex in addition to the mononuclear complex.

UV/VIS spectral data can also yield speciation data by the occurrence of isosbestic points. An isosbestic point is defined as a point at which the absorbance of a solution remains constant while a solution variable such as pH is being changed. This point is the result of at least two species in equilibrium which have overlapping absorption bands. There will be a specific wavelength at which the molar absorptivities of the two species are equal and if the sum of the concentration of the two species is held constant (ie. change of a solution variable only), then there will be no change in absorbance at the isosbestic point as the ratio of the two species may vary. Therefore the existence of an isosbestic point is evidence that a chemical equilibrium exists between at least two species with overlapping spectra.

1.3.2 ESR

Vanadium (IV) systems are accessible to esr studies for three major reasons:

(1) The presence of a single d electron outside a closed shell;

(2) isotopic purity of naturally occurring ^{51}V; and,

(3) a high nuclear spin of 7/2[2].

Francavilla and Chasteen[24] obtained esr data from the aqueous $VO(H_2O)_5^{2+}$ system as a function of pH. They used the first derivative peak to peak intensity of the $M_I = -3/2$ line (see figure 1.5) as a measure of the relative concentration of vanadyl species. Referring to figure 1.6, it can be seen that as the pH increased, the concentration of detectable vanadyl species decreased, and that three distinctive regions over the pH range 1.00 to 6.00 can be identified. Between pH 1.00 and 4.50 a gradual decrease in intensity is observed. The author attributed this to the formation of an esr silent dimer of the form $(VOOH)_2^{2+}$ (equation 22). The sharp drop in esr intensity between pH 4.50 and 5.00 was rationalized through the precipitation of $VO(OH)_2$ (equation 23 and 24). The last gradual decrease between a pH of 5.00 and 6.00 was attributed to the onset of amphoterism in which the formation of $VO(OH)_2$ offsets the formation of $VO(OH)_3^-$.

$$2VO^{2+} + 2H_2O \Longleftrightarrow (VOOH)_2^{2+} + 2H^+ \text{ (esr silent)} \quad (22)$$

$$VO^{2+} + H_2O \Longleftrightarrow VOOH^+ + H^+ \text{ (esr active)} \quad (23)$$

$$VO^{2+} + 2OH^- \Longleftrightarrow VO(OH)_2 \text{ (insoluble - esr silent)} \quad (24)$$

** note: coordination molecules left out

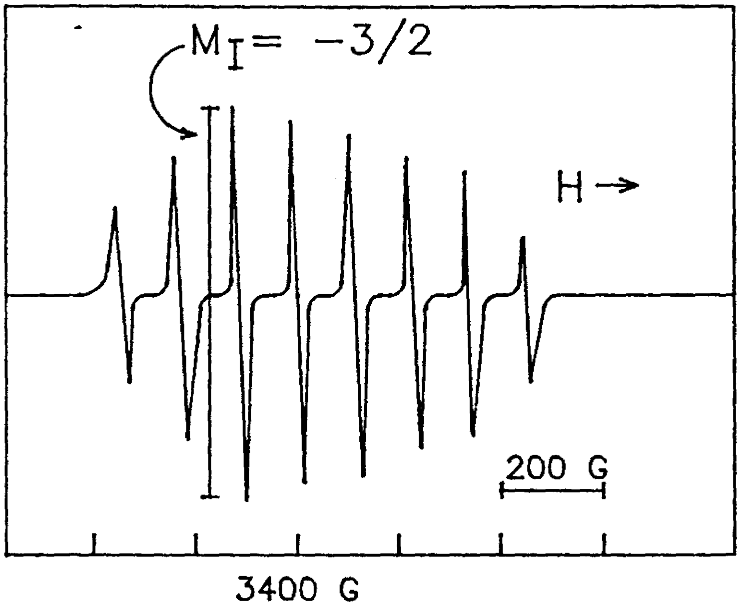

Figure 1.5:

First derivative isotropic ESR spectrum of $VO(H_2O)_5^{2+}$. The signal height of the $M_I = -3/2$ line is used in the determination of the relative concentration of vanadium(IV) ESR active species.[18]

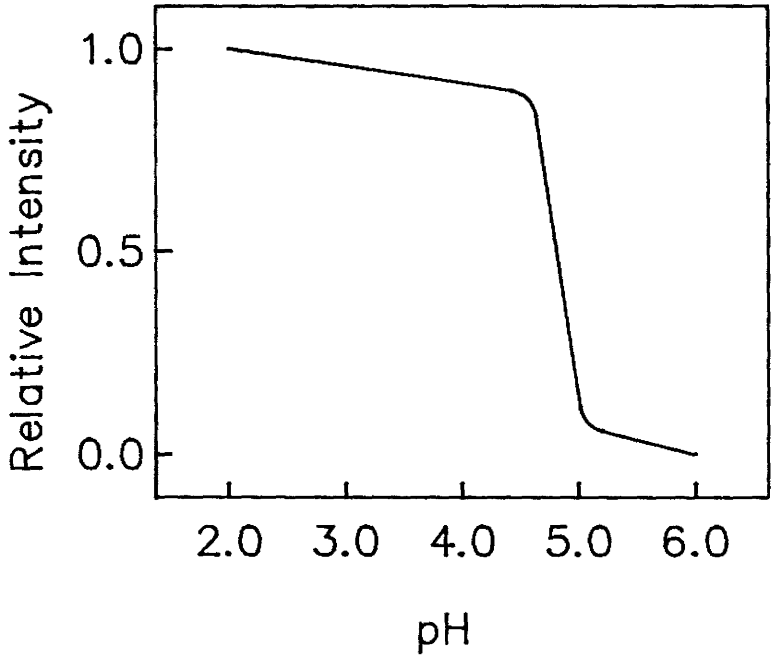

Figure 1.6

Relative ESR intensity of $VO(H_2O)_5^{2+}$ as a function of pH. (Ref. 24)

Further evidence for the existence of more than one esr active species is inferred from a small (but real) variation of relative intensities of the M_I= -3/2 and M_I= -1/2 lines. At pH 2.5 the M_I= -3/2 was more intense while at pH of 5 the M_I= -1/2 was the more intense line. When the pH was increased to 11.5 a strong eight line spectra was once again recorded which had a similar <g> value (a measure of the number of unpaired electrons) and a similar hyperfine coupling constant as reported by Iannuzzi[13]. This was attributed to the $VO(OH)_3^-$ species. The existence of this esr signal in basic solution may be taken to indicate that V(IV) is monomeric in basic solutions. But alternatively, an polymer may be present in which the spin-spin coupling is so weak that each unpaired electron "sees" only one vanadium nucleus. This, however, is rather unlikely in the absence of any complexing ligands. Alternatively, an esr active monomer may be in equilibrium with an polymer which is either diamagnetic or exhibits undetectable broad lines.[13]

1.3.3 NMR

Oxygen-17, proton and carbon-13 nmr techniques have previously been used to investigate the nature of vanadyl(IV)-aquo complexes (ref. 5,6,7,25,26,27,28). Specifically, these studies have added additional support to structures which have been proposed for vanadium (IV) complexes in a wide variety of systems.

There exists no documented studies of the use of vanadium-51 nmr in conjunction with a vanadium(IV) system. Vanadium-51, however, is a suitable nucleus for nmr studies for three reasons:

(1) the high natural abundance of vanadium-51 (99.7%);

(2) a nuclear spin of 7/2; and,

(3) a low quadrupolar moment.

These properties result in an nmr signal which displays narrow linewidths in the range of 20 to 200 Hz. The sensitivity of vanadium-51 nmr with respect to proton nmr is approximately 0.4 at constant magnetic field and 5.5 at a constant frequency. Reher[29], upon comparison with other transition metals, considers vanadium-51 to be one of the most favourable (which have a nuclear spin greater than 1/2) for nmr studies.

This sensitivity of vanadium-51 nmr, along with the experimental results of Francavilla and Chasteen[24] (which indicate that over a specific pH ranges the paramagnetic properties of vanadium(IV) solutions may disappear) would tend to suggest that vanadium-51 nmr may be a useful spectroscopic method with which to probe the vanadium(IV): citrate system, at least over a limited pH range.

1.4 Research Goals

Spectroscopic methods including UV/VIS, ESR and ^{51}V-FT NMR have been used to investigate the speciation of vanadium(V). It is proposed here to extend these methods to the investigation of vanadium(IV) speciation over a wide range of pH levels in solutions containing citrate. The primary goal is to establish the relative concentration ratios of the species as well as the pH range over which the various species are present in appreciable amounts in solution.

CHAPTER TWO

Experimental Details

Chapter Two - Experimental Details

In this section brief outlines of the experimental procedures which were used to investigate the vanadium(IV):citrate aqueous system are presented. A detailed explanation of each procedure is presented in Appendices E and F. Figure 2.1 contains a flow diagram outlining the experimental procedure which was utilized.

2.1 Preparation of Samples

Initially, the percent composition (with respect to vanadium) of $VOSO_4 \cdot X\ H_2O$ was determined using conventional titrametric procedure (see Appendix E). This was necessary to determine the quantity of the solid which would be required to prepare solutions with the appropriate vanadium concentration (0.3M for NMR and ESR; 0.016M for UV/VIS).

Aqueous samples of vanadium(IV): citrate were prepared (see Appendix F) by dissolving the appropriate quantity of the reagents, without purification, (under nitrogen) in distilled water which had been boiled under nitrogen to remove carbon dioxide. Furthermore, any remaining dissolved gases (eg. oxygen) were removed using a ultrasonic bath and reduced pressure. The pH of the solution was then altered using either 9M H_2SO_4 or a saturated solution of sodium hydroxide. The sulfuric acid and sodium hydroxide solution were both degassed before use.

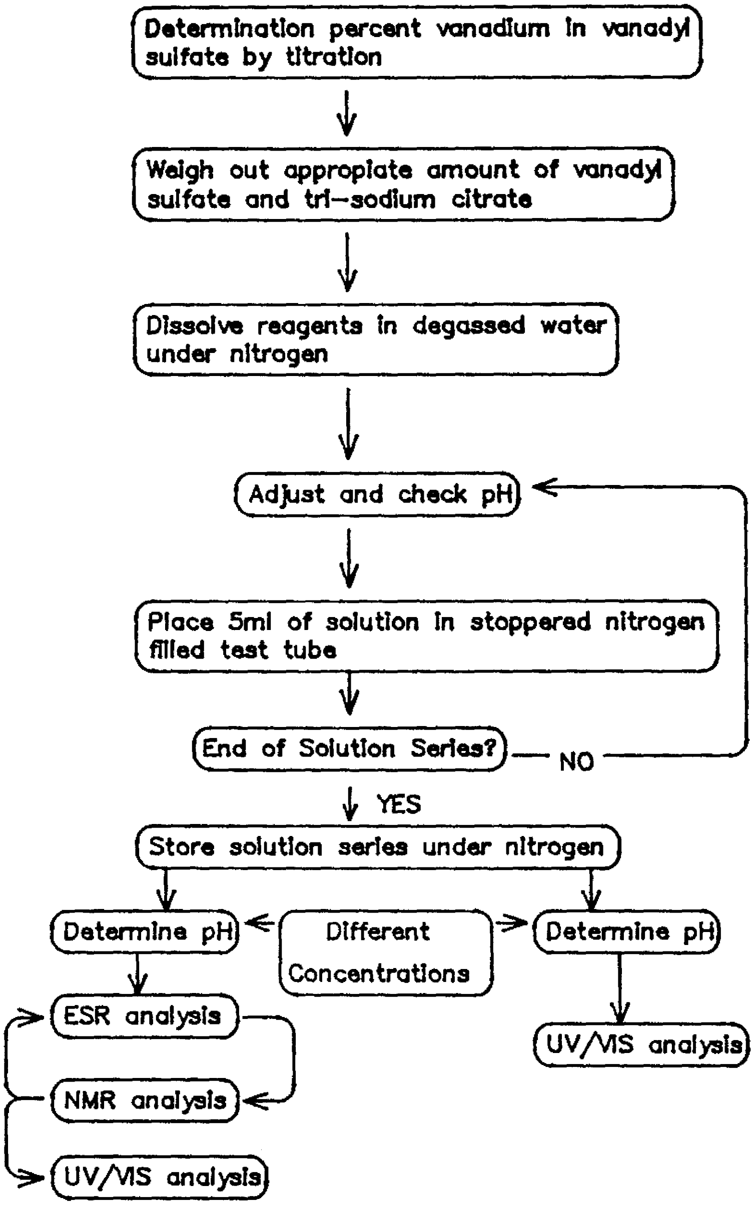

Figure 2.1: Flowchart of Experimental Procedure

Five to ten millilitre samples of the solution were then removed from the main reaction vessel at various pH levels. These samples were withdrawn from the reaction vessel using a syringe and were injected into nitrogen filled test tubes which were sealed with serum caps. All samples were then stored for a minimum of one week under nitrogen to allow time for the solution to come to equilibrium. After this time period, the appropriate spectroscopic measurements were made. This entire procedure was carried out under a nitrogen atmosphere utilizing a glove box.

2.2 Sample Analysis

2.2.1 UV/VIS

UV/VIS spectra of vanadium(IV): citrate solutions (0.016M) over the pH range 0.50 to 12.5 were obtained using a Hewlett-Packard 8450A diode array spectrophotometer. The spectra were recorded over a wavelength range of 200 to 800 nm.

A UV/VIS method of analysis was also utilized to qualitatively determine the degree of oxygen sensitivity of the prepared solutions at various pH levels. This was achieved by recording the UV/VIS spectra of the specific solutions repeatitively after set intervals of exposure to oxygen. (see Appendix F for details)

2.2.2 ESR

ESR signals were obtained for the prepared vanadium(IV): citrate solutions (0.3M) over the pH range of 0.50 to 12.50 using a Bruker ER100D spectrometer (see Appendix F for details). From this spectral data, the following two parameters were measured and compared:

(1) the relative intensity of the signal, and;

(2) the hyperfine coupling tensor <a>.

The absolute error associated with the relative intensity measurements is estimated to be +/- 0.05 while the hyperfine coupling tensor has an estimated error of +/- 7.00.

2.2.3 <u>NMR</u>

Vanadium-51 NMR spectra were obtained for the prepared vanadium(IV): citrate solutions (0.3M) over the pH range of 6.50 to 12.5 using a Bruker WH-90 spectrometer interfaced to a Bruker WP-80 data system. Field-frequency stabilization was achieved by locking onto the ^{2}H-resonance of D_2O which was contained in an inner tube. Initially, spectral widths of 25kHz using a 90 degree pulse (30 microseconds) were used. Later the spectral width was reduced to 10kHz or less to improve resolution. Spectra were recorded using a rotating, cylindrical 10mm OD sample which was externally referenced to neat $VOCl_3$. Chemical shift data were calculated in ppm with negative values in the low frequency direction relative to $VOCl_3$. The resolution of overlapping peaks and peak areas were determined using the Nicolet-1180 Curve Analysis Program (CAP). The error associated with each chemical shift value is estimated to be +/- 0.2 ppm in the high pH region and +/- 1 ppm in the low pH region. All reported linewidths were measured at half-height with an estimated uncertainly of approximately +/- 10 Hz.

The esr spectrum of the nmr samples were recorded before and after the nmr measurements were made to verify that no oxygen contamination occurred during the nmr measurement period. (see Appendix F for more details).

CHAPTER THREE

Results and Discussion

Chapter Three - Results and Discussion

The UV/VIS, ESR, and vanadium-51 FT-NMR measurements were carried out on the prepared solutions of vanadium(IV): citrate as outlined in the Experimental Section and Appendices E and F. From these measurements, the following observations and results were drawn.

3.1 UV/VIS

The UV/VIS absorption spectra of solutions containing vanadium(IV): citrate complexes as a function of pH are shown in figures 3.1 to 3.8. Each is consistent with preliminary work previously carried out in this laboratory[33] and appear to be consistent with spectra acquired by Nikolova for a 1:2 ratio of vanadium(IV): citrate solution (see tables 3.1 and 3.2). Nikolova concluded from his data that vanadium(IV):citrate complexes were only stable to a pH of about 9.00 as was shown by the existence of a band at approximately 650 nm. Our data showed the presence of this band up to a pH of approximately 9.50. Above this pH, our spectral data agree with those of Nikolova and indicate the presence of some bands which have been attributed by Iannuzzi[8] to result from the presence of $VO(OH)_3^-$. The spectral data for the vanadium(IV): citrate system, however, are not exactly the same as the $VO(OH)_3^-$ system (see table 1.1) which would tend to indicate that other UV/VIS active species must be in equilibrium with the $VO(OH)_3^-$ at these pH values. It is unlikely that a vanadium(IV): citrate complex could exist in this region above a pH of

Table 3.1: UV/VIS Data for Vanadium(IV): Citrate Solution[20]

pH	Band Maxima (in nm)			
	Band I	BandII	Band III	Band IV
3.60	1075	649	571	
6.00	1053	654	568	
8.00	1053	649	571	
>9.00	775	671	556	
>9.00	847		532	417

Note: ratio of Citrate: Vanadium in this study was 2:1

Table 3.2: UV/VIS Results for the Vanadium(IV): Citrate System

pH	Band Maxima (in nm)		
	Band II	Band III	Band IV
1.2	770	625	254
2.00	760	625	254
3.00	710	557	314
3.70	683	561	318
6.50	650	565	330
8.20	645	567	335
9.40	670	555	350
>10.00		530	410

Note: ratio of Vanadium: Citrate is 1:1

9.50, however, the UV/VIS spectra would indicate some other complex in addition to $VO(OH)_3^-$ maybe present as a minor constituent in the solution with a UV/VIS spectra hidden under that of the $VO(OH)_3^-$.

The oxygen sensitivity of the solutions at a pH level of 7.00 and 12.3 were qualitatively determined by recording consecutive spectra after fixed periods of oxygen contamination (see Appendix F for procedure). The resulting spectra (see figures 3.1 and 3.2) indicate that the solution of pH 12.3 was extremely oxygen sensitive, while spectra of the neutral solution showed no change after 20 minutes of exposure. The oxygen contaminated spectra of the solution with a pH of 12.3 also indicates that spectrum of the vanadium(V): citrate system is drastically different than that for the vanadium(IV): citrate system.

In a preliminary study carried out previously in this laboratory[33], it was found that several isosbestic points could be identified. One isosbestic point at a wavelength of 750 nm was observed to remain intact over the pH region of 2.00 to 7.00. Two further isosbestic points were also observed at a wavelength 425 nm and 465 nm in the pH range 4.00 to 7.00 (see figures 3.3 and 3.4). These last two isosbestic points, however, occurred over a small range in wavelengths and were not as well defined as the first isosbestic point.

In this study, the spectra were consistent with those obtained earlier, however, only the isosbestic point located at 750 nm was observed over the entire pH range 2.00 to 7.00 (see figures 3.5 and 3.6). The other two isosbestic points were not observed and their presence in the preliminary study may be attributed to small changes

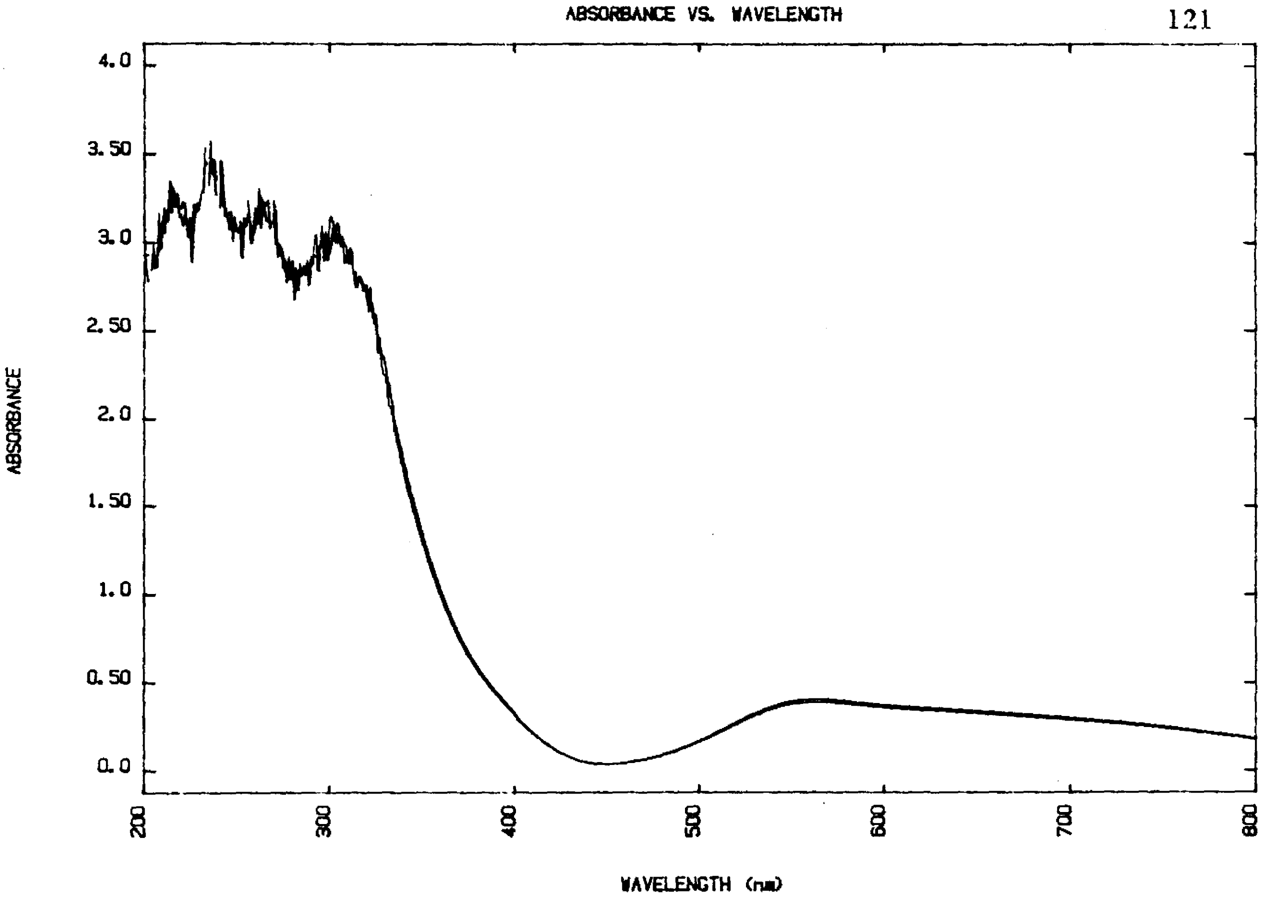

Figure 3.1:

Effect of oxygen on the UV/VIS spectrum of a vanadium(IV): citrate solution at a pH level of 7.00. The upper spectrum is before exposure to oxygen, while the lower spectral line is the result of exposure to oxygen for a 20 minute period. Notice the effect of oxygen on this solution is very slight.

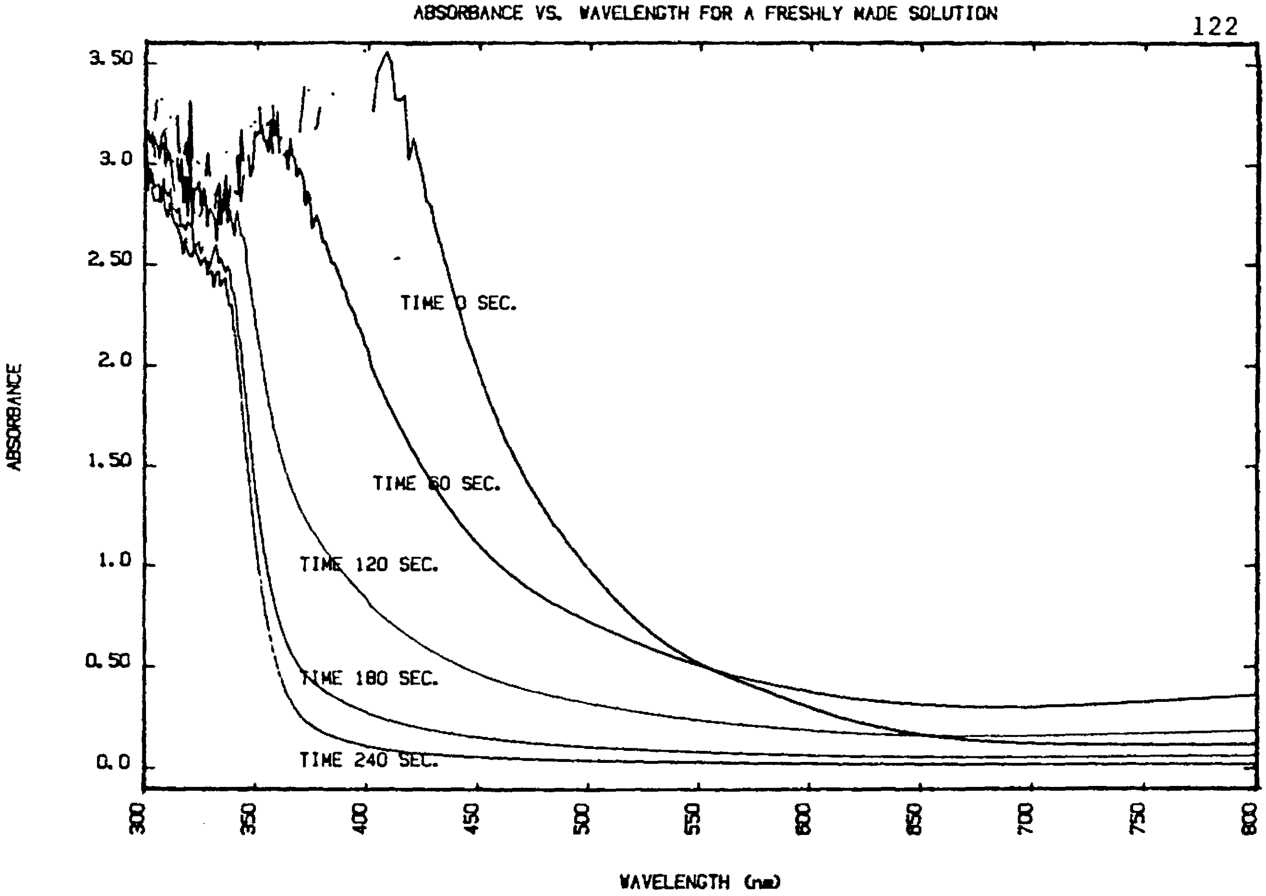

Figure 3.2:

Effect of oxygen exposure on the UV/VIS spectrum of a vanadium(IV): citrate solution as a function of time. The pH value of the initial solution was 12.30.

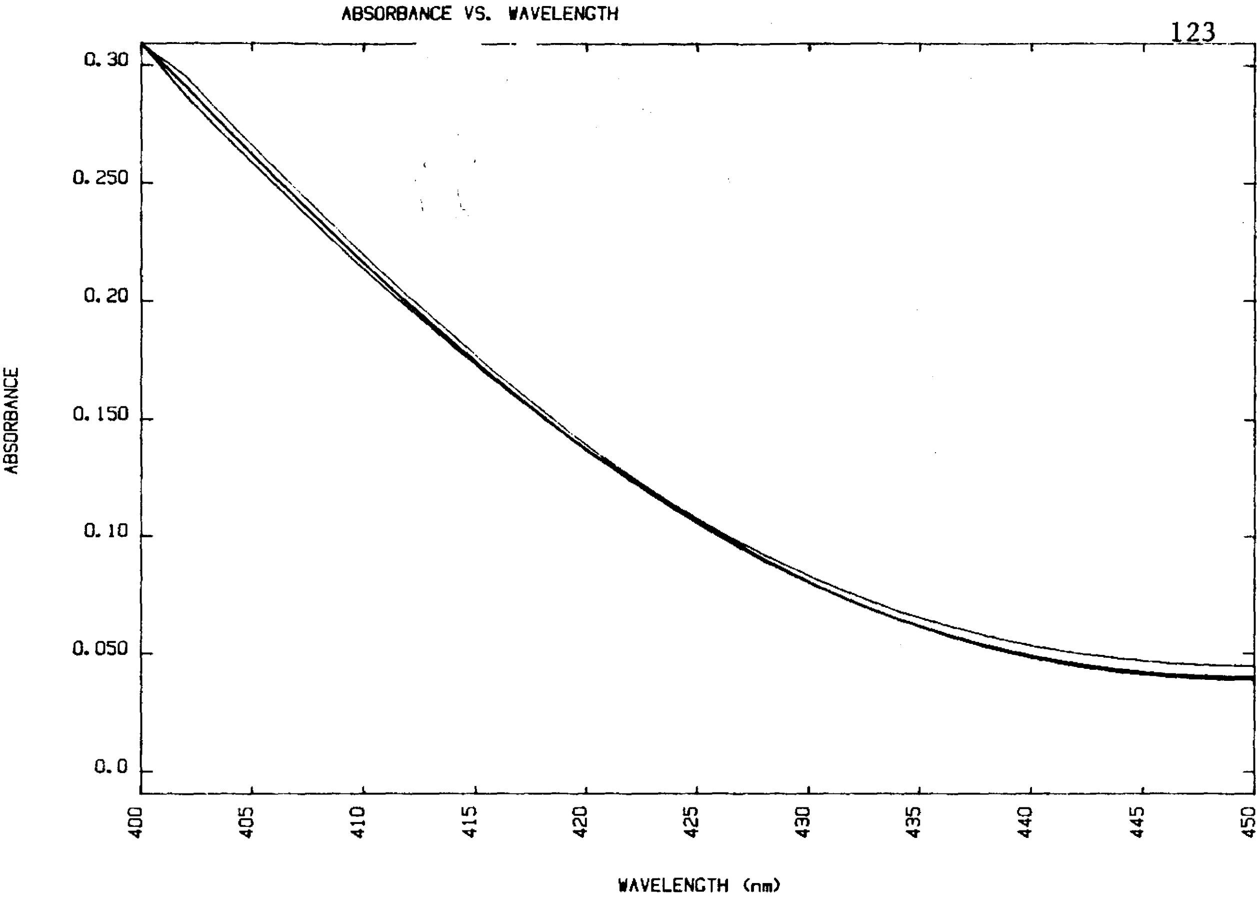

<u>Figure 3.3</u>:

The above UV/VIS spectra were recorded during the preliminary study and indicate a possible isosbestic point at 425 nm. The pH values of the solutions were 5.10, 6.15, and 7.15 from top to bottom, at 405 nm. In the present study this isosbestic point was not observed.

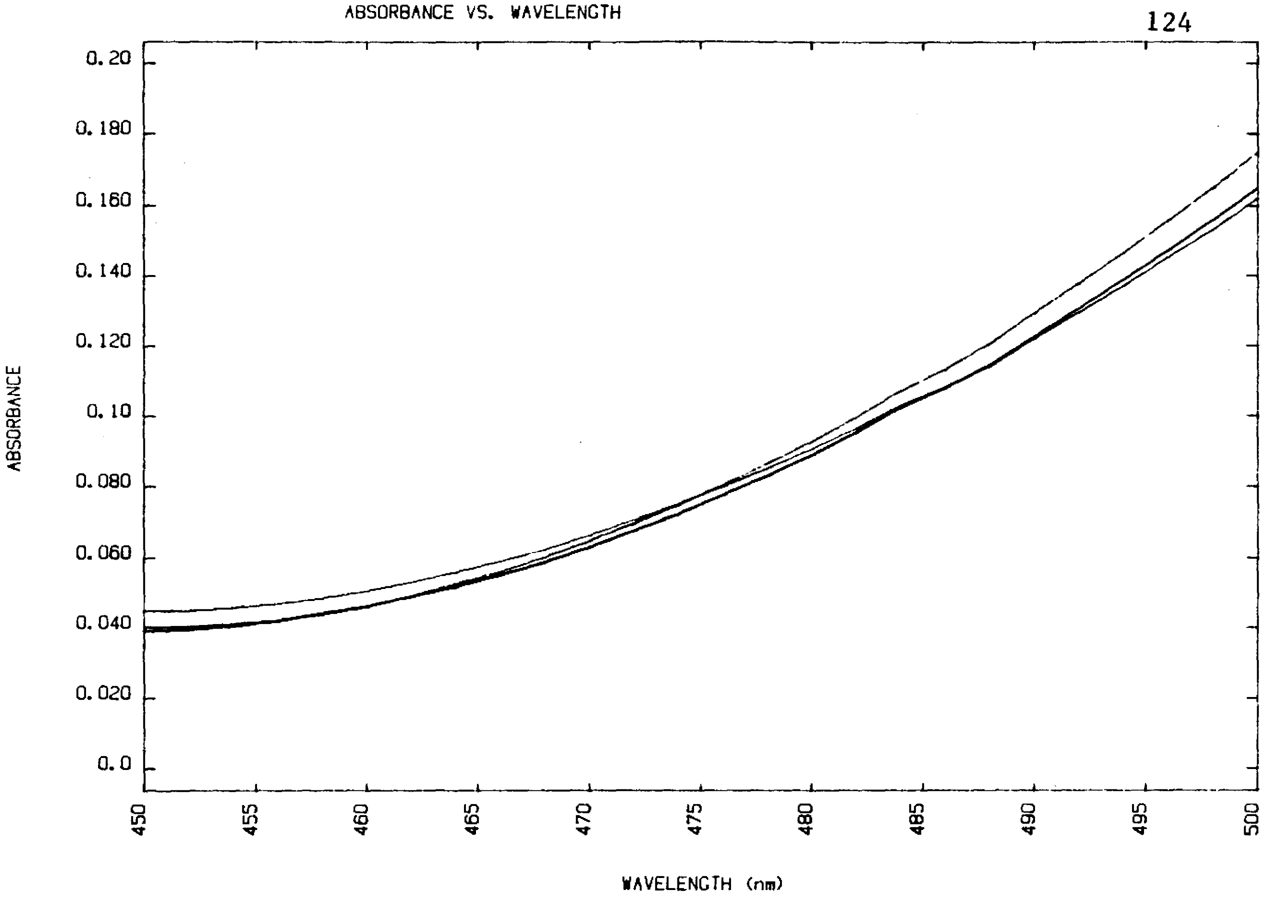

Figure 3.4:

The above UV/VIS spectra were recorded during the preliminary study and indicate a possible isosbestic point at 465 nm. The pH values of the solutions were 5.10, 6.15, and 7.15 from top to bottom, at 495 nm. In the present study this isosbestic point was not observed.

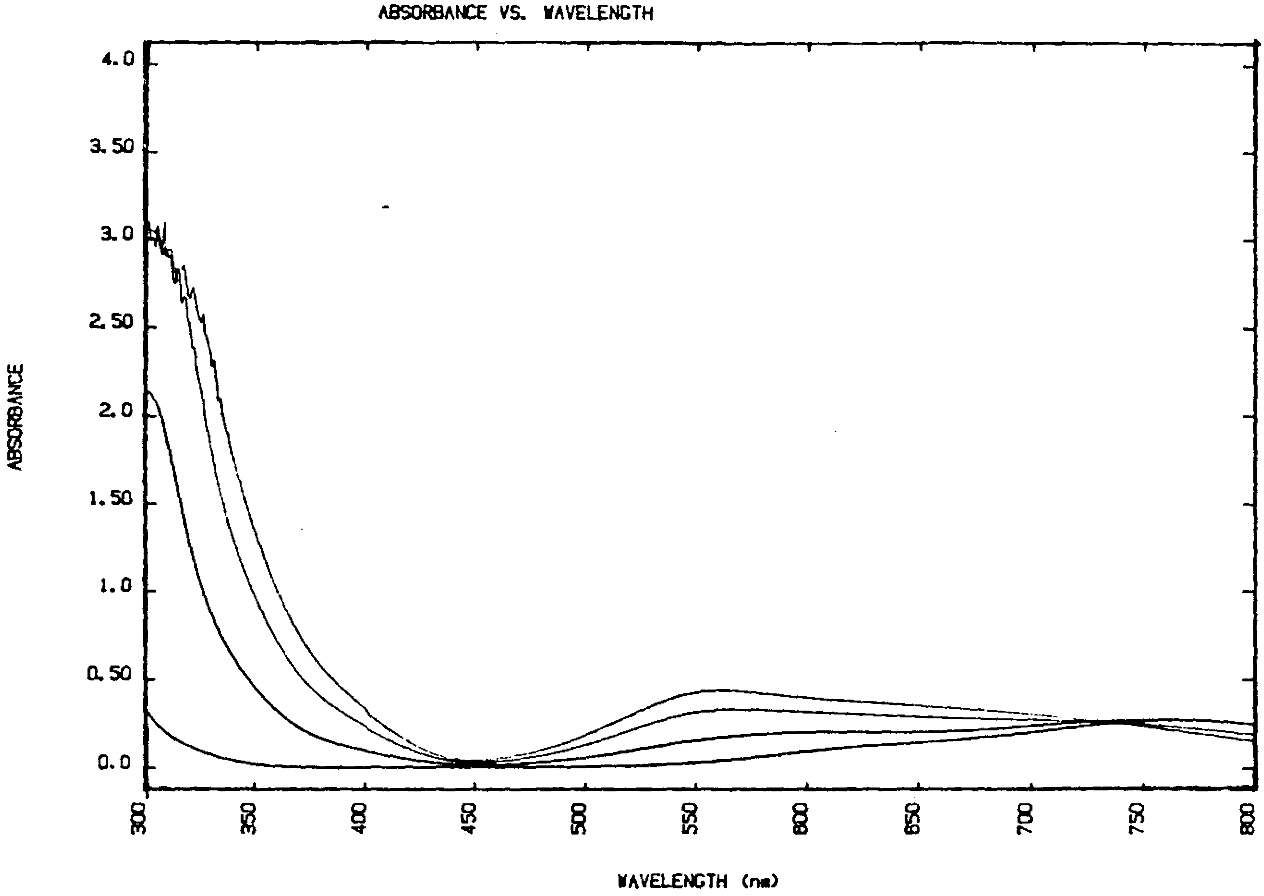

Figure 3.5:

The above UV/VIS spectra of vanadium(IV): citrate solutions display an isosbestic point at approximately 750 nm. The respective pH values of these solutions were 4.20, 3.10, 2.70 and 1.10 from top to bottom, at 550 nm.

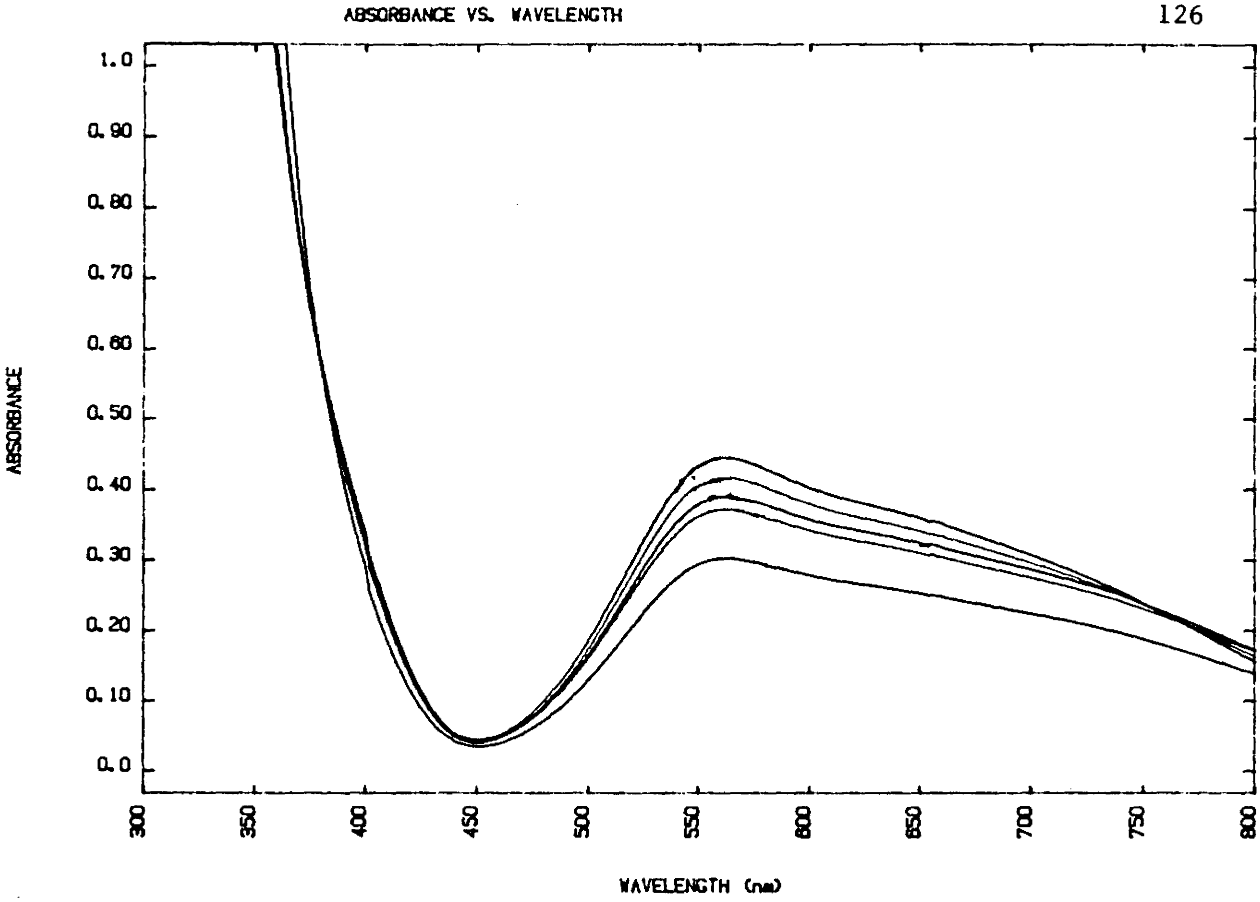

Figure 3.6:

The above UV/VIS spectra of vanadium(IV): citrate solutions displays an isosbestic point at approximately 750 nm. The respective pH values of these solutions were 4.15, 5.10, 6.15, 7.15 and 7.55 from top to bottom, at 550 nm.

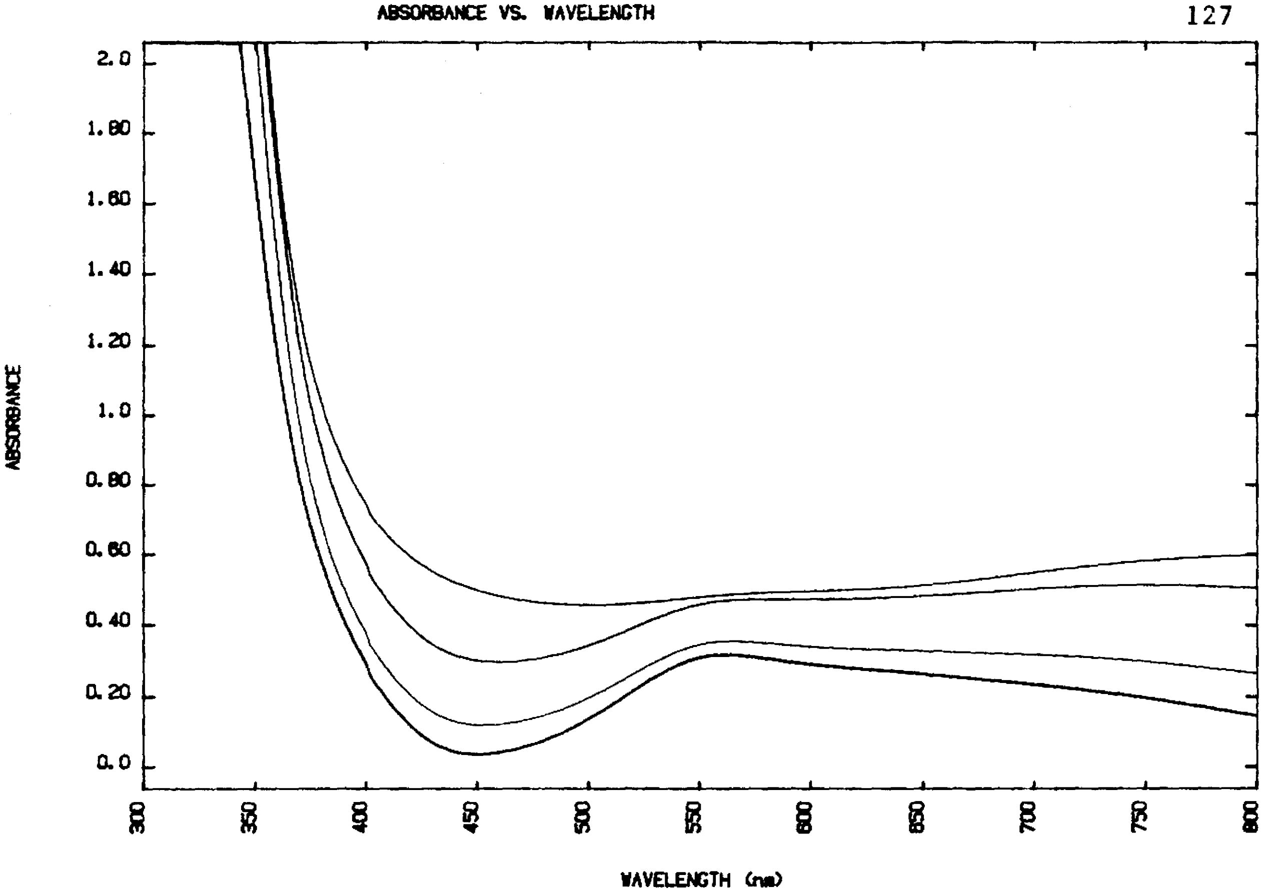

Figure 3.7:

The above UV/VIS spectra are typical of vanadium(IV): citrate solutions which have a pH value in excess of 7.00. In this pH range no isosbestic points are evident. The respective pH values of these solutions were 7.65, 8.40, 8.85 and 9.60, from top to bottom, at 550 nm.

in vanadium concentration within a sample series.

From the presence of this one isosbestic point, it is inferred that at least two species or more are present in equilibrium between a pH of 2.00 and 7.00. The apparent lack of an isosbestic point above a pH of 7.00 (see figure 3.7) provides no evidence concerning speciation, however, it can be inferred that if two species are in equilibrium in this region their respective absorption spectra and ultimately their structural configuration must be quite different.

3.1.1 Summary of UV/VIS Data

From the analysis of the UV/VIS spectra, it is apparent that basic solutions of vanadium(IV): citrate are extremely oxygen sensitive and upon exposure to oxygen the spectra changes drastically. Due to this great difference between the spectra of the vanadium(V): citrate system and the vanadium(IV): citrate system, it is possible to quickly determine by the UV/VIS spectra whether any oxygen contamination has occurred to the vanadium(IV): citrate solutions (see figure 3.8).

The UV/VIS spectra of the vanadium(IV): citrate solutions at different pH levels were consistent with spectra obtained by Nikolova[20]. The spectral data indicate the definite present of vanadium(IV): citrate complexes up to pH of 9.5. Above this pH, the spectra begin to take on some characteristics which have been attributed[8] to the presence of $VO(OH)_3^-$. Subtle differences, however, are apparent, which would indicate either several species are in equilibrium with the $VO(OH)_3^-$ or a species exists which is similar to the $VO(OH)_3^-$ species with respect to structure and bonding.

The presence of an isosbestic point at 750 nm would indicate that at least two species are in equilibrium in the pH range 2.00 to 7.00. Even though no isosbestic points were observed in the pH region above 7.00, this does not rule out the possiblity that more than one species was present.

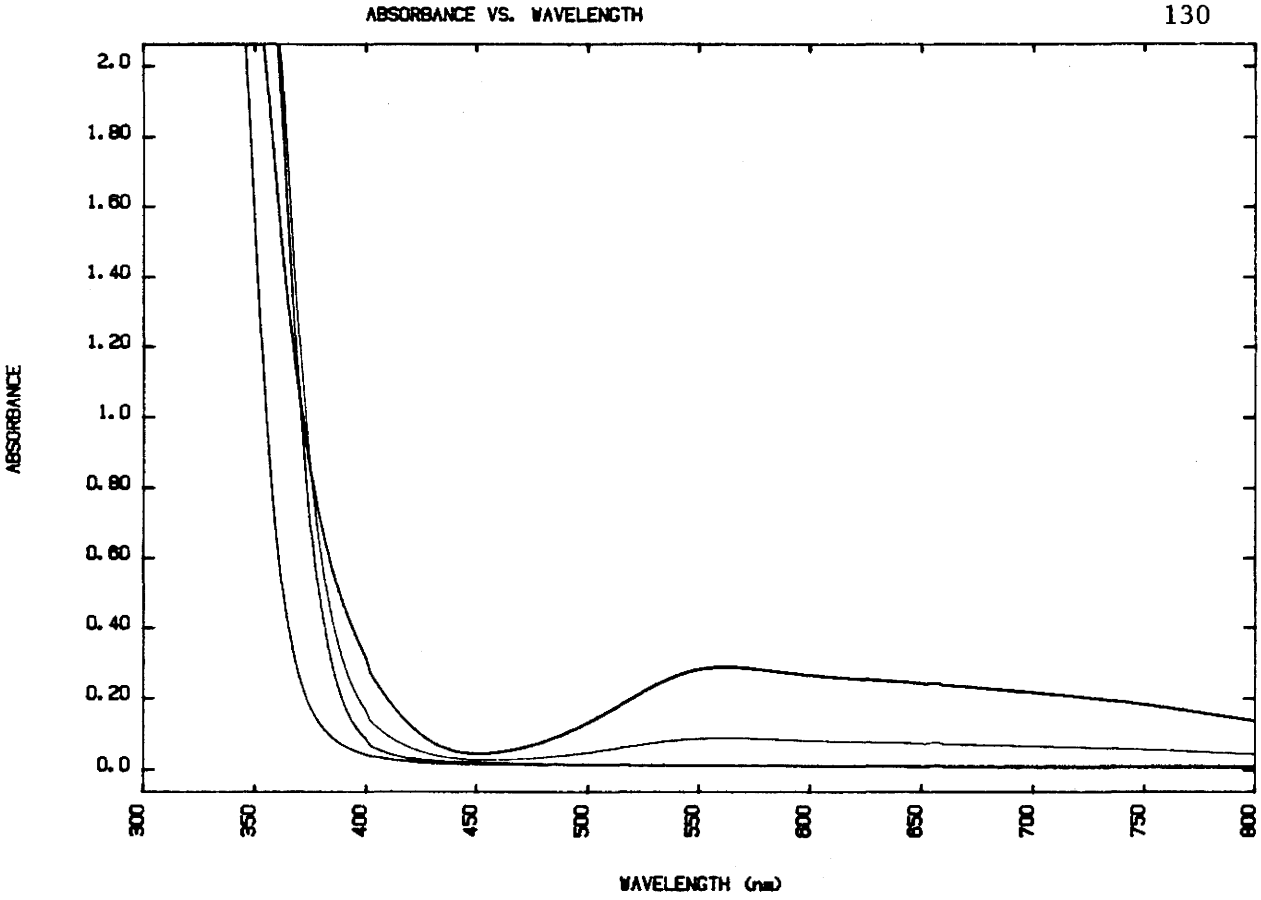

Figure 3.8:

Oxygen contamination of vanadium(IV): citrate solutions is easily identified on the basis of UV/VIS spectra. The above UV/VIS spectra are typical of vanadium(IV): citrate solutions which have been contaminated by oxygen. Notice that the absorptivity decreases with increasing pH values, which is in contrast to what is observed when oxygen is excluded from the solutions (see figure 3.7). The respective pH values of these solutions were 7.60, 8.30, 8.75 and 9.75, from top to bottom, at 400 nm.

3.2 ESR

The characteristic eight line spectrum reported for vanadium(IV) complexes was observed over the complete pH range 0.50 to 12.50 with the intensity varying to different degrees depending on pH. This is in contrast to the data acquired in the preliminary study[33] which indicated the absence of ESR active species in the pH region 6.00 to 9.00 and 11.00 to 12.50. In this present study, particular care was taken in this pH region to determine if an ESR active species could be detected. When the sensitivity of the ESR machine was increased to the maximum level, a poorly defined eight line spectra of vanadium(IV) could be resolved. The intensity of this signal was less than .2% of the reference ESR signal recorded at a pH of 1.00.

From the accumulated ESR spectra, the values of two parameters were determined and compared:

(1) relative intensity of the signal; and,

(2) hyperfine coupling tensor <a>.

(Details of the acquisition of these parameters are outlined in Appendix F)

The variation of these two parameters as function of pH can be used to provide evidence for the existence of various vanadium(IV) complexes in equilibrium. A drop in the intensity of the signal indicates a decrease in the number (or concentration) of paramagnetic complexes. Such a decrease in the ESR signal can be attributed to formation of dimers (or polymers) or the loss from solution by precipitation of ESR active material.

The <a> tensor value is determined by the environment of the unpaired electron. A change in this value is an indication of a overall change in the environment of the unpaired electron and thus a definite change in speciation.

The relative intensity and <a> tensor values changed as a function of pH as shown in Figure 3.9 to 3.14. From these data the following observations can be made:

(1) A sharp drop in ESR signal intensity was observed between a pH value of 1.00 and 3.00.

(2) A more gradual decrease in signal intensity was observed over the pH range of 3.00 to 6.00

(3) In the pH range 6.00 to 9.00 the ESR intensity drops to approximately .2% of the reference solution (pH= 1.00).

(4) Above 9.25 precipitation of an ESR active black coloured solid occurs.

(5) At a pH of 9.00 the ESR intensity started to increase and reached a maximum at a pH of approximately 10.00. This maximum intensity was approximately 5% to 7% of the signal intensity at a pH of 1.00.

(6) Above a pH of 10.00 the ESR signal intensity once again decreased until it was approximately less than 1% of the reference solution (pH= 1.00) at pH values above 11.00.

(7) The <a> tensor value of the solution at a pH of 1.00 and in the pH range 9.00 to 11.00 are consistent, within experimental error, with values determined by Iannuzzi[13] for the vanadium(IV) system in the absence of citrate.

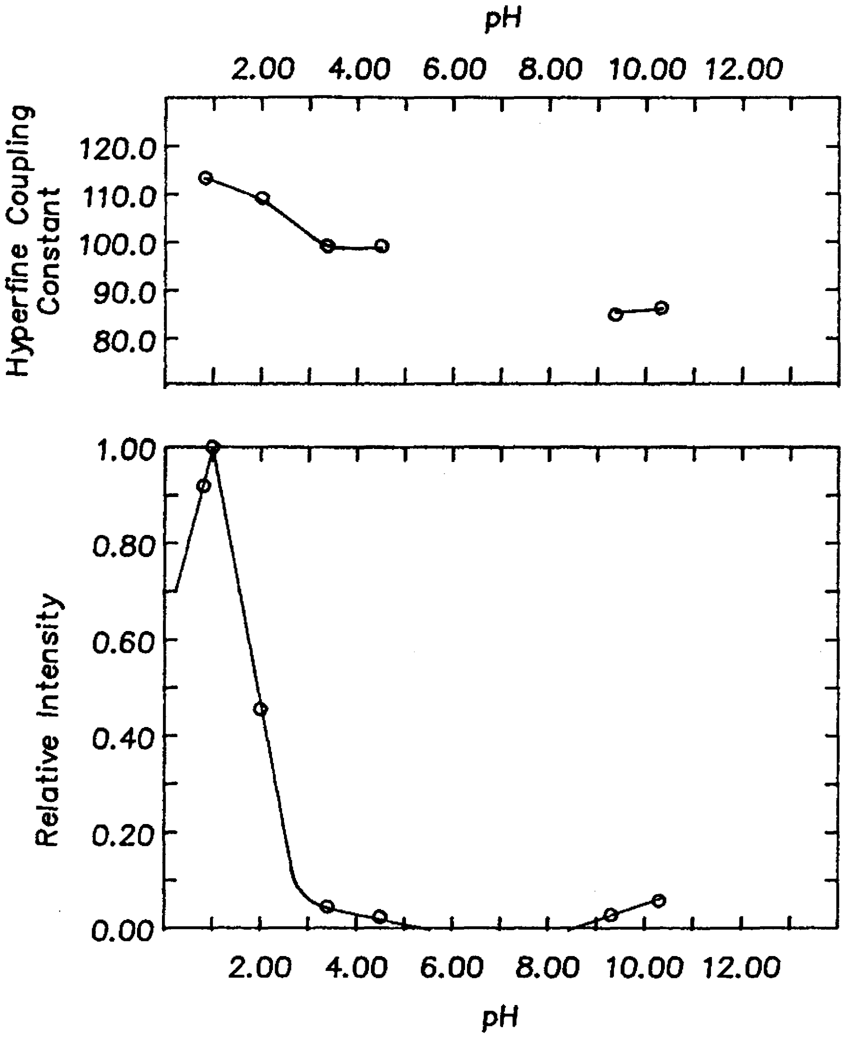

Figure 3.9:

Relative ESR intensity and hyperfine coupling constant as a function of pH for solution series A.

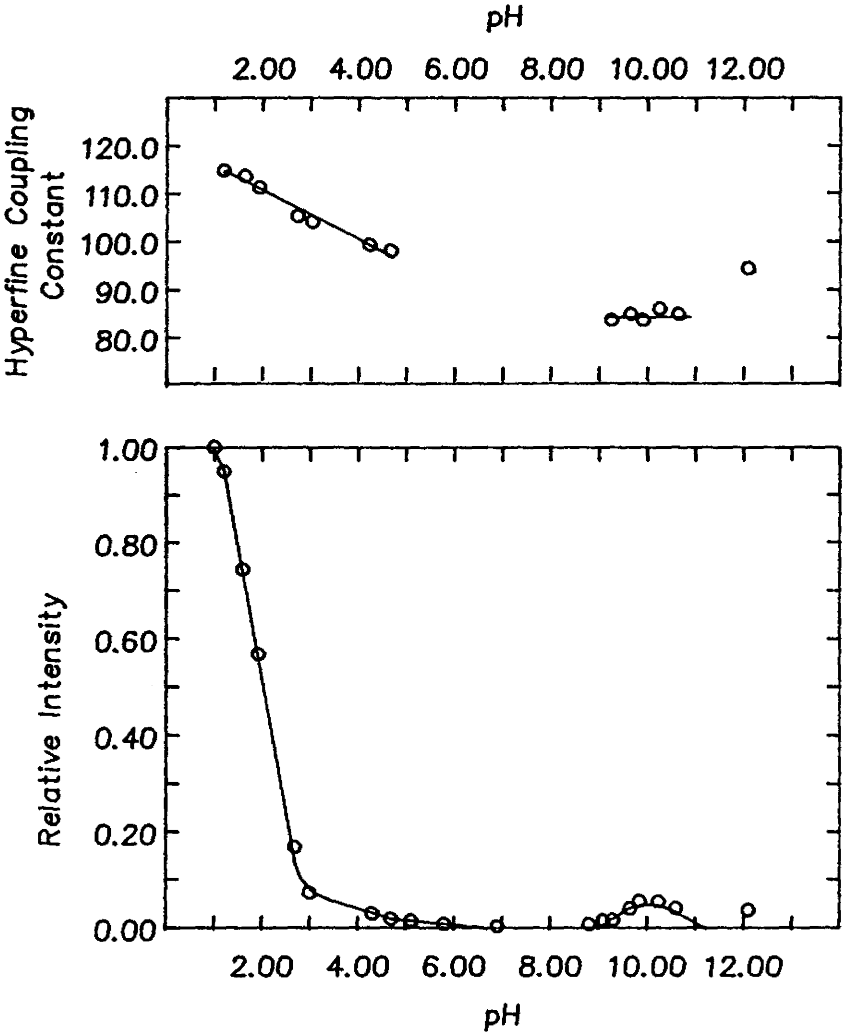

Figure 3.10:

Relative ESR intensity and hyperfine coupling constant as a function of pH for solution series B.

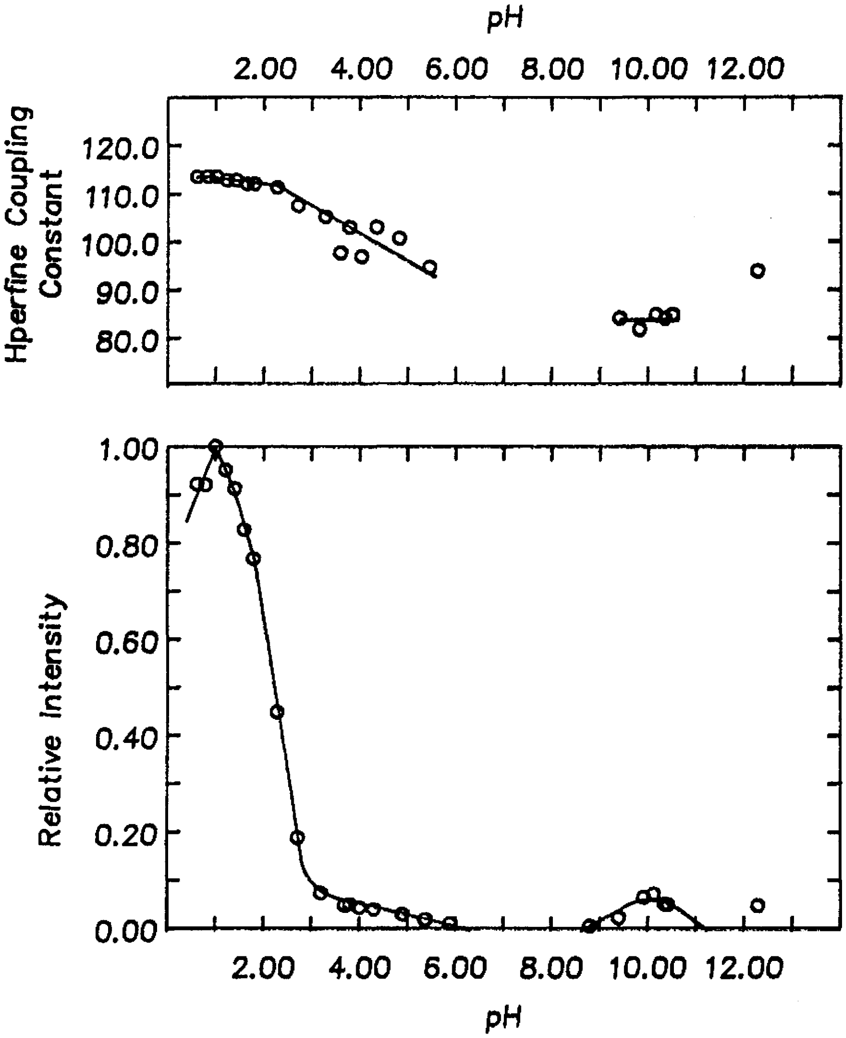

Figure 3.11:

Relative ESR intensity and hyperfine coupling constant as a function of pH for solution series C.

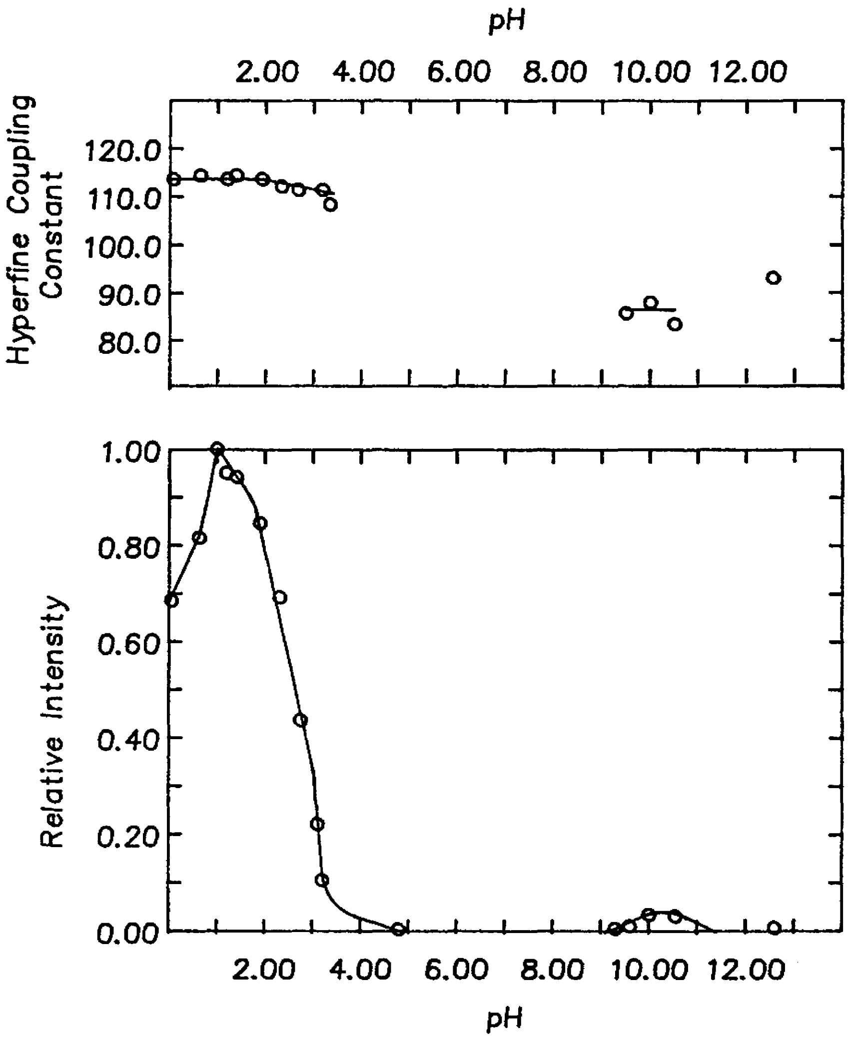

Figure 3.12:

Relative ESR intensity and hyperfine coupling constant as a function of pH for solution series D.

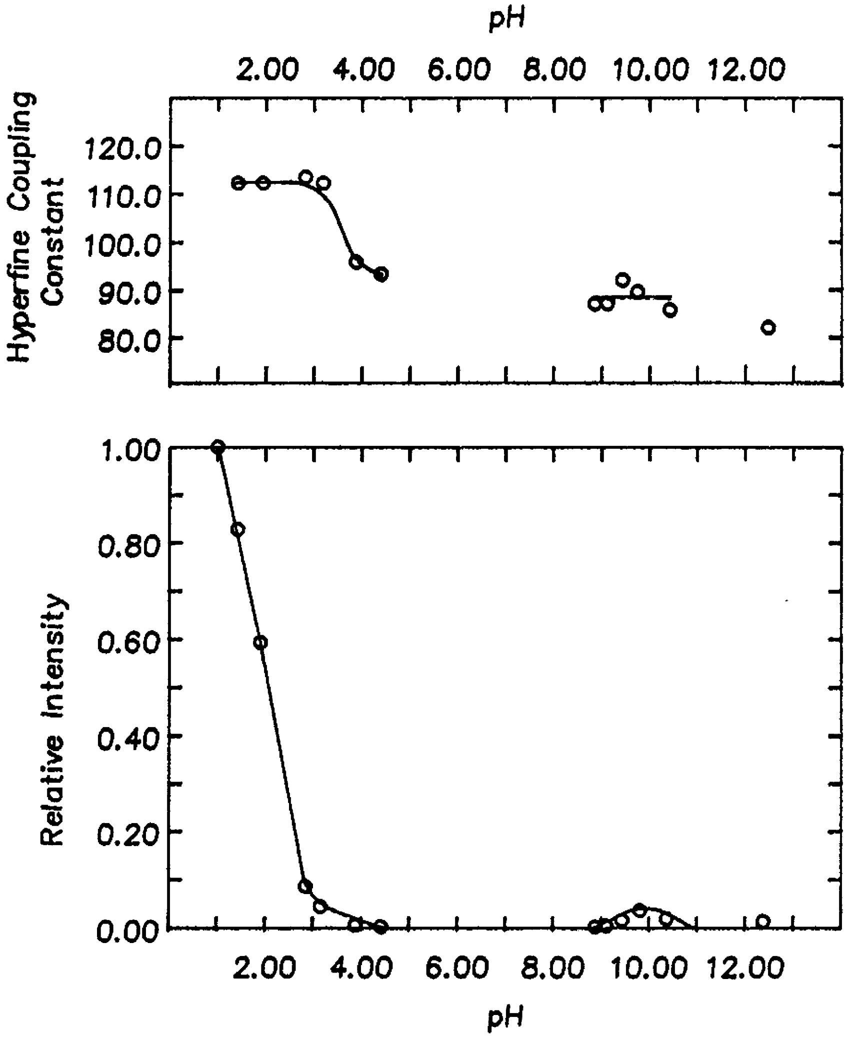

Figure 3.13:

Relative ESR intensity and hyperfine coupling constant as a function of pH for solution series E.

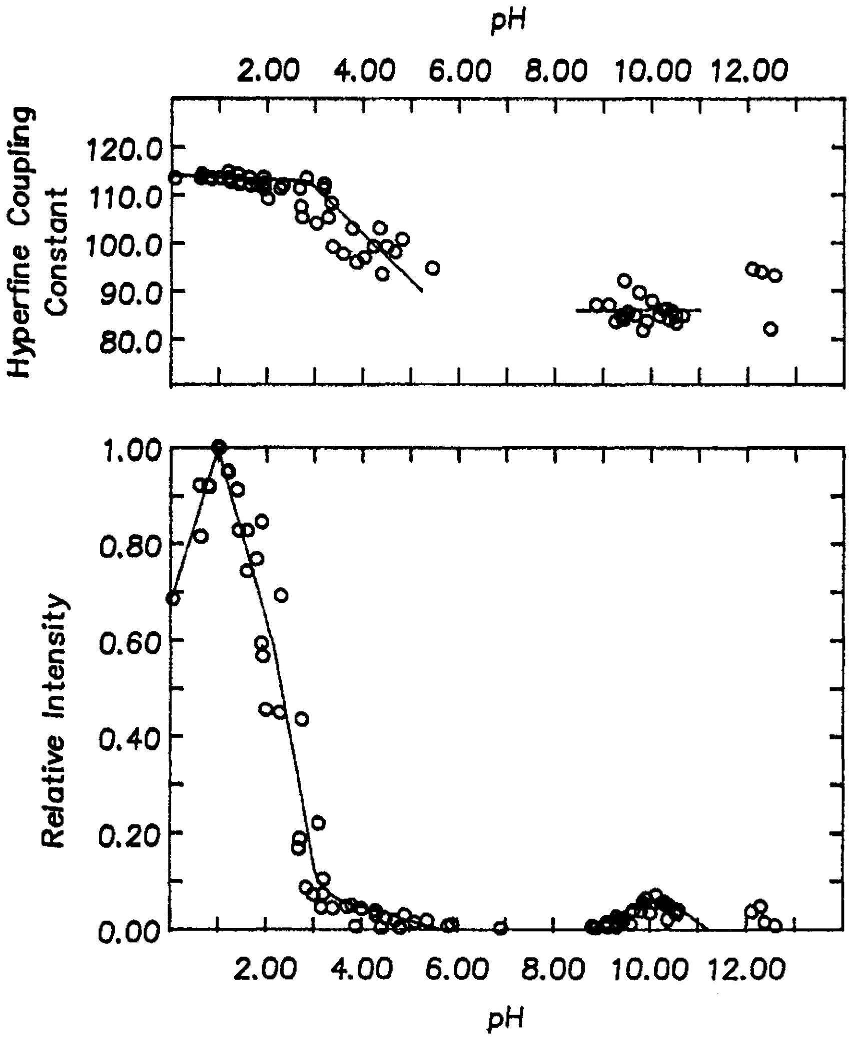

Figure 3.14:

Composite diagram of the relative ESR intensity and hyperfine coupling constant as a function of pH.

The manner in which the intensity of the ESR signal changed as a function of pH at values less than 6.00 was significantly different than the data reported by Francavilla and Chasteen[24] for the vanadium(IV) system in the absence of citrate. As shown in Figure 1.6, the intensity of the ESR signal for the vanadium(IV) system in the absence of citrate decreased as the pH was increased. Three distinctive regions over the pH range 1.00 to 6.00 can be identified[24]. Between a pH of 1.00 and 4.50, a gradual decrease in intensity is observed and was attributed to the formation of an ESR silent dimer of the form $(VOOH)_2^{2+}$ (equation 22). The sharp drop in ESR intensity between a pH of 4.50 and 5.00 was rationalized by the precipitation of $VO(OH)_2$ (equation 23 and 24). The last gradual decrease between a pH of 5.00 and 6.00 was attributed to the onset of amphoterism, in which the formation of $VO(OH)_3^-$ offsets the the formation of $VO(OH)_2$[24].

In contrast, the vanadium(IV): citrate system showed a sharp decrease in intensity in the pH range 1.00 to 3.00. This difference in pH would indicate that the sharp drop in signal intensity cannot be attributed solely to the formation of $(VOOH)_2^{2+}$ and that the citrate ligand has a significant effect on the vanadium(IV) system. Furthermore, as the pH was increased, no precipitation of $VO(OH)_2$ was observed. This absence of the precipitation of the $VO(OH)_2^{2+}$ would further indicate that it maybe possible that the citrate ligand inhibits the hydrolysis of vanadium(IV), at least in this pH range.

In the vanadium(IV) system (in the absence citrate), evidence for the existence of more than one ESR active species is reflected by a very small but real variation in the relative intensities of the M_I=

-3/2 and the M_I= -1/2 lines.[24] Francavilla and Chasteen[24] observed that at a pH value of approximately 2.5 the M_I= -3/2 line was slightly more intense than that of the M_I= -1/2 line and that when the pH was increased to approximately 5.00 the intense of these two lines were equal. In the present study of the vanadium(IV): citrate system, a similar trend was observed except that the M_I= -3/2 line was only more intense than the M_I= -1/2 line at pH values less than approximately 1.20. This, coupled with the fact that the <a> tensor value slowly decreases as the pH increases (see figures 3.9 to 3.14) would tend to infer that more than one ESR active species is present in the pH range of 1.00 to 6.00. It should be noted that this change in <a> tensor value cannot be explained by the formation a dimer, since a dimer would be ESR silent and have no effect on the <a> tensor value.

The existence of a very weak ESR signal in the pH range of 6.00 to 9.00 indicates that almost all of the previously unpaired electrons are now paired up, probably due to the formation of a dimerized species.

In basic solutions (pH in excess of 12) containing vanadium(IV) in the absence of citrate, Iannuzzi[13] reported an eight line ESR spectrum which was similar in intensity and splitting constant as that for similar acidic solutions. He attributed this ESR signal to the presence of $VO(OH)_3^-$ species. In the present study, an ESR signal of moderate intensity (10% of reference solution at a pH of 1.00) was observed only in the pH range of 9.00 to 11.00. These spectra displayed <a> tensor values which are consistent, within experimental error, with those reported by Iannuzzi[13]. The fact that this ESR signal is only observed over a limited pH range, and that the intensity is only approximately 10% of that reported by Iannuzzi, would tend to indicate that in the vanadium(IV): citrate system the $VO(OH)_3^-$ species is a minor constituent in basic solutions and exists over a limited pH range only.

3.2.1 Summary of ESR Data

ESR signals were observed over the entire pH range 0.50 to 12.50, however, in the pH range 6.00 to 9.00 and 11.00 to 12.50 the observed signal was extremely weak. At a pH of 1.00 the spectra of vanadium(IV): citrate system is similar to that reported for the vanadium(IV) system in the absence of citrate (ie. $VO(H_2O)_5{}^{2+}$). As the pH increased, the ESR signal intensity dropped quickly. This cannot be explained solely by the formation of a dimer of the form $(VOOH)_2{}^{2+}$. Based on this fact, it is apparent that the citrate must be involved in the formation of dimers or polymers which have no unpaired electrons. There is also evidence which supports the possibility of the presence of more than one ESR active species. As the pH is increased further, no precipitation of $VO(OH)_2$ was observed, which would indicate that citrate inhibits the hydrolysis of vanadium(IV), at least in this pH range. In basic solution (pH= 9.00 to 11.00), an ESR signal is observed which is consistent with the presence of $VO(OH)_3{}^-$, however, this signal is observed over this limited pH range only and the intensity is only about 10% of that expected for the vanadium(IV) system in the absence of citrate.

3.3 Vanadium-51 FT-NMR

The vanadium(IV): citrate solutions which displayed low intensity ESR signals were subsequently analyzed using vanadium-51 FT-NMR. These NMR data are displayed in figures 3.15 to 3.20 and are tabulated in Appendix G. The reader should consult these diagrams during the following discussion.

Six resonances were observed in all over the chemical shift region of -573 ppm to -533 ppm (with respect $VOCl_3$ reference). The resonances in the above group can be further subdivided into four resonances that were observed below a pH of 9.00 and two resonances that were observed only above this pH level (see table 3.3).

Upon comparing the nmr spectra obtained with that of similar vanadium(V) systems,[1] it is apparent that similar resonances are observed. The manner in which these resonances vary as a function of pH, however, is quite different (see table 3.4). At this point subsequent UV/VIS analysis of basic nmr solutions were conducted to determine whether or not the solutions contained vanadium(IV) or vanadium(V). The resultant spectra were consistent with those of the vanadium(IV): citrate system. Therefore, it was concluded that the solutions contained primarily vanadium in oxidation state (IV).

The possibility that the nmr signals may have resulted from an extremely low concentration of vanadium(V), so low in fact, that it did not affect the UV/VIS spectra of the solutions, was considered. The spectral width setting of the nmr spectrometer was increased to

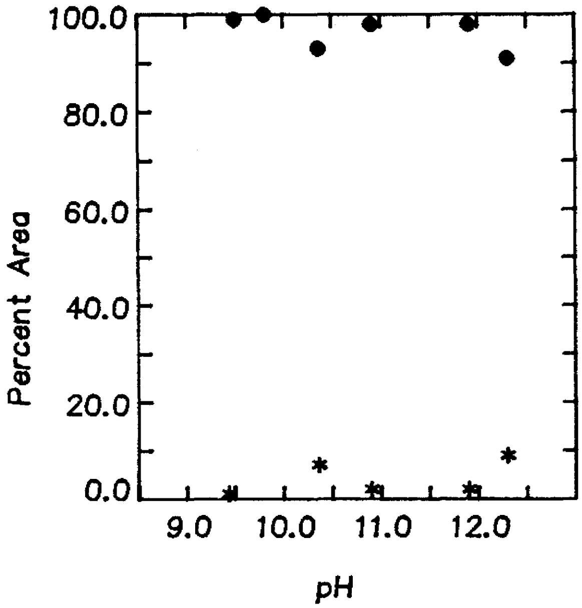

Figure 3.15: NMR Results

Percent peak area as a function of pH for vanadium(IV): citrate solutions which had been prepared for one week.

Legend:

Symbol	Chemical Shift (in −ppm)
●	533
*	556

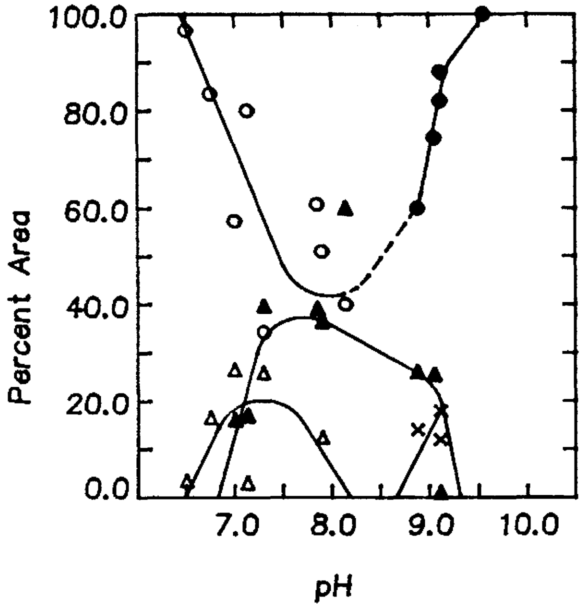

Figure 3.16: NMR Results

Percent peak area as a function of pH for vanadium(IV): citrate solutions which had been prepared for two weeks. The dashed line denotes a gradual change in the observed chemical shift value.

Legend:

Symbol	Chemical Shift (in −ppm)
●	533
○	543
Δ	553
*	556
×	563 to 560
▲	573

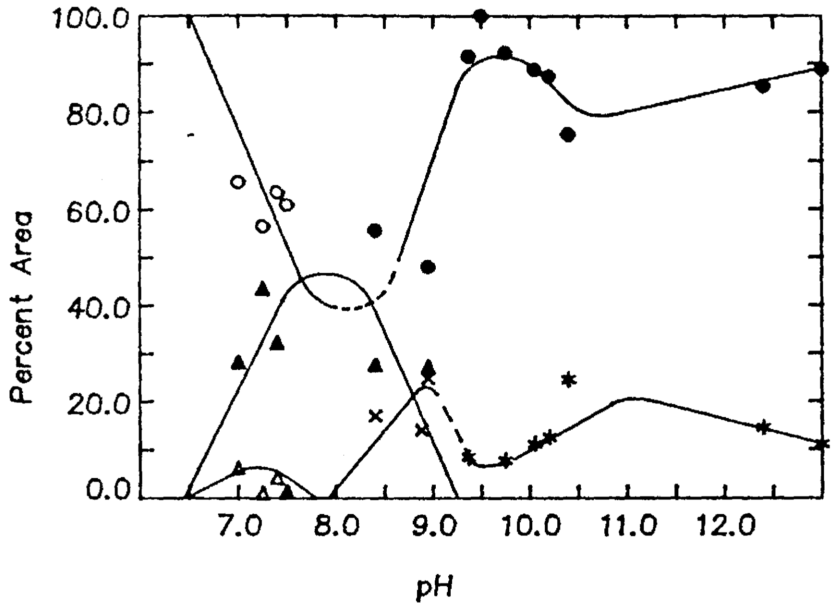

Figure 3.17: NMR Results

Percent peak area as a function of pH for vanadium(IV): citrate solutions which had been prepared for three weeks. The dashed line denotes a gradual change in the observed chemical shift value.

Legend:

Symbol	Chemical Shift (in –ppm)
●	533
○	543
△	553
✱	556
×	563 to 560
▲	573

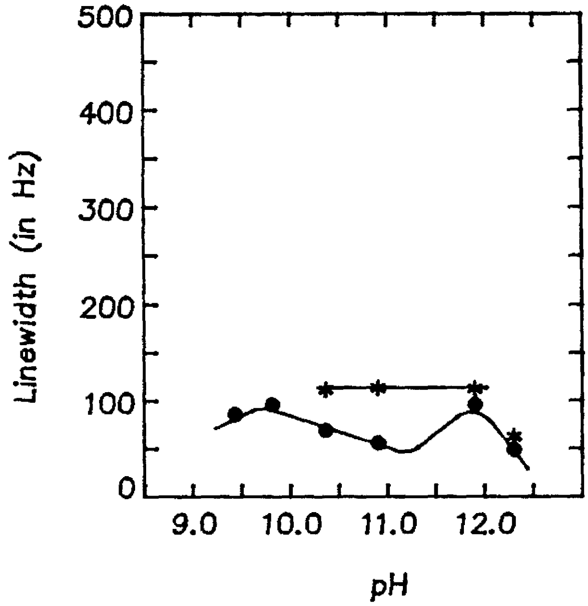

Figure 3.18: NMR Results

NMR linewidths as a function of pH for vanadium(IV): citrate solutions which had been prepared for one week.

Legend:

Symbol	Chemical Shift (in −ppm)
●	533
○	543
△	553
*	556
×	563 to 560
▲	573

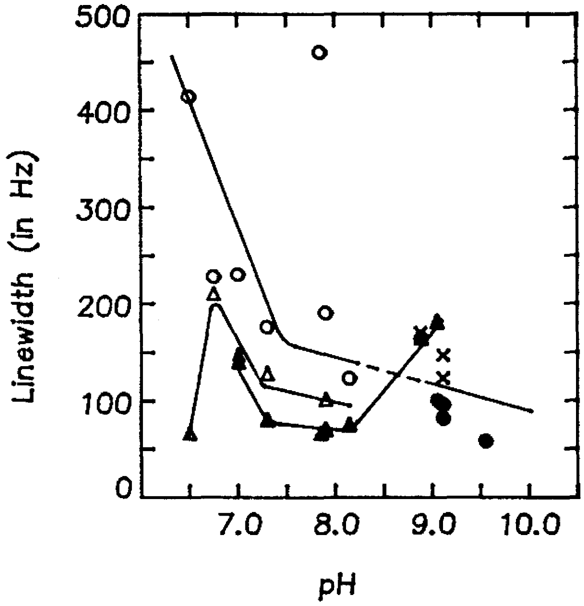

Figure 3.19: NMR Results

NMR linewidth as a function of pH for vanadium(IV): citrate solutions which had been prepared for two weeks. The dashed line denotes a gradual change in the observed chemical shift value.

Legend:

Symbol	Chemical Shift (in −ppm)
●	533
○	543
△	553
*	556
×	563 to 560
▲	573

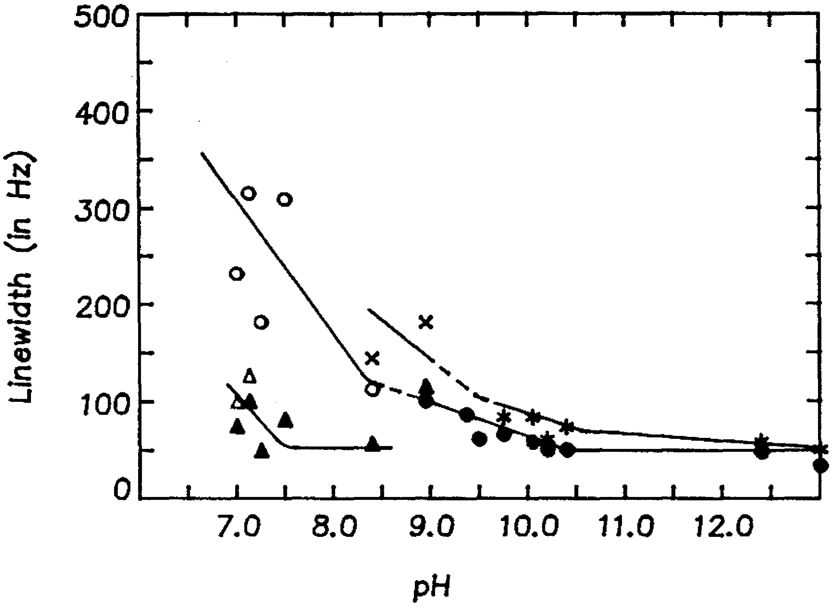

Figure 3.20: NMR Results

NMR linewidths as a function of pH for vanadium(IV): citrate solutions which had been prepared for three weeks. The dashed line denotes a gradual change in the observed chemical shift value.

Legend:

Symbol	Chemical Shift (in −ppm)
●	533
○	543
△	553
*	556
×	563 to 560
▲	573

Table 3.3: Specific pH Regions of Observed Resonances for the Vanadium(IV): Citrate System

Resonances Observed Below pH of 9.00

Chemical Shift (in - ppm)	pH Region
543	6.50 to 8.50
553	6.50 to 8.50
563	8.50 to 9.20
573	6.50 to 9.00

Resonances Observed Above pH of 9.00

Chemical Shift (in - ppm)	pH Region
533	9.00 to 12.50
556	9.00 to 12.50

Table 3.4: Specific pH Regions of Observed NMR Resonances for Vanadium(IV) and Vanadium(V): Citrate Systems

Chemical Shift (in - ppm)	Vanadium(IV): Citrate	Vanadium(V): Citrate
533	9.00 to 12.50	9.50 to 12.80
543	6.50 to 8.50	6.00 to 9.00
553	6.50 to 8.50	not observed
556	9.00 to 12.50	10.00 to 12.80
563	8.50 to 9.20	9.00 to 10.20
573	6.50 to 9.00	6.90 to 10.00

25,000 Hz, to determine if any new resonances could be observed. No additional nmr signal were observed and subsequent measurements were made using a narrow spectral width of 10,000 Hz covering the spectral area of interest.

The possibility that the vanadium(IV): citrate solutions were being oxidized by oxygen to vanadium(V) during the time that the nmr measurements were being made was considered as a possible explanation of the observed spectra. To determine if any change occurred during the nmr analysis time, the ESR spectra were acquired for the solution before and after. In every case, the intensities of the ESR signals were the same, within experimental error, before and after the nmr spectra were acquired. This result indicates that the manner in which the nmr tubes were sealed was effective in protecting the sample from oxygen contamination.

Upon initial inspection of Figure 3.21, it may appear that a correlation between shielding and formal oxidation state exists. This observation would imply a significant contribution to the variations in the overall shielding due to the local diamagnetic term. It is well established, however, that the variations in the overall shielding (and the chemical shift) are dominated by variations in a paramagnetic term. This term has its origin in the residual paramagnetism imparted by excited states and represents the major deshielding contribution.[29] Based on these facts, Rehder[29] concluded that there is no necessary correlation between chemical shift and oxidation state. Therefore, any similarity in chemical shift between the vanadium(V): citrate system and the vanadium(IV): citrate system must be due to similar nuclear

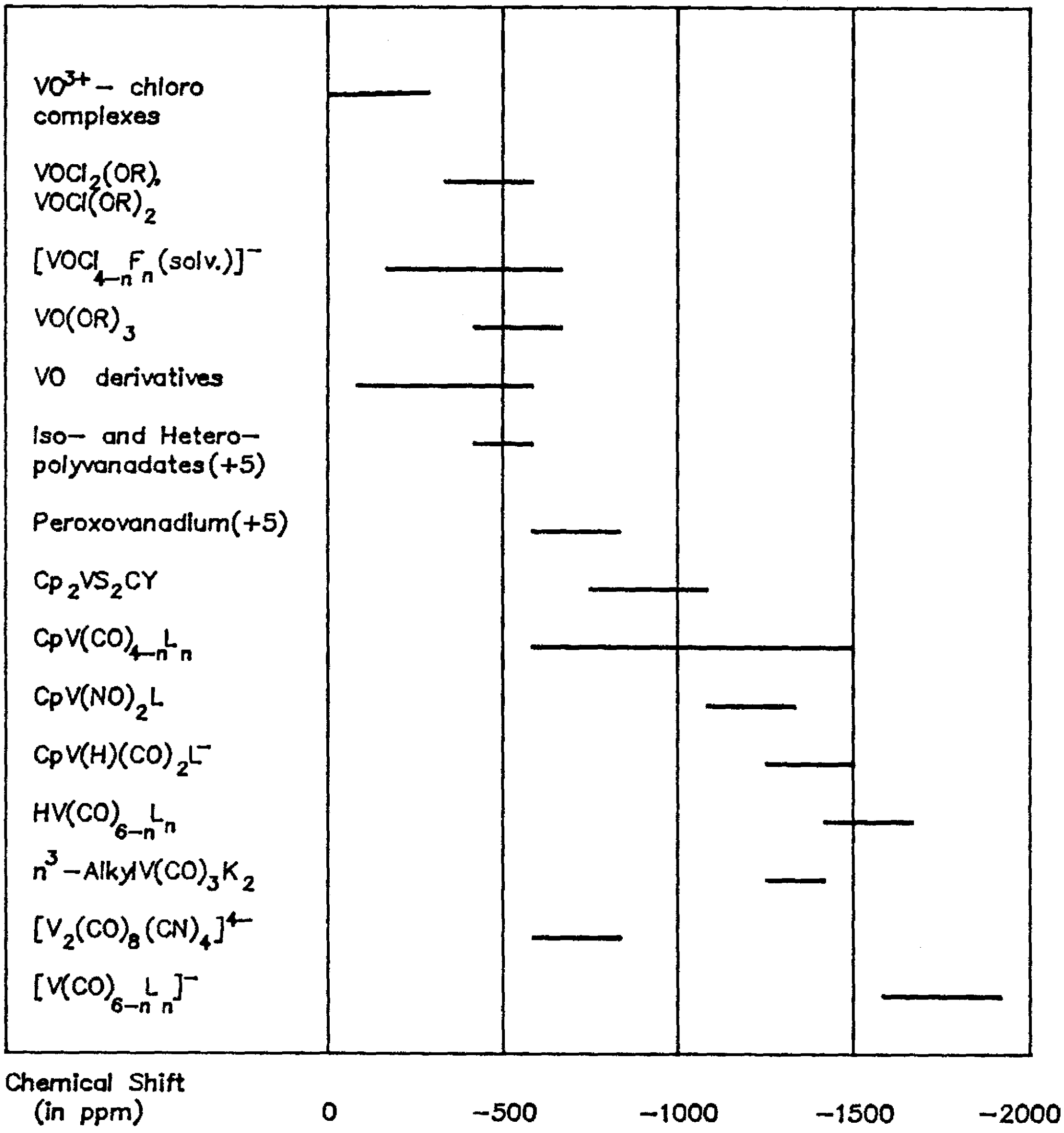

Figure 3.21: Typical Vanadium–51 Chemical Shifts in ppm Relative to $VOCl_3$.

environments and is not dependent on formal oxidation state.

From the nmr data acquired, the ratio of the peak areas and the linewidths at half-height were observed "to fluctuate" somewhat. This appears to be dependent on the maturing time of the solutions, small pH changes, and small changes in the total vanadium concentration. This is consistent with the fact that vanadium(IV) systems are slow to attain equilibrium and that the ratio of the polyanions is highly pH and total vanadium concentration dependent.

NMR spectra were obtained of solutions which had a vanadium to citrate ratios of 1:1 and 1:1.6. No differences in terms of chemical shift, linewidth, or percent peak area were observed. This would indicate that the species in solutions are insensitive to change in total citrate concentration.

At pH value greater than approximately 9.00 only two resonances exhibiting relatively narrow linewidths were observed; namely, -533 and -556 ppm. The species responsible for these resonances also appeared to be in equilibrium. As maturing time increased, so did the percent area of the -556 ppm resonance, which increased until the relative ratio of the -533 to -556 resonace was approximately 4:1 (see figures 3.15 and 3.17).

The linewidth of the -533 resonance (40 to 80 Hz) was always observed to be less than that of the -556 resonance (50 to 100 Hz). This observation would infer that the species which gives rise to the -533 resonance must have a more symmetrical electronic environment about the vanadium nuclei which results in inefficient quadrupolar relaxation and, therefore, narrower linewidths (see figures 3.18 to

3.20).

These trends are similar to those in the vanadium(V): citrate system which have been investigated.[1]. The -535 resonance in the vanadium(V) system has been attributed to the $[VO_4]^{3-}$ species.

In the vanadium(IV): citrate system, the resonance at -533 cannot be attributed to such a mononuclear vanadium species, since such a species would contain an unpaired electron and the nmr spectra would probably not be obtainable. The ESR data in this pH range indicates the presence of an ESR active species in extremely low concentration. It is possible for an ESR active species to be observed using nmr techniques under certain circumstances; however, the nmr resonance observed would have an increased linewidth due to the increased relaxation of the vanadium nucleus. Clearly, this is not the case in the present situation, since the linewidth displayed by this resonance is rather narrow (40 to 80 Hz). Therefore, the resonances at -533 can not be attributed to a mononuclear vanadium species and must be the result of a dimer or polymer.

In the vanadium(V) system, the -555 ppm resonance has been associated with the $[V_2O_7]^{4-}$ species. In the vanadium(IV): citrate system it is possible that this chemical shift may result from a vanadium(IV) species which has a similar nuclear environment, such as $V_2O_5^{2-}$. Such a species should not only give rise to a similar chemical shift but also a similar linewidth, due to similar symmetry which could exist between these vanadium(IV) and vanadium(V) species. The linewidth observed for this resonance in the vanadium(IV): citrate system is equal, within experimental error, to that reported for the vanadium(V) system[30]. This supports the idea of the species having a similar nuclear environment.

As the pH decreased below 9.00, the resonance at -533 ppm broadened and slowly shifted upfield until a maximum of -546 ppm was observed at a pH value of approximately 8.00. As the pH decreased further, this peak shifted slightly downfield to -543 ppm.

A similar behaviour is observed in the vanadium(V) system (in the absence of citrate),[31] in which the peak broadens and shifts from -533 to -537. This has been attributed to the protonation of the $[VO_4]^{3-}$ species coupled with an exchange process between $[HVO_4]^{2-}$ and $[HV_2O_7]^{3-}$.[31]

In the vanadium(IV): citrate system, a similar increase in the linewidth and the upfield shift are observed, but the shift goes further upfield. This would indicate that protonation is occurring. The increase in linewidth cannot be explained by the presence of an ESR active species in solution, since the ESR data indicates the highest concentration of ESR active species occurs at a pH value of 10.00. At this pH value, the nmr linewidths arising from both resonances are still relatively narrow. Therefore, the increased linewidths must be due to an exchange process or possibly due to the formation of species which have lower symmetries and/or longer correlation times.

In the vanadium(V) system, in the absence of citrate, no resonance is observed at -543 ppm, however, when citrate is present with the vanadium(V), a new resonance is observed at -543 ppm. Based on this fact, this resonance has been assigned to a vanadium(V): citrate complex.

In the vanadium(IV) system, it is not possible to acquire the nmr spectra of vanadium(IV) in the neutral pH range in the absence of citrate due to the precipitation of $VO(OH)_2$. Based on information acquired from the vanadium(V): citrate system, the -543 resonance in the vanadium(IV): citrate system is assigned to a vanadium(IV): citrate complex which must be at least a dimer. The observation that as the pH is increased the -543 resonance shifts upfield before it begins to shift downfield may indicate that the vanadium(IV): citrate complex may be cyclic and the shift upfield could be the result of the cyclic structure opening up in analogous manner to the species responible for the -573 and -583 resonances in the vanadium(V) system. The subsequent downfield shift is probably the result of deprotonation which converts this complex to the one responsible for the resonance at -533 in basic solutions.

As the pH drops below 9.5 the resonance at -556 also slowly shifts upfield to -563 and then disappears at a pH of approximately 8.00 to 8.50.

In the vanadium(V) system, a resonance at -556 is observed to broaden and slowly shift upfield to a value of -568 at a pH of approximately 10.00. This upfield shift was attributed to the protonation of $[V_2O_7]^{4-}$ to $[HV_2O_7]^{4-}$. It was suggested that the increase in linewidth was the result of the protonation reaction coupled with exchange between $[HVO_4]^2$ and $[HV_2O_7]^{3-}$. The exchange between these vanadium(V) species is supported by evidence which indicates $[HVO_4]^{2-}$ has a tendency to form hydrogen bonded dimers.[31] As the pH level of the vanadium(V) system is further decreased to 7.5 it was observed that the resonance at -568 coalesced with a resonance observed at -573[31].

In the vanadium(IV): citrate system, a similar shift upfield was observed, but not to the same extent and not over the same pH range. This would infer that the species being protonated must have a similar structure to the species in the vanadium(V) system, though differences do exist as is reflected by difference in the extent of the chemical shift. Furthermore, as the pH was decreased in this region a noticeable increase in the linewidth of both the -563 and the -573 resonances was observed. This suggests the possibility that these two complexes are in equilibrium and undergo exchange.

The resonance at -573 ppm was only observed in the pH range 6.50 to 9.00. Over this pH range the linewidth remained more or less constant - increasing slightly at the extreme pH limit of approximately 8.90.

In the vanadium(V) system, this resonance is attributed to the presence of anion of the form $[(VO_3)_X]^{X-}$. There has been controversy over whether this anion is tetrameric or trimeric. Based on the most recent work done in this laboratory[30] on the vanadium(V) system, it would appear that the exact structure may depend on the analytical concentration of the vanadium and that the resonance actually is the result of both species being in equilibrium. Furthermore, in the vanadium(V) system a further resonance is observed at -582 in this pH range. This resonance has been attributed to the acyclic form of the species which gives rise to the -573 ppm resonance. Since this chemical shift is identical in the vanadium(IV) and (V) systems, this would indicate that the species which gives rise to the -573 ppm in the vanadium(IV) system must be similar in nuclear environment to that of the vanadium(V) system. The absence of the peak at -582 ppm would infer that either the species responsible for the -573 ppm resonance is either stabilized by the presence of citrate, thus not allowing the cyclic species to open, or that the species is slightly different from that found in the vanadium(V): citrate system. With these facts in mind, the -573 ppm resonance in the vanadium(IV): citrate is assigned to the $V_4O_7^{2-}$ species.

Below a pH of 8.00, another new resonance is observed at -553 ppm. This peak remains at this resonance over the complete pH range 6.50 to 8.00. The nmr spectra of some solutions were acquired both after a maturing time of 8 days and 24 days. Upon standing, the resonance at -553 showed a marked decrease while the the resonance at -543 increased. This may infer a slow attainment of equilibrium between the two species responsible for these resonances.

From the vanadium(V) system, it has been concluded that such a chemical shift at -553 arises from a dimer of the form $(V_2O_7)^{4-}$. Since a similar chemical shift is observed in the vanadium(IV): citrate system, it may be inferred that this also is due to a dimer or, at least, a species with a similar nuclear environment. From the nmr spectra gathered as a function of time, it appears that the species which give rise to the resonances at -543 and -553 ppm are in equilibrium. Upon inspection of the tabulated linewidths of these peaks, it may appear that the resonance at -553 has a linewidth that is narrower than that of the -543 resonance. This, however may not be the case, since the peak located at -553 ppm is a shoulder on the -543 ppm resonance and the linewidth at half-height had to be subsequently estimated using a curve fitting program. With this in mind, it is proposed here that the two resonances observed at -543 and -553 ppm actually have, within experimental error, the same linewidths.

As was previously mentioned, in the vanadium(V) system the species at -573 is attributed to a cyclic complex of the form $[(VO_3)_X]^{X-}$, while the resonance at -582 is attributed to a similar acyclic species. Therefore, it appears that an upfield shift of approximately 10 ppm is associated with the opening of the cyclic complex.

In the vanadium(IV): citrate system, it would appear that an analogous situation exists between the -543 and -553 ppm resonance. The -543 ppm peak has been assigned here to a citrate complex which must be at least a dimer. Therefore, the existence of a peak 10 ppm upfield which is observed to be in slow equilibrium with the complex responsible for the -543 resonance would infer the possibility that the -553 ppm resonance may be the result of an acyclic species which has a structure similar to the complex responsible for the -543 ppm resonance.

3.3.1 Summary of NMR Data

Based on a survey of vanadium-51 nmr data and on theoretical considerations, Rehder[29] concluded that there is no necessary correlation between chemical shift and oxidation state. This, coupled with the UV/VIS and ESR data gathered during this study has led to the conclusion that the six nmr resonances observed are the result of vanadium(IV) species which have similar nuclear environments to those responsible for corresponding resonances in the nmr spectra of vanadium(V): citrate solutions. This gives rise to similar chemical shifts. The following observations and conclusions based on the data have been proposed:

(1) Peak areas and linewidths in the vanadium(IV): citrate system were observed to vary somewhat and appeared to depend on solution "maturing" time, small pH changes and small changes in total vanadium concentration across a solution series.

(2) NMR spectra of solutions, which contained 1:1 and 1:1.6 ratios of vanadium(IV):citrate yield identical nmr spectra, indicating that the species present are insensitive to total citrate concentration.

(3) The species responsible for the -533 resonance is more symmetrical and/or has a shorter correlation time than the species responsible for the -556 ppm resonance, but both appear to be in equilibrium.

(4) Species at -533 must have a similar nuclear environment as the vanadium(V) $[VO_4]^{3-}$ but must be a dimer or a polymer due to the lack of esr activity.

(5) The species responsible for the resonance at -533 ppm appears to be related to the -543 species as reflected by the gradual peak shift. Since the peak is observed to shift on the nmr time scale, this would infer a fast reaction such as deprotonation may be important.

(6) The species which displays the resonance at -543 is assigned, by analogy to the vanadium(V): citrate system, to a vanadium(IV): citrate complex.

(7) From the slight upfield shift of the -543 resonance before a subsequent downfield shift to -533 as the pH is increased suggests that the proposed cyclic vanadium(IV): citrate complex may be opening as deprotonation occurs.

(8) The evidence tends to suggest that the species responsible for the -543 ppm resonance and the -553 resonance are in equilibrium. The 10 ppm shift difference would infer that the -553 peak maybe the result of an acyclic complex which is similar to the vanadium(IV): citrate species responsible for the -543 ppm resonance. Since no gradual shift is observed between these peaks, it would infer that the interconversion reaction is slow on the nmr time scale.

(9) The -556 ppm resonance in basic solution is assigned, by analogy to the vanadium(V) system, to be the result of presence of $[V_2O_7]^{4-}$. The shift upfield as the pH is decreased is then attributed to protonation of this species.

(10) Linewidth considerations would infer that the species responsible for the -563 ppm shift may also be in equilibrium with species which gives rise to the -573 resonance.

(11) The -573 resonance was assigned, by analogy with the vanadium(V)

system, to be the result of the $[V_4O_7]^{2-}$ species. The lack of a resonance at −582 infers that this cyclic complex must be stabilized perhaps by the presence of the citrate ligand in the solution.

The specific pH ranges over which these species exist are outlined in figures 3.22 and 3.23.

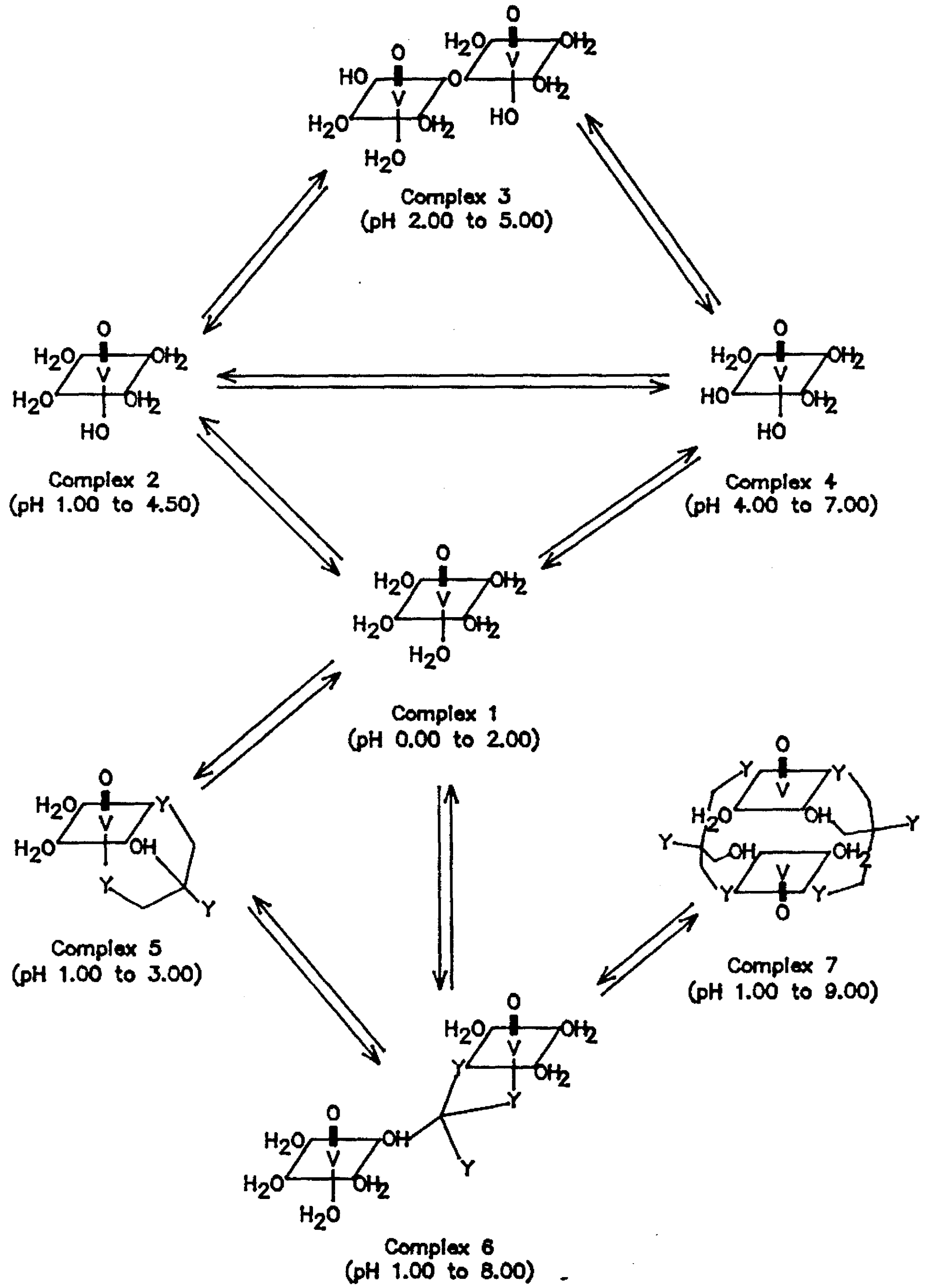

Figure 3.22:

Proposed structures for the vanadium(IV): citrate system in acidic and neutral solution. Complex 2,3 and 4 are minor constituents.

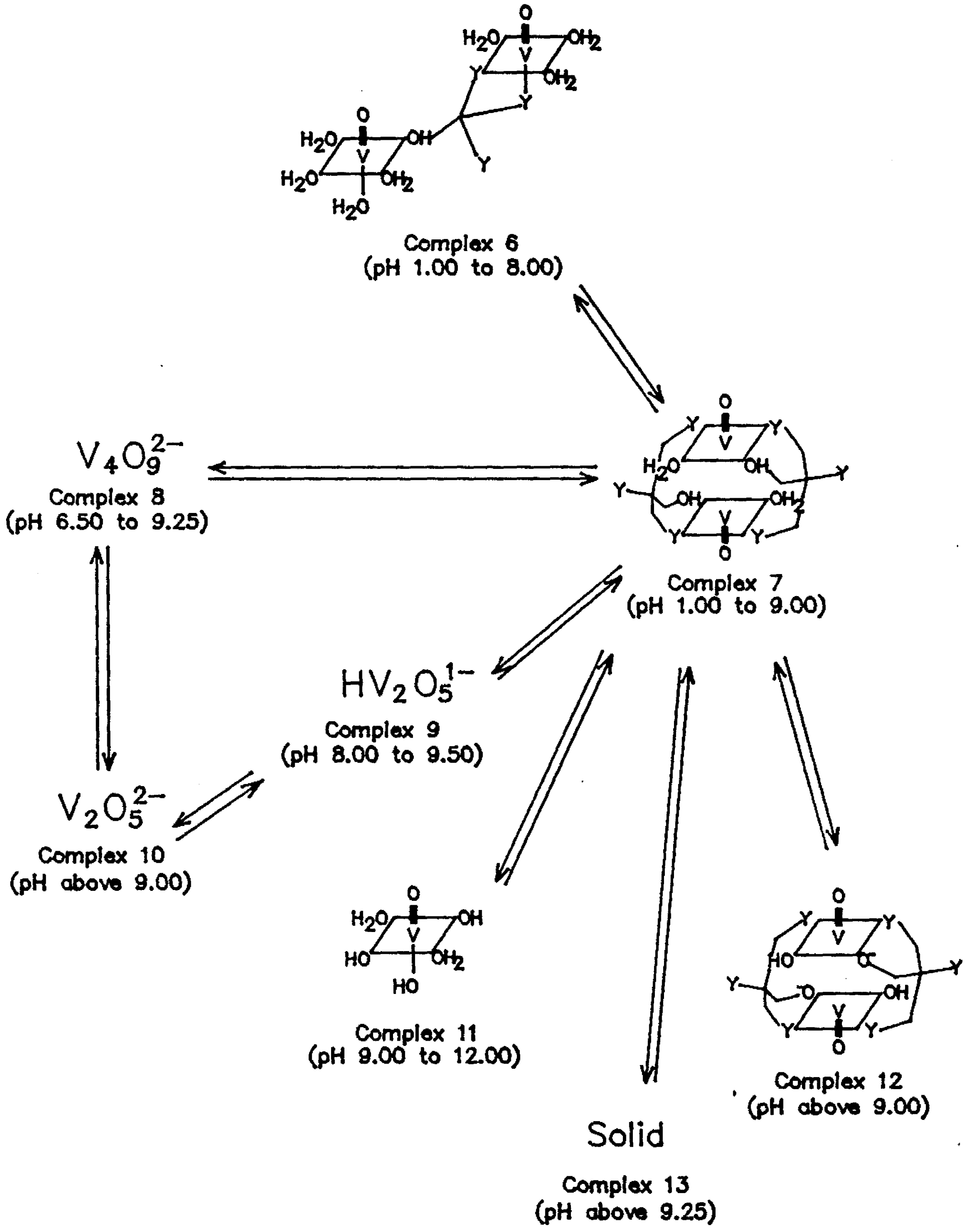

Figure 3.23:

Proposed structures for the vanadium(IV): citrate system in neutral and basic solution.

3.4 Proposed Structures

UV/VIS, ESR and vanadium-51 FT-NMR results and conclusions are summarized in table 3.5. Based on these results, the species illustrated in Figures 3.22 and 3.23 have been proposed.

In the pH range 1.00 to 2.00, the ESR spectral data display a sharp drop in relative signal intensity accompanied by little change in the hyperfine coupling constant until a pH of approximately 1.50. The hyperfine coupling constant in this pH range is consistent with that reported by Francavilla and Chasteen[18] for the esr active hydrated VO^{2+} species, complex I (see figure 3.22). The sharp drop in signal intensity was not observed by Francavilla and Chasteen[18] in the vanadium(IV) system (in the absence of citrate). They observed only a gradual decrease in intensity over the pH range 2.00 to 4.50, which they attributed to the formation of $(VOOH)_2^{2+}$. In the vanadium(IV): citrate system, this rapid decrease in signal intensity which was observed cannot be solely attributed to the formation of this dimer. Therefore, it is proposed that this rapid drop in signal intensity is the result of two possible vanadium: citrate complexes, complex 6 and complex 7 (see figure 3.22). The complex must be a least a dimer to result in the coupling of the unpaired electrons and subsequent drop in esr activity of the solution but whether it is a 1:2 or a 2:2 binuclear complex (with respect to vanadium) is unclear and cannot be concluded from the present data. The formation of a dimer of the form $(VOOH)_2^{2+}$ (complex 3) can not be excluded; however, the rapid

Table 3.5: Summary of Results

Source	pH range	Comment
UV/VIS	up to 9.50	-Spectra consistent with vanadium(IV): citrate
UV/VIS	above 9.50	-Spectra is the result of species in addition to $VO(OH)_3^-$ and, therefore the citrate ligand has a significant effect even in basic solution
UV/VIS	basic	-Solution are extremely oxygen sensitive and the resulting spectra is significantly different from the vanadium(IV): citrate system
UV/VIS	2.00- 7.00	-Isosbestic point present at 750 nm which indicates at least two species in equilibrium over this pH range
ESR	1.00- 3.00	-Drastic drop in esr intensity; cannot be attributed solely to $(VOOH)_2^{2+}$ -Citrate ligand has significant effect on esr spectra probably due to dimer formation

Table 3.5: Summary of Results cont'd

Source	pH range	Comment
ESR	1.00- 5.00	-Evidence of more than one esr active species
ESR	4.00- 7.00	-No sign of $VO(OH)_2$ precipitation
ESR	6.00- 9.00	-Low intensity esr signal, approximately .2% of reference solution
ESR	9.00-11.50	-Low intensity esr signal (about 10% reference solution); similar line splitting as $VO(OH)_3^-$ -Species only observed over limited pH range
ESR	above 9.25	-Precipitation of esr active black solid
ESR/ UV-VIS	above 6.50	-Verification that no oxygen contamination had occurred to the nmr solutions
NMR	6.50- 12.50	-Peak areas and linewidths appear to be affected by solution age, pH changes and total vanadium concentration -Spectra not affected by a change in vanadium: citrate ratio from 1:1 to 1:1.6 .

Table 3.5: Summary of Results cont'd

Source	pH range	Comment
NMR	6.50- 8.50	-Resonance at -543 ppm assigned to cyclic vanadium(IV): citrate complex with 1:1 ratio
NMR	6.50- 8.50	The -553 ppm resonance appears to be in equilibrium with -543 ppm resonance -Resonance at -553 assigned to acyclic form of vanadium(IV): citrate which was responsible for resonance at -543 ppm
NMR	6.50- 9.00	-Resonance at -573 ppm assigned to $V_4O_9^{2-}$
NMR	8.50- 9.00	-Disappearance of -553 ppm resonance
NMR	above 8.50	-Gradual shift of -543 resonance upfield then downfield to -533 which is attributed to opening of cyclic vanadium(IV): citrate complex followed by deprotonation -Species must be similar to vanadium(V) species (VO_4^{3-}) which gives rise to similar resonance, except it must be polymeric due to lack of esr activity

Table 3.5: Summary of Results cont'd

Source	pH range	Comment
NMR	above 8.50	-Appearance of resonance at -563 ppm, which shifts downfield upon deprotonation -563 ppm species maybe in equilibrium with species at -573 - The -563 ppm resonance assigned to $V_2O_5^{2-}$ and its' protonated form
NMR	above 9.25	- only two resonances observed: -533 and -556 - The species responible for these resonances appear to be in equilibrium, with the concentration of -556 increase with time

drop in signal intensity in this low pH range would indicate that if this dimer is present it is probably a minor constituent.

At a pH of approximately 1.50, the hyperfine coupling constant shows a gradual decrease in magnitude which would indicate the presence of at least another esr active species (complex 2) in equilibrium with the hydrated VO^{2+} species. This maybe the result of the hydrolysis of the VO^{2+} moiety or maybe attributed to a 1:1 vanadium: citrate mononuclear complex (complex 5). Based on UV/VIS data, Nikolova[20] has reported the presence of two vanadium: citrate complexes in acidic solutions:

(1) a strong 1:1 (mononuclear) vanadium: citrate complex over the pH range 2.00 to 9.00; and,

(2) a 2:1 (binuclear species with respect to vanadium) in acidic solution over the pH range 2.00 to 3.50[10].

The presence of a 2:1, binuclear vanadium(IV): citrate complex, complex 6, is consistent with the esr spectral data. The presence of the hydrolysis product of VO^{2+} cannot be excluded, based on the data observed, however, the lack of precipitation of $VO(OH)_2$ (complex 4) at higher pH levels would tend to infer that the presence of citrate inhibits the hydrolysis of vanadium(IV).

The UV/VIS spectra observed in the pH range 2.00 to 9.00, are consistent with that of vanadium: citrate complexes[20]. The presence of an isosbestic point over the range 2.00 to approximately 7.00 indicates the presence of at least two species in equilibrium. This coupled with the esr results and the data reported by Nikolova would suggest that in the pH range 1.00 to 7.00 there probably exists three vanadium: citrate complexes which are in equilibrium: a 1:1 mononuclear complex (complex 5), a 2:2 binuclear complex (complex 7) and a 1:2 binuclear complex (complex 6). Nikolova's[20] data showed that above a pH level of approximately 3.5 a vanadium: citrate complex with a 1:1 ratio was stable, however, based on esr results obtained it appears that this complex is a 2:2 binuclear complex (complex 7) as is illustrated by the lack of esr activity in this pH range (see Figure 3.14).

The presence of the hydrolysis products of VO^{2+}, namely $VO(OH)^+$ (complex 2) and $(VOOH)_2{}^{2+}$ (complex 3), can not be excluded on the basis of the observed data. The lack of precipitation of $VO(OH)_2$ (complex 4), however, would indicate that the solubility product ($S = 10^{-22}$) is not exceeded, therefore, if these species are present then they must be minor constituents.

NMR signals observed in the pH region above 6.50 were assigned to vanadium(IV) species which had similar structure and, therefore, similar nuclear environment as vanadium(V) species, thus giving rise to similar chemical shifts. The assumption that chemical shift and oxidation state are not necessarily correlated is supported by Rehder[29], who based his finding on a survey of vanadium-51 nmr data, as well as theoretical considerations. This was further supported by esr and UV/VIS data which indicated that nmr resonances observed resulted from solutions containing vanadium in an oxidation state of +4.

In the pH region 7.00 to 9.00, four resonances were observed, namely -543,-553,-563 and -573 ppm (with respect to an external $VOCl_3$ reference). The data obtained indicates that the species responsible for the chemical shifts at -543 and -553 are in equilibrium. The species responsible for the -543 ppm resonance appears to be the most thermodynamically stable, as it relative peak area increased as a function of time. In the similar vanadium(V): citrate system[30], the resonance at -543 ppm was assigned to a 1:1 vanadium(V): citrate complex, subsequently the similar resonance in the vanadium(IV): citrate system is assigned to a species with a similar structure: complex 7. The structure of the cyclic complex 7 is similar to the structure which has been proposed for a solid state vanadium: tartrate[32] complex.

The 10 ppm difference between -543 and -553 could be rationalized in an analogous manner to the vanadium(V) system where the -573 ppm resonance is attributed to a cyclic species whereas the -582 ppm resonance is assigned to the related acyclic complex. This coupled with the fact, that species responsible for the -543 ppm resonance appears to be in equilibrium with the -553 species supports the idea that the -553 resonance could the be the result of a acyclic species (complex 6) which is related to complex 7 (see Figure 3.23). Additional support is added to this proposal by the fact that in the vanadium(V) system a similar resonance which has been attributed to a vanadium dimer. This resonance in the vanadium(V) system, however, does not occur over the same pH range. This would infer that the resonance observed in the vanadium(IV): citrate system has a similar nuclear environment, however, it does not arise from a citrate-free species.

The slight upfield shift to -546 and the subsequent gradual downfield shift to -533 of the original -543 ppm resonance can be rationalized by the opening of the cyclic complex 7 followed by rapid exchange of protons which results in the gradual increase in the concentration of complex 12. This is consistent with a shift to lower negative chemical shift values upon substituting of a ligand which is a weaker sigma donour into the complex (ie. OH^- is a weaker sigma donour than H_2O).

The species which give rise to the -573 ppm resonance in the vanadium(V): citrate system was concluded to arise from a citrate free complex of the form $V_3O_9^{3-}$ and/or $V_4O_{12}^{4-}$. On this basis, our observed resonance at this value is attributed to the presence of an isopolyanion of the form $V_4O_9^{2-}$ (complex 8). It is proposed that the presence of the oxygen moieties can result in a similar vanadium nuclear environment as $V_4O_{12}^{4-}$, thus giving rise to a similar chemical shift.

In the vanadium(V): citrate system, the resonance observed at -563 over the pH range 8.00 to 9.00 has been attributed to the presence of a protonated isopolyanion of the form HV_2O_7. Similarly, in the vanadium(IV): citrate system, this resonance is assigned to a similar species, namely $(HV_2O_5)^-$ (complex 9). As the pH increases, a gradual shift to -556 is observed, as well as a decrease in linewidth. These observations are consistent with the formation of complex 10 (see Figure 3.23). The gradual shift in the observed resonances and the decrease in linewidth is rationalized by an exchange process between these two complexes in which the protons "flip on and off" very rapidly on the nmr time scale.

The increase in esr signal intensity in the pH range 9.00 to 12.00 can be rationalized by the decomposition of complex 7 in basic solution to yield the esr active species: $VO(OH)_3^-$ (complex 11).

The formation of a esr active black precipitate (complex 13) was observed in basic solutions (pH > 9.00). Upon X-ray crystal diffraction analysis of the solid, an extremely large unit cell was observed. However, attempts to carry out a more detailed X-ray diffraction analysis was not possible as subsequent samples were found be amorphous in nature.

3.5 Summary and Conclusions

The vanadium(IV): citrate system was investigated over the pH range 0.50 to 12.50 using UV/VIS, ESR and vanadium-51 FT-NMR spectroscopic methods. The data obtained suggested the formation of at least 13 aqueous species (complex 1 to 13, see Figures 3.22 and 3.23) over the pH range studied. Of these 13 aqueous species, at least four were attributed to vanadium(IV): citrate complexes while the other eight were attributed to aqueous vanadium(IV) species. The vanadium(IV): citrate species appear to exist in the pH region 2.00 to 12.50. It also appears that the presence of citrate in these solutions inhibited, to some degree, the hydrolysis of the vanadium(IV). The equilibrium concentrations of all the species appear to be extremely sensitive to small pH changes, as well as the total vanadium concentration.

References:

(1) Habayeb, M.A., ^{51}V, ^{13}C, and ^{1}H FT-NMR Studies on Vanadium(V) species in Aqueous Solution, Ph.D. Thesis, McMaster University, April, 1981.

(2) Selbin, J., Chem. Rev., 65(2), 153(1965).

(3) Selbin, J., Coord. Chem. Rev., 1, 293(1966).

(4) Dodge, R.P., Templeton, D.H., and Zalkin, A., J. Chem. Phys., 35, 55(1961).

(5) Wuthrich, K., and Connick, R.E., Inorg. Chem., 7(7), 1377(1968).

(6) Reuben, J., and Fait, D., Inorg. Chem., 6(3), 579(1967).

(7) Reuben, J., and Fait, D., Inorg. Chem., 8(9), 1821(1969).

(8) Hart, A.B., and Partington, J.R., J. Chem. Soc., 1532(1940).

(9) Balhausen, C.J., and Gray, H.B., Inorg. Chem., 2, 426(1963).

(10) Ducret, L., Ann. Chem., 6, 700f(1951).

(11) Rossotti, F.J.C., and Rossotti, H.S., Acta Chemica Scandinavia, 9, 1177(1955).

(12) Dean, G.A., and Herringshaw, J.F., Talanta, 10, 793(1963).

(13) Iannuzzi, M.M., and Reiger, P.H., Inorg. Chem, 14(12), 2895(1975).

(14) Ostrowetsky, S., Bull. Soc. Chim. France, 1012f(1964).

(15) Lingane, J.J., and Meites, L. Jr., J.A.C.S, 69, 102(1947).

(16) Lingane, J.J., J.A.C.S., 67, 182(1945).

(17) Griffith, W.P., and Wilkinson, T.D., J. Chem. Soc. A, 8, 1087(1966).

(18) Lingane, J.J., J.A.C.S., 69, 1882(1947).

(19) Pecsok, R.L., and Juvet, R.S., J.A.C.S., 75, 1202(1952).

(20) Nikolova, D.M., and Nikolova, G.S., J. Inorg. Nucl. Chem., 29, 1017(1966).

(21) Werguin, C.H., and Friedman, D., Bull. Soc. Chim. France, 25, 972(1958).

(22) Canneri, G., Gazz. Chim. Ital., 56, 637(1926).

(23) Ballhausen, C.J., and Gray, H.B., Inorg. Chem., 1(1), 111(1962).

(24) Francavilla, J., and Chasteen, N.D., Inorg. Chem., 14(11), 2860(1975).

(25) Wuthrich, K., and Connick, R.E., Inorg. Chem., 6(3), 583 (1967).

(26) Copenhafer, W.C., and Riegler, P.H., Inorg. Chem., 16(10), 2431(1977).

(27) Dodrell, D.M., and Gregson, A.K., Chem. Phy. Letters, 29(4), 512(1974).

(28) Wilkie, C.A., and Haworth, D.T., J. Inorg. Nucl. Chem., 40, 195(1978).

(29) Rehder, D., Quaterly Review of "ISMAR", 4(1/2), 33(1983).

(30) Habayeb, M.A., and Hileman, O.E., Jr., Canadian J. of Chem., 58(21), 2255(1980).

(31) O'Donnell, S.E., and Pope, M.T., J.C.S Dalton, 2290(1976).

(32) Forrest, J.G., and Prout, C.K., J. Chem. Soc. (A), 1312(1967).

(33) Walker, T.A., "Speciation Studies of the Vanadium(IV): Citrate System", Senior Thesis, McMaster University, Hamilton(1983).

APPENDICES

Appendix E: Determination of the Percent Composition of Vanadyl Sulfate

The percent composition with respect to vanadium of vanadyl sulfate was determined by the following conventional titrametric procedure, so as to determine the quantity of solid vanadyl sulfate required to prepare vanadium(IV): citrate solutions of the appropriate vanadium concentration.

E1.1 Required Reagents:

(1) sulfamic acid, 1:1 v/v aqueous solution

(2) concentrated nitric acid

(3) concentrated orthophosphoric acid

(4) saturated potassium permanganate solution

(5) sodium nitrate solution, 0.5% w/v

(6) concentrated sulfuric acid

(7) sodium diphenylamine sulphonate indicator tablets ("analoid")

(8) potassium dichromate, 0.05N

(9) ferrous ammonium sulfate, 0.05N (prepared by dissolving 19.6g ferrous ammonium sulfate hexahydrate in 1L of 25% (v/v) sulfuric acid - the sulfuric acid is present to prevent excessive deterioration of the ferrous reagent)

E1.2 Analysis Procedure:

The following analysis procedure is performed at least in duplicate:

(1) add 10 ml water and 5 ml sulfuric acid to a 500 ml conical flask,

(2) heat to boiling in a fume hood,

(3) pipette 10 ml of the vanadium sample into the flask - slowly and cautiously - allowing the solution to run down the side of the flask,

(4) add approximately 2 ml of nitric acid,

(5) boil the solution for approximately 15 minutes,

(6) allow the solution to cool for 1 hour,

(7) add the saturated potassium permanganate solution dropwise until a permanent pink colour is obtained which persists for at least on minute (approximately 15-20 drops),

(8) rinse down sides of the flask with distilled water,

(9) destroy the excess permanganate by addition of the 0.5% sodium nitrate, adding five drops at a time,

(10) add 10 drops in excess,

(11) rinse down the sides of the flask with distilled water,

(12) add 5 ml of 10% sulfamic acid and mix well,

(13) add 10 ml concentrated orthophosphoric acid and 7 drops of the indicator,

(14) titrate with 0.05N ferrous ammonium sulfate solution until the colour changes from purple to green.

E2.1 Calculation of Percent Composition (with respect to vanadium) of Vanadyl Sulfate:

The titration of vanadium with a standardized Fe^{2+} solution using the procedure outlined above was carried out. The freshly prepare Fe^{2+} solution was titrated with dichromate solution to determine the normality. This calculation is shown below:

Normality of dichromate used = N_a = 0.05493N
Volume of dichromate used = V_a = 9.25 ml
Normality of iron solution = N_b = ?
Volume of iron solution = V_b = 10 ml

Given that $N_aV_a = N_bV_b$

we can rearrange the expression to solve for the normality of the iron solution:

$$N_b = N_aV_a / V_b$$
$$= (0.05493)(9.25)/ 10$$
$$= 0.05081N \ (= 0.05081M \text{ in this case})$$

Therefore, the normality of the iron solution used in the subsequent vanadium titration was determined to 0.05081N.

In the subsequent titration of the vanadyl sulfate solution, 4.6 ml of the 0.05081N iron solution was consumed. Since one mole of Fe^{2+} reacts with one mole of vanadium, then the number of moles of vanadium in the 10 ml aliquot of solution containing 0.06028 g of vanadyl sulfate is = (4.6)(0.05081)/ 1000 = 0.0002337 moles

E2.2 Determination of Quantity of Water Associated with Vanadyl sulfate:

The quantity of vanadyl sulfate used in the 10 ml aliquot was 0.06028g. The molecular weight of $VOSO_4$ is 163 g/mole. From the titration we known there were 0.0002337 moles of vanadium present (ie. (0.0002337)(163) = 0.03809 g of vanadium). Therefore, there is (0.06028 - 0.03809 =) 0.02219 g (0.001233 moles) of water associated with the $VOSO_4$. Based, on this the ratio of the number of waters associated with $VOSO_4$ was determined to be 5.3.

The titration was carried out for four more samples with similar results being obtained. It was concluded that the number of water associated with $VOSO_4$ was approximately 5.00. This information was necessary to determine the quantity of vanadyl sulfate required to produce sample solution with a known vanadium concentration.

Appendix F: Preparation and Handling of the Vanadium(IV): Citrate Solutions

F1.1 Reagents Used:

Vanadyl sulfate ($VOSO_4 \cdot 5H_2O$)

Trisodium citrate ($Na_3C_6H_5O_7 \cdot 2H_2O$)

Sodium hydroxide (NaOH)

Sulfuric acid (H_2SO_4)

F1.2 Procedure

Solution series with a composition of 0.3M vanadyl sulfate and 0.3M tri-sodium citrate were prepared for the esr and nmr measurements. For the UV/VIS measurements, solutions with a composition of 0.016M vanadyl sulfate and 0.0274M tri-sodium citrate were prepared. A lower solution concentration was required for the UV/VIS measurements so that the absorptivity would not be greater than 3.00 in the spectral region of interest. The ratio of vanadium to citrate for the solution series used for esr and nmr measurements was 1:1, while that for the UV/VIS solution was 1:1.7. Excess citrate was used in the UV/VIS solutions to ensure excess was available for complexation with the vanadium. This excess citrate, however, did not affect the overall UV/VIS spectra of the solution, since it did not absorb in the spectral region of interest. Later, UV/VIS solutions were prepared with a 1:1 ratio to observe if this effected the spectra data significantly. The subsequent spectra which were observed appeared to be identical to those obtained from solution with a 1:1.7 ratio.

The appropriate amounts of the two reagents were weighed out. The reagents were then dissolve, under nitrogen, in 200 ml of distilled water which had been boiled (under nitrogen) to remove any carbon dioxide. Furthermore, any remaining dissolved gases (eg. oxygen) were removed using a ultrasonic bath and reduced pressure. The pH of the solution was then adjusted by the addition of 9M H_2SO_4 or a saturated solution of NaOH. Both were degassed prior to use.

Five to ten millilitres aliquots of the solution were then extracted at set pH levels using a syringe and were injected into nitrogen filled test tubes fitted with serum caps. All samples were then stored for a minimum of one week under nitrogen to allow time for the solution to come to equilibrium. After this time period, the pH of the samples were determined, once again under a blanket of nitrogen. The pH was measured using a Fisher pencil combination, gel filled electrode which was responsive over the pH range 0.00 to 14.00. The error associated with these measurements is estimated to be +/- 0.1 pH unit. The appropriate spectroscopic measurements were subsequently made. This entire procedure was carried out a nitrogen atmosphere utilizing a glove box.

F1.3 UV/VIS Analysis of Vanadium(IV): Citrate Solutions

Under a blanket of nitrogen, approximately three millilitres of the prepared solution were placed in an open rectangular UV/VIS absorption cell which had a path length of 10 cm. The cells were constructed of Spectosil UV silica, which is good for use in the range 170 to 25000 nm. The cells were then fitted with a telfon cap to prevent oxygen contamination and placed in the spectrophotometer.

The absorption spectra of the solution, which ranged in pH from 0.50 to 12.50, were measured using a Hewlett-Packard 8450A diode array spectrophotometer over a range of 200 to 800 nm. The samples were referenced against a distilled water sample contained in a similar absorption cell.

The oxygen sensitivity of solutions with a pH value of 12.40 and 7.00 were qualitatively determined by repeatitively recording the spectra of the sample after oxygen had been bubbled through it for set intervals of time.

F1.4 ESR Analysis of Vanadium(IV): Citrate Solutions

Samples of the prepared solution (at various pH levels) were loaded into 2 mm OD quartz esr sample tubes in a glove box under a blanket of nitrogen. The esr signals were recorded with a Bruker ER100D spectrometer operating at 9.77 GHz with a field modulation of 100 KHz and a microwave power of 12 dB. The mid-range field was set at 3440 G with a field sweep of 2000 G.

Two parameters of the resulting eight line spectra were measured and compared:

(1) The relative intensity of the $M_I = -3/2$ and $-1/2$ lines compared to solution at a pH level of 1.00; and,

(2) The hyperfine coupling tensor <a>.

The relative intensities of the esr signal were determined by measuring the first-derivative peak to peak intensity of the $M_I = -3/2$ and $-1/2$ lines. The value of the intensity of the signal at a pH level of one was assigned unity and all other intensities were assigned on a relative basis. The <a> tensor value was determined by measuring the distance along the base line between consecutive in phase sections of the esr signal. Both these parameters were measured for all solutions and subsequently compiled and compared on the basis of pH.

F1.5 NMR Analysis of Vanadium(IV): Citrate Solutions

Under a blanket of nitrogen approximately 2.0 ml of the prepared solutions were place in a 10 mm standard nmr tube which was fitted with a inner tube containing D_2O. The samples in the nmr tubes were isolated from the atmosphere by the use of a rubber sealing ring at the top of the tubes.

The nmr spectra for each sample was acquired at 23.66 MHz in a magnetic field of 2.1 T using a FT-NMR technique on a Bruker WH-90 spectrometer interfaced with a Bruker WP-80 data system. Frequency field stabilization was provided by locking onto the ^2H resonance of the D_2O located in the inner tube. A 90 degree pulse was used and was applied for periods of 30 microseconds, with a subsequent detection delay time of 100 microseconds. Initially, the spectral width was 25 KHz but was later reduced to 10 KHz to provide improved resolution over the desired range. All samples were externally referenced to neat $VOCl_3$ and chemical shifts were calculated in ppm, with negative values in the low frequency direction relative to the reference. The error associated with the chemical shifts is estimated to be +/- 0.20 ppm in the high pH region and +/- 1 ppm in the neutral solutions.

The resolution of overlapping peak areas were calculated using the Nicolet-1180 Curve Analysis Program (CAP). All linewidths were measured at half-height ($W_{1/2}$) and have an estimated uncertainty of +/- 10 Hz.

Appendix G: ESR and NMR Results

G1.0 ESR Results:

The vanadium(IV): citrate solutions were prepared and analyzed as outlined in Appendix B. The following tables of relative intensity of the M_I= -3/2 and -1/2 lines as well as the hyperfine coupling tensor <a> were obtained for five discrete solution series. An ESR signal was observed for all samples, however, in specific pH ranges the intensities were too low to accurately measure and are represented in the following tables by the use of a dashed line.

Table G1.1: ESR Results of Solution Series A

pH	M_I= -3/2	M_I= -1/2	<a>
0.81	0.920	0.960	112
2.00	0.456	0.504	109
3.40	0.045	0.058	99
4.50	0.024	0.035	99
6.51	-.---	-.---	---
7.20	-.---	-.---	---
8.15	-.---	-.---	---
9.31	0.028	0.036	83
10.30	0.058	0.077	84
12.30	-.---	-.---	---

Table G1.2: ESR Results for Solution Series B

pH	M_I= -3/2	M_I= -1/2	<a>
1.20	0.950	0.950	114
1.60	0.744	0.760	113
1.93	0.568	0.591	111
2.60	0.169	0.190	106
3.00	0.073	0.092	105
4.30	0.030	0.039	99
4.70	0.019	0.025	97
5.12	0.015	0.018	---
5.80	0.008	0.010	---
6.90	0.003	0.003	---
8.10	-.---	-.---	---
8.50	-.---	-.---	---
8.81	0.008	0.012	---
9.10	0.016	0.017	84
9.30	0.017	0.023	85
9.65	0.040	0.049	84
9.85	0.056	0.067	85
10.24	0.055	0.065	86
10.60	0.041	0.048	85
12.10	0.037	0.047	95

Table G1.3: ESR Results for Solution Series C

pH	$M_I = -3/2$	$M_I = -1/2$	<a>
0.61	0.922	0.907	114
0.79	0.921	0.962	114
1.00	1.00	1.00	114
1.21	0.951	0.954	113
1.40	0.913	0.926	113
1.60	0.829	0.854	113
1.80	0.769	0.771	112
2.29	0.450	0.483	111
2.72	0.189	0.227	108
3.20	0.074	0.099	106
3.69	0.048	0.069	98
3.80	0.051	0.069	103
4.00	0.044	0.066	97
4.30	0.040	0.056	103
4.90	0.030	0.038	101
5.37	0.019	0.024	95
5.89	0.011	0.016	---
6.50	-.---	-.---	---
6.95	-.---	-.---	---
7.00	-.---	-.---	---
7.25	-.---	-.---	---
7.35	-.---	-.---	---
8.11	-.---	-.---	---
8.80	0.006	0.011	---
9.40	0.023	0.030	83
9.92	0.065	0.079	81
10.12	0.072	0.085	84
10.35	0.051	0.066	83
10.42	0.050	0.063	84
12.29	0.048	0.058	93
13.05	0.091	0.102	94
13.32	-.---	-.---	---
13.55	0.161	0.176	95

Table G1.4: ESR Results for Solution Series D

pH	$M_I = -3/2$	$M_I = -1/2$	$\langle a \rangle$
0.05	0.686	0.673	113
0.63	0.816	0.810	114
1.20	0.950	0.950	114
1.41	0.942	0.942	114
1.90	0.846	0.861	114
2.31	0.693	0.716	112
2.75	0.436	0.466	111
3.10	0.221	0.238	111
3.21	0.105	0.118	108
4.80	0.004	0.005	---
6.80	-.---	-.---	---
8.40	-.---	-.---	---
8.91	-.---	-.---	---
9.30	0.006	0.006	---
9.60	0.011	0.017	87
10.00	0.035	0.046	89
10.55	0.032	0.041	84
12.60	0.008	0.009	93
13.30	-.---	-.---	---

Table G1.5: ESR Results for Solution Series E

pH	$M_I = -3/2$	$M_I = -1/2$	<a>
1.42	0.829	0.853	111
1.90	0.594	0.615	111
2.85	0.087	0.090	112
3.16	0.046	0.051	111
3.88	0.007	0.009	96
4.42	0.004	0.004	93
5.09	-.---	-.---	---
5.73	-.---	-.---	---
6.62	-.---	-.---	---
7.13	-.---	-.---	---
8.05	-.---	-.---	---
8.14	-.---	-.---	---
8.88	0.004	0.004	88
9.11	0.006	0.008	88
9.44	0.018	0.025	92
9.81	0.038	0.049	90
10.37	0.021	0.035	87
12.38	0.015	0.019	82

G1.2 NMR Results:

The vanadium(IV): citrate solutions were prepared, and the nmr spectra were obtained using the procedure outlined in Appendix B. The following table contains the chemical shift data and linewidth as a function of pH level and age of solution in days.

Table G1.6: NMR Results

pH	Age (in days)	Chemical Shift (in ppm)	Linewidth (in Hz)	Percent Area
6.50	14	-544.9	414	96.6
		-554.1	66	3.4
6.75	14	-544.2	218	83.4
		-553.0	210	16.5
7.00	15	-542.8	229	57.3
		-553.8	147	26.5
		-573.7	147	16.1
7.00	23	-543.4	231	65.6
		-553.1	99	6.1
		-572.8	74	28.2
7.13	19	-542.2	315	80.0
		-554.1	126	3.0
		-572.7	100	17.0
7.25	23	-544.3	181	56.4
		-553.8		0.1
		-573.0	49	43.4
7.30	14	-543.9	176	34.3
		-553.9	128	25.9
		-573.4	80	39.7

Table G1.6: NMR Results Cont'd

pH	Age (in days)	Chemical Shift (in ppm)	Linewidth (in Hz)	Percent Area
7.40	24	-543.4	275	63.5
		-552.5	178	4.2
		-573.0	73	32.2
7.50	23	-544.3	308	60.9
		-553.3	81	37.7
		-572.7	81	1.3
7.85	14	-545.0	459	60.8
		-573.3	66	39.1
7.90	15	-544.2	187	51.0
		-552.8	101	12.4
		-573.1	70	36.5
8.14	17	-546.4	123	40.0
		-572.9	75	60.0
8.40	23	-541.8	112	55.7
		-563.9	144	16.5
		-573.3	56	27.6
8.88	18	-537.8	165	60.0
		-562.6	165	14.0
		-572.0	142	26.0
8.95	23	-536.4	99	48.0
		-561.3	181	24.7
		-572.9	115	27.1
9.05	14	-538.2	100	74.4
		-573.3	183	25.5
9.11	15	-536.3	82	82.0
		-560.6	123	17.9
		-573.0		0.1
9.11	17	-534.6	96	88.0
		-559.5	147	12.0
9.37	23	-534.4	76	91.6
		-558.4	101	8.3

Table G1.6: NMR Results Cont'd

pH	Age (in days)	Chemical Shift (in ppm)	Linewidth (in Hz)	Percent Area
9.43	8	-532.9	86	99.0
		-554.2		
9.50	24	-533.94	61	100.0
9.55	13	-533.9	58	100.0
9.75	24	-533.6	66	92.3
		-557.1	83	7.6
9.81	8	-532.7	96	100.0
10.05	24	-533.5	58	88.9
		-557.4	83	11.0
10.20	24	-533.3	50	87.5
		-557.2	66	12.4
10.36	7	-532.5	69	93.0
		-556.6	111	7.0
10.40	24	-533.2	50	75.5
		-556.8	73	24.4
10.9	7	-533.1	56	98.0
		-556.3	113	2.0
11.9	7	-533.2	96	98.0
		-556.5	122	2.0
12.3	7	-533.4	49	91.0
		-555.9	62	9.0
12.4	24	-533.5	48	85.4
		-556.2	58	14.5
13.1	24	-535.3	34	88.9
		-555.9	50	11.0